# REGULATION OF EXOPOLYSACCHARIDE PRODUCTION IN *MYXOCOCCUS XANTHUS*

Wesley P. Black

Dissertation submitted to the faculty of the
Virginia Polytechnic Institute and State University
in partial fulfillment of the requirements for the degree of

Doctor of Philosophy
In
Biological Sciences

Zhaomin Yang, Chair

David L. Popham

Jill C. Sible

Ann M. Stevens

December 15, 2005
Blacksburg, VA

Keywords: *Myxococcus xanthus*, exopolysaccharide (EPS), type IV pili (Tfp), Dif chemotaxis proteins, signal transduction, gliding motility, fruiting body development

Copyright 2005, Wesley P. Black

# REGULATION OF EXOPOLYSACCHARIDE PRODUCTION IN *MYXOCOCCUS XANTHUS*

Wesley P. Black

Zhaomin Yang, Chair

Department of Biological Sciences

(ABSTRACT)

The surface gliding motility of *Myxococcus xanthus* is required for a multicellular developmental process initiated by unfavorable growth conditions. One form of the *M*. *xanthus* surface motility, social (S) gliding, is mediated by the extension and retraction of polarly localized type IV pili (Tfp). Besides Tfp, exopolysaccharides (EPS), another cell surface associated component, are also required for *M*. *xanthus* S motility. Previous studies demonstrated that the Dif chemotaxis-like signal transduction pathway is central to the regulation of EPS production in *M*. *xanthus*. Specifically, *difA*, *difC* and *difE* mutants were found to be defective in EPS production and S motility. DifA, DifC and DifE, homologous to methyl-accepting chemotaxis proteins (MCPs), CheW and CheA, respectively, are therefore positive regulators of EPS. This study, undertaken to better understand the regulation of EPS production, led to a few major findings. First, DifD and DifG, homologous to CheY and CheC, respectively, were found to be negative regulators of EPS production. Both DifD and DifG likely function upstream of the DifE kinase in EPS regulation. DifB, which has no homology to known chemotaxis proteins, was found not to be involved in EPS production. Secondly, this study led to the recognition that Tfp likely function upstream of the Dif pathway in the regulation of EPS production. Extracellular complementation experiments suggest that Tfp may act as sensors instead of signals for the Dif chemotaxis-like pathway. We propose a regulatory feedback loop that couples EPS production with Tfp function through the Dif signaling proteins. Lastly, we sought to identify additional genes involved in EPS production. Our efforts identified a mutation in a separate chemotaxis gene cluster as a suppressor of *difA* mutations, suggesting potential cross-talks among the multiple chemotaxis-like pathways in *M. xanthus*. In addition, we identified twenty-five previously uncharacterized genes that are predicted to be involved in *M. xanthus* EPS production. These genes appear to encode additional EPS regulators and proteins with biosynthetic function.

# DEDICATION

I dedicate this dissertation to my entire family for all their love and support over the years. To my grandmother, who made me go to college in the first place. And yes mom and dad, after only a decade of college, I am finally finished!

# AKNOWLEDGEMENTS

I would like to first acknowledge my mentor, Zhaomin Yang. Thank you for taking me into your lab after I was abandoned and for bringing me to Blacksburg, which has been a great experience. You have truly been a great advisor throughout this entire process and your encouragement, support and guidance is always greatly appreciated. To the remainder of my committee, Drs. Dave Popham, Jill Sible and Ann Stevens, thank you for all the advice, comments and guidance you have provided.

To all past and present members of the Yang lab and other members of the labs on the 4th floor, thank you for assistance in and around the lab. To all my past and present friends at Virginia Tech, Dave O’Brien, Mike Woodman, John Varga, Danny Schu, Matt Mastropaolo, Josh Williams, and Ian Auckland for all the “stress relieving” activities we have and will likely continue to participate in. A special thank you to Catalina Troche for cutting my foot and for all your support and encouragement, especially in the later stages of writing this dissertation.

# TABLE OF CONTENTS

**CHAPTER 1: Introduction and Review of Literature** **1**

- A. General introduction to the myxobacteria 2
  - 1. Roland Thaxter and the discovery of myxobacteria 2
  - 2. Phylogeny of the myxobacteria 5
  - 3. Ecology of the myxobacteria 7
  - 4. Nutrition and growth of the myxobacteria 9
- B. General characteristics of surface gliding motility 11
  - 1. Tfp-mediated motility 11
  - 2. Gliding motility 13
- C. Type IV pili 17
  - 1. Structure of Tfp 17
  - 2. Tfp assembly and function 19
- D. Review of bacterial chemotaxis 22
  - 1. The bacterial chemotaxis signal transduction pathway 24
    - a. Excitation 24
    - b. Adaptation 26
  - 2. Comparison between different chemotaxis systems 30
  - 3. Non-conventional chemotaxis-like pathways 31
- E. General review of *Myxococcus xanthus* 34
  - 1. Overview of *Myxococcus xanthus* development 34
    - a. Development and the starvation signal 34
    - b. Cell-cell communication signals during development 36

c. Involvement of other signaling pathways in development 39

2. *Myxococcus xanthus* motility 40

a. Adventurous motility 41

b. Social motility 42

c. Regulation *M. xanthus* motility 44

3. Review of the *Myxococcus xanthus dif* locus 47

a. Identification and characterization of the *dif* locus 47

b. Interactions among Dif proteins 49

c. Signaling by DifA, the chemoreceptor homologue 50

d. The Dif pathway and lipid chemotaxis 50

e. Research questions 52

**CHAPTER 2: *Myxococcus xanthus* Chemotaxis Homologs DifD and DifG Negatively Regulate Fibril Polysaccharide Production 55**

ABSTRACT 56

INTRODUCTION 57

MATERIALS AND METHODS 60

RESULTS 64

DISCUSSION 77

ACKNOWLEDGEMENTS 84

**CHAPTER 3: Type IV Pili Function as Remote Sensors for the Dif Chemotaxis Pathway in *Myxococcus xanthus* EPS Regulation 85**

ABSTRACT 86

INTRODUCTION 87

MATERIALS AND METHODS 89
RESULTS 91
DISCUSSION 103
**CHAPTER 4: A Mutation in *cheW7* Suppresses *difA* Deletion in *Myxococcus xanthus* 110**
ABSTRACT 111
INTRODUCTION 112
MATERIALS AND METHODS 113
RESULTS 118
DISCUSSION 127
**CHAPTER 5: Identification of Additional Genes Involved in *Mycococcus xanthus* EPS Production 130**
INTRODUCTION 131
MATERIALS AND METHODS 132
RESULTS 134
DISCUSSION 140
**REFERENCES 141**
**CURRICULUM VITAE 157**

## LIST OF FIGURES

### CHAPTER 1:

Figure 1-1. Phylogenetic tree of the myxobacteria. 6

Figure 1-2. Electron micrograph of type IV pili. 18

Figure 1-3. Schematic of a biased random walk. 23

Figure 1-4. Comparison of a two-component system with a chemotaxis system. 25

Figure 1-5. Chemotaxis systems in *E. coli* and *B. subtilis*. 27

Figure 1-6. Cartoon of *M. xanthus* vegetative growth and development. 35

Figure 1-7. The *M. xanthus dif* locus. 48

Figure 1-8. A model of the regulation of EPS production by the Dif pathway. 54

### CHAPTER 2:

Figure 2-1. The *M. xanthus dif* locus and homology. 65

Figure 2-2. Homology of DifG and DifD to CheC and CheY. 66

Figure 2-3. Phenotypic analysis of *dif* mutants. 68

Figure 2-4. Agglutination assay of *dif* mutants. 72

Figure 2-5. Immunoblot analysis of the fibril protein FibA. 73

Figure 2-6. Binding of calcofluor white. 75

Figure 2-7. Two models for the Dif pathway. 79

### CHAPTER 3:

Figure 3-1. Quantitative analysis of EPS production. 92

Figure 3-2. Qualitative analysis of EPS production. 95

Figure 3-3. Quantitative analysis of EPS production. 96

Figure 3-4. Immunoblot of Dif proteins in *pil* mutants. 98

Figure 3-5. Extracellular complementation experiment. 100

Figure 3-6. Extracellular complementation assay. 101

Figure 3-7. Model of Tfp-Dif regulation of EPS. 104

**CHAPTER 4:**

Figure 4-1. Analysis of S motility and development. 120

Figure 4-2. Analysis of EPS production. 121

Figure 4-3. Schematic of the *M. xanthus che7* locus. 124

**CHAPTER 5:**

Figure 5-1. Example of *M. xanthus* binding Congo red. 135

# LIST OF TABLES

CHAPTER 2:

Table 2-1. *M*. *xanthus* strains and plasmids. 61

Table 2-2. Binding of Congo red and Trypan blue. 76

CHAPTER 4:

Table 4-1. *M*. *xanthus* strains and plasmids used in this study. 114

Table 4-2. Cotransformation frequencies of kan$^r$ and *che7*. 125

CHAPTER 5:

Table 5-1. Selected *magellan4* insertions causing defects in EPS production. 137

# CHAPTER 1

# Introduction and Review of Literature

## A. General introduction to the myxobacteria

Myxobacteria are an interesting group of Gram-negative bacteria that have remarkable morphogenic potentials. They tend to behave in a social manner throughout their lifestyle and have been traditionally referred to as “social bacteria” (53, 56, 158). A striking feature of myxobacterial movement is that it appears to be highly coordinated and often occurs as cohesive cell groups. When deprived of nutrients, myxobacteria undergo a complex morphogenic process to form a multicellular fruiting body with one to several hundreds of thousands of cells (53, 56, 158). The shape of myxobacterial fruiting bodies can range from simple mounds to elaborate stalked or branched structures. Within fruiting bodies, the majority of the population further differentiates into environmentally resistant myxospores that may remain dormant until conditions improve. The process of fruiting body formation by myxobacteria is highly dependent on cell-cell signaling and their gliding motility. The following subsections will focus on the discovery, phylogeny, ecology and nutrition of myxobacteria.

### 1. Roland Thaxter and the discovery of myxobacteria

Roland Thaxter, a mycologist at Harvard University, is undoubtedly the founding father of the myxobacterial field. He made an astounding observation that would lead to the separation of myxobacteria, initially *Chondromyces crocatus*, from fungi (83). He noticed that these peculiar organisms exhibited two distinct life cycles: a single cell vegetative cycle and a multicellular developmental cycle (174). Although Thaxter published only three papers on the subject, his work was fundamental because he recognized *C. crocatus* as a bacterium and set in motion the scientific inquires into the myxobacteria.

Thaxter's first publication focused primarily on observations of the duel life cycles of *C. crocatus*. Thaxter documented his observations of the two distinct life cycles of myxobacteria with meticulous and detailed drawings. He recognized the first as a vegetative cycle that included the slow locomotion of single rod-shaped cells, the swarming of cell groups and cell division by binary fission (174). In the second, a developmental cycle, *C. crocatus* cells were observed to pile up into discrete points that eventually rose off the surface to form structures with distinct projections. He referred to these structures as fructifications or pseudofructifications, which are now known as fruiting bodies. In addition, his first publication introduced several other myxobacterial species that he had isolated. He observed that the fruiting bodies by different myxobacterial strains could range from simple raised mounds to complex tree-like branched structures that terminated consistently at defined lobes. Furthermore, he noticed that these lobes might contain cysts or spores, which could give rise to rod-shaped cells and reenter the vegetative cycle. Thaxter concluded that these peculiar organisms were "altogether so unique in the group of Schizomycetes, to which they should undoubtedly be referred, that their separation as a distinct order seems unavoidable" and thus designated the new group as "Myxobacteriaceae" (174).

Thaxter's second publication (172) was mostly focused on describing the sporulation and germination of myxobacteria, which he believed was left in doubt in his first publication. He provided detailed descriptions of the various stages of fruiting body formation and the differences between sporulation and germination. Thaxter also developed a technique that allowed him to isolate single spores and monitor their germination. He observed individual rod-shaped cells emerge from single spores. These newborn cells eventually commenced growth and binary cell division. This second publication also introduced eight more myxobacterial species.

Thaxter's third and final account of myxobacteria (173) appeared twelve years after his initial publication. Thaxter was apparently quite unhappy about the lack of attention and research on the myxobacteria since his first two publications. He mentioned that during the twelve years since the discovery of myxobacteria, they had received inadequate treatment and did not even appear in general textbooks, such as the *Pflanzenfamilien* or the the *System der Bacterien* (173). In fact, they were only mentioned in the publications of three other scholars who provided hasty and/or vague contributions on the myxobacteria. He thoroughly expressed his displeasure on the contributions by these researchers, and E. Zederbauer got the worst of Thaxter's criticism. Zederbauer had apparently claimed at one time that the myxobacteria did not really exist and that Thaxter most likely described a symbiont of fungi. Thaxter pointedly criticized Zederbauer for not being very well acquainted with myxobacteria and was convinced of these beliefs when a culture from Zederbauer proved to be the conidial state of a fungus. He also mentioned that he would make no further contributions on myxobacteria and only reexamined his own preparations so that "he had not been guilty of such blunders as were, perhaps unconsciously, attributed to him in Dr. Zederbauer's account" (173). It was suggested later that Thaxter let go of the group because he was disgruntled about the nomenclatural nightmares that myxobacteria had encountered and likely would encounter (56). He stated that "one can but look with no small interest, and perhaps with some misgivings, to such further taxonomic vicissitudes as may be in store for them" (56, 173). Nevertheless, Thaxter concluded that it would be critical to conduct more careful and detailed studies of myxobacteria, especially on their motility and social characteristics. Indeed, the contemporary research on myxobacteria is mainly focused on their motility and social interactions.

## 2. Phylogeny of the myxobacteria

At one point in time, myxobacteria had been grouped as a separate class within the division of Schizomycetes, which included Eubacteriae, Myxobacteriae, and Spirochaetae (56). The classification of myxobacteria had since undergone many changes primarily based on the morphology of their fruiting bodies and limited biochemical tests. Such criteria resulted in a certain level of confusion in the classification of myxobacteria, because not all species formed structurally well defined fruiting bodies and thus could not be reliably placed into taxonomical groups.

Analysis of rDNA sequence revealed that myxobacteria belong to a coherent order within the class of δ *Proteobacteria* (153). Their closest relatives include certain bdellovibrios and sulfate reducers. The 16S rDNA sequence, their predicted secondary structure and certain biochemical properties suggested that there are three separate suborders of myxobacteria (Fig. 1-1). The first is *Cystobacterineae*, which includes the better known genera *Myxococcus* and *Stigmatella* (153). Species in *Cystobacterineae* generally undergo dramatic morphological changes during development, including the transition from rod-shaped cells to spherical spores. These species also produce ridges of cells, a phenomenon called rippling, during the aggregation process (53, 56). In addition,

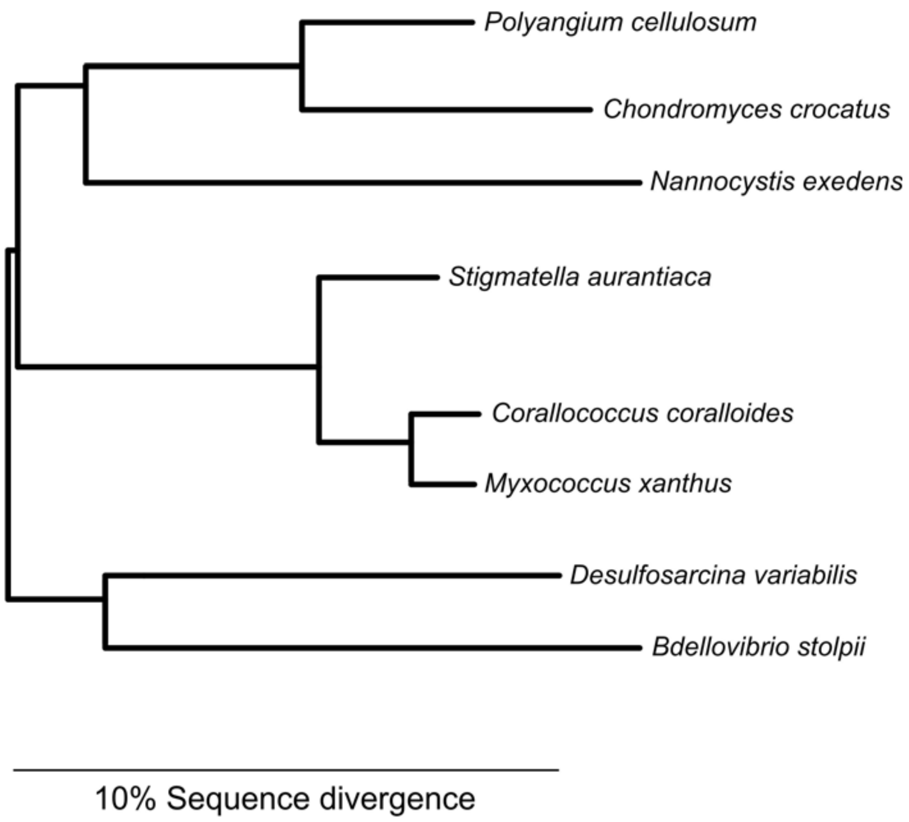
Polyangium cellulosum
Chondromyces crocatus
Nannocystis exedens
Stigmatella aurantiaca
Corallococcus coralloides
Myxococcus xanthus
Desulfosarcina variabilis
Bdellovibrio stolpii
10% Sequence divergence

**Figure 1-1.** Phylogenetic tree of the myxobacteria.

The indicated line represents 10% sequence divergence of the 16S rDNA. The tree is rooted with other members of the δ-proteobacteria for reference. Figure based on Shimkets and Woese (153).

they produce monocyclic keto-carotenoid glucosides, have 2- and 3-hydroxy branched fatty acids in their membranes and their colonies bind the dye Congo red. The second suborder, *Sorangineae*, contains the genera *Chondromyces* and *Polygangium*. The third contains only *Nannocystis* and two other recently described halophilic genera (60, 77, 153). These latter two suborders produce myxospores that differ little in shape from their vegetative cells. In addition, they do not exhibit developmental rippling and lack the ability to absorb Congo red (53, 56). Both of these subgroups have low levels of branched-chain fatty acids and do not possess hydroxy fatty acids. Members of the *Sorangineae* subgroup also lack the keto groups found in the carotenoids of *Cystobacterineae*. The *Nannocystis* group contains monocyclic aromatic carotenoids, which are unique to this group.

## 3. Ecology of the myxobacteria

Myxobacteria are apparently a very successful group of bacteria as they are nearly ubiquitous in nature. They have been isolated from many altitudes and climates from the tropics to Antarctica (138). Environments with the richest myxobacterial micro floras are usually in semi-dry and warm areas. It is unclear whether myxobacteria isolated from the more extreme environments naturally thrive there or have merely persisted there due to incidental translocation of myxospores. The complex life style of the myxobacteria is probably influenced and selected for by the environmental niches that they inhabit.

Myxobacteria are mostly known as soil-dwelling bacteria (50, 138). They can be found in all soil types ranging from sandy and rocky soils such as psamment to soils rich in organic matter such as chernozem (black earth) (138). It has been estimated that a single gram of soil from a favorable environment may yield up to one million myxobacterial cells representing 5-10 species. In addition to soil, they are often found on living or decaying organic matter such as tree leaves and bark, rotting wood and herbivorous mammal dung. Traditionally, dung has served as a reliable source for the isolation of various myxobacteria. It is unclear why myxobacteria have frequently been found in association with dung because convention maintains that vegetative cells do not survive in animals. However, isolation of myxobacteria from dung samples on the surface of deep snow suggests that myxospores may safely pass through the digestive track of certain animals, possibly as a means for myxobacterial dispersal.

Myxobacteria can also be readily isolated from water sources, although it is unclear whether they persist in such environments (138). Until recently, it was assumed that myxobacteria did not exist naturally in marine environments because all the early myxobacterial isolates failed to grow at salinities higher than 1%. However, several research groups in China and Japan have discovered many species of marine myxobacteria that are closely related to the *Cystobacterineae* or *Nannocystis* subgroups (78, 106). These new isolates have been shown to be true halophiles and grow at optimal salinities ranging from 2-4%. It is perhaps relevant to note that marine myxobacteria have only been found in Pacific waters but not the Atlantic as all attempts to isolate myxobacteria from Atlantic samples were unsuccessful (138). Perhaps further testing using the isolation method recently described for marine myxobacteria (106) could reveal myxobacteria in the Atlantic Ocean.

## 4. Nutrition and growth of the myxobacteria

The general growth characteristics of myxobacteria correlate with their environmental niches and feeding style. Most known myxobacteria isolated from topsoil are mesophilic and culturable between 6 and 35°C (138). They are almost exclusively strict aerobes. The only known exception is *Anaeromyxobacter dehalogenans* (147), which was isolated from various soil samples by enrichment for halorespiration. Despite the name, *A. dehalogenans* is likely not a strict anaerobe since oxygen was shown to support microaerophilic growth. Myxobacteria can persist over a wide pH range and generally prefer to grow in neutral to slightly alkaline conditions (138). Myxobacterial feeding is a communal effort analogous to "microbial wolf-packs". They surround and digest their food sources, whether insoluble macromolecules or preys like other microorganisms (52). It was determined initially that at least 17 amino acids were required to provide the carbon and energy sources for the growth of *Myxococcus xanthus* (54). Later studies found that only 6 amino acids were necessary if pyruvate or acetate were provided as energy sources (41). Several studies have found that sugars are not utilized as energy sources by the myxobacterium *M. xanthus* (41, 54).

Since myxobacteria consume macromolecules and microbes as food, they must secrete many hydrolytic enzymes capable to digest them. Many attempts have been made to characterize the various bacteriolytic and proteolytic activities associated with myxobacteria. The most comprehensive analysis was preformed by Sudo and Dworkin (166), who demonstrated the presence of bacteriolytic and/or proteolytic activities from the crude fractions of culture supernatants of *M. xanthus*. These fractions were tested for lytic activity on whole cells, Gram-positive cell walls and purified casein. They concluded that there were four distinct enzymatic activities: glucosaminidase, amidase, protease and peptidase. Another study suggested that myxobacteria feeding is cooperative because it requires a threshold of exoenzymes (143). Specifically, it was found that more than $10^3$ cells/ml of *M. xanthus* were required to initiate growth on low levels of casein. In contrast, fewer than $10^3$ cells/ml were able to initiate growth on the same concentration of casitone, which is enzymatically digested casein. In addition, it was shown that the extracellular protease activity correlated with and was approximately proportional to the density of the culture. These findings are consistent with the notion that myxobacteria are cooperative feeders and their social behavior in nature extends beyond their developmental cycle.

## B. General characteristics of surface gliding motility

Motility is a trait that is scattered throughout the living world and provides a means for organisms to move about in their environment. In the bacterial world, there exist several distinct mechanisms of motility. Flagella mediated swimming motility is the most extensively studied and well understood form among them. Flagella, membrane-anchored helical filaments, generate motility through rotation driven by the translocation of either protons or sodium ions (11, 20, 113). In general, flagellated bacteria move in aqueous or semi-aqueous environments. It has also been demonstrated that some bacteria can move on solid surfaces using a form of flagella-driven motility known as swarming (65, 66). Gliding motility, another form of surface translocation, is widespread among bacteria. Gliding is defined as an energy dependent surface locomotion of a cell without the aid of flagella (69, 115). Because gliding motility appears in many phylogenetic branches of bacteria, there likely exist multiple mechanisms for movement (115). It appears that there are at least two major classes of surface gliding motility: those that involve type IV pili (Tfp) and those that do not.

### 1. Tfp-mediated motility

Tfp-mediated surface motility has been observed in a variety of Gram-negative bacteria. In *Pseudomonas aeruginosa*, *Neisseria* sp. and many other bacteria, it is know as twitching motility (115). In myxobacteria, Tfp-mediated motility is referred to as social gliding motility. The differences between these two are relatively minor. Twitching appears slightly less coordinated or organized when compared to social gliding (164). It is now generally accepted that twitching motility and social gliding share the same underlying mechanisms (149) and they will be discussed together.

Twitching motility was first described as intermittent jerky movements of cells on a surface without the aid of flagella (69). Henrichsen observed and categorized the surface movements of an exhaustive list of bacterial species. One of these groups, representing some 20 or so different species of bacteria, contained bacteria that exhibited twitching motility. One of his most important observations was that all strains exhibiting twitching motility possessed polar pili whereas the strains of the same species that had lost their pili also lost the ability to twitch. He proposed that polar pili were likely responsible for twitching motility.

The first proposed mechanism of twitching motility came from David Bradley, who suggested that pilus retraction may power twitching (36). It had been known that loss of Tfp and hyperpiliation coincided with resistance to certain phage in *P. aeruginosa* (35, 37). His new discoveries were that phage or antibodies specific to Tfp inhibited twitching motility and that certain twitching motility mutants were hyperpiliated (36). He noticed that although these non-motile hyperpiliated mutants still had phages attached to the pilus fibers, they remained resistant to infection. In strains that possessed functional twitching motility, most of the phage particles were localized at the base of the pilus near the cell surface. In contrast, phage particles decorated the entire length of pili in hyperpiliated non-twitching mutants. It was suggested that the pilus must be able to retract to bring the phage in contact with the cell surface.

More direct methods have now been used to demonstrate the retraction of Tfp and have provided sufficient evidence to validate Bradley's model. In *Neisseria gonorrhoeae*, laser tweezers were utilized to determine that pilus retraction powers motility (122). It was shown that laser trapped beads (1 µm) coated with Tfp specific antibodies were pulled toward wild-type cells attached to larger latex beads (3 µm). This was not seen in *pilT* mutant cells, which presumably assemble paralyzed or non-retractable Tfp. Using this technique, they were also able to show that the pilus is one of the strongest molecular motors with a predicted force approaching 100 pico Newtons. In *P. aeruginosa*, an alternative approach led to the same conclusion. Skerker and Berg directly observed and documented the retraction of Cy3 labeled Tfp on single cells and the translocation of one cell towards another (161). In *M. xanthus*, wild-type cells were found to become tethered to surfaces when submerged in a viscous solution containing methylcellulose whereas non-piliated cells failed to do so (167). The tethered cells were observed to occasionally stand on one end and move toward the surface. To support that it was Tfp that mediated this movement, it was shown that *pilT* mutants, which assemble paralyzed Tfp, became tethered to surfaces but did not show any movement towards the surface. These observations, which were all made within one year, proved beyond reasonable doubt that pilus extension and retraction is the mechanism for Tfp mediated surface motility.

## 2. Gliding motility

Tfp-independent surface gliding motility has been observed in many phylogenetic branches of bacteria. The best studied members include representatives from myxobacteria, cyanobacteria and flavobacteria (69, 115). Although Tfp-independent gliding motility has been studied extensively, it remains one of the most mysterious forms of motility. Proposed mechanisms include directional wave propagation, slime or surfactant secretion, rotary motor propulsion and moving tracks or belts on cell surfaces (115, 133). The following section will focus on the studies of gliding motility in the *Cytophaga-Flavobacterium-Bacteriodes* (CFB) phylogenetic group and certain cyanobacteria. A discussion of myxobacterial gliding motility will be presented in a later section.

Some key observations have been made pertaining to the mechanism of gliding in the CFB group. *Flavobacterium johnsoniae* (formerly *Cytophaga johnsoniae*) moves incredibly fast. Speeds of 2-10 μm/sec have been observed on glass surfaces, which are roughly ten times faster than on agar surfaces (115, 116). *F. johnsoniae* cells have been observed to attach to glass surfaces by their cell poles and rotate at speeds around 100 rpm, leading to the proposal of rotary motors as the gliding engine (133, 134). In addition, latex beads attached to the cell surface have been observed to move along the length and width of the cell (101, 134). In some instances, several beads attached to one cell can travel in opposite directions and pass each other on the same side of the cell. These beads have also been observed to stop and spin on the cell surface, especially at the poles. Experimental evidence suggests the mechanism moving these beads may be the same as that for gliding. For instance, beads move at approximately the same speed as that observed for the cells. Non-motile mutants fail to move these beads and regain the ability to do so when complemented with appropriate genes (4, 75, 76, 134). These observations provide some support for a rotary gliding motor or a moving belt. It was proposed that the movement of track-like structures, which could be embedded in the outer membrane, may provide the force for gliding (134).

Recent genetic studies in the McBride laboratory have identified many genes required for gliding motility in *F. johnsoniae* (4, 38, 39, 74-76, 116, 117). These genes encode potential ABC transporters, lipoproteins and a few other proteins with no known homology or function. A new model or a variation on an old model was proposed based on these genetic studies (116). It involves the export and import of macromolecules, like polysaccharides. In this model, the export of a long polysaccharide chain could be followed by import at another site on the cell surface. The movement of this macromolecule along the cell surface could function as a conveyor-belt that may propel the cell along a surface. In agreement with this model, non-motile strains have been found to be defective in chitin degradation, which is believed to involve chitin transport across the outer membrane (6, 7).

Studies from *Oscillatoria* sp., *Phormidium uncinatum* and *Anabaena variabilis* have led to the proposal of two mechanisms for gliding motility in filamentous cyanobacteria. The secretion of mucilage or slime is implicated in both mechanisms (72, 191). In *Oscillatoria* sp. and *P. uncinatum*, cells rotate around the long axis as they glide. Ultrastructure analysis revealed bands of helically arranged protein fibrils on the cell surface of these two genera. The orientation of these bands always correlated with the direction of rotation (1, 72). It is proposed that slime secretion causes contraction of the fibrils and creates traveling surface waves along the length of the cell. The traveling waves are proposed to cause cell rotation and gliding. In agreement with this model, India ink staining of secreted slime revealed helical patterns similar to the helical bands of fibrils (73). The gliding of *A. variabilis* is somewhat similar to that of the other two filamentous cyanobacteria. The difference is that helical fibrils are absent and the cells do not rotate about their axis. India ink staining of secreted slime was observed to radiate perpendicular to and away from the cell body. As with slime secretion, another common component in all of the gliding cyanobacteria is the presence of junctional pore complexes (JPC) (73). Slime secretion and gliding motility always correlate with presence of JPC's. JPC's appear to be made of an outer membrane pore complex attached to a tube that extends through the peptidoglycan into the cytoplasm (72, 73, 191). It is hypothesized that polyelectrolyte gel initially enters the tube unhydrated and as it approaches the outer membrane pore, it becomes hydrated, swells, and gets secreted. The secreted slime contacts and adheres to the substratum and provides the force necessary to propel the cell. Although observations in cyanobacteria are consistent with slime secretion as a mechanism for gliding motility, it is not clear how slime secretion through different JPC's can be coordinated or what the genetic basis for such a slime secretion model is.

## C. Type IV pili

Type IV pili (Tfp) have been implicated in a variety of cellular process, including DNA uptake, biofilm formation, pathogenesis, bacteriophage infection, and surface motility (43). Tfp are usually polarly localized (except for cocci such as *Neisseria* sp.) thin protein filaments that extend off the surface of the cell membrane (Fig. 1-2). They are generally 5-7 nm in diameter and can be as long as four microns (114, 115). It is now generally accepted that extension and retraction of the Tfp filament is crucial for the processes listed above. The following is a brief review of the structure and assembly of Tfp.

### 1. Structure of Tfp

The structure of the Tfp filament has been studied extensively in *P. aeruginosa* and *N. gonorrhoeae* (47). The filament is generally a homopolymer of the pilin protein or PilA, which arranges in a helical fashion with five monomers per helical turn (47, 59, 114, 180). PilA has a highly conserved N-terminal hydrophobic region containing a leader peptide sequence. Portions of the C-terminal region of pilin vary greatly among bacterial species and are proposed to provide the specificity for Tfp substrate binding and antigenic variability (59, 114). The crystal structures of several pilins have given much insight into Tfp structure. The filament is predicted to have three layers (47, 59). The inner-most layer or core of the fiber is composed of packed α-helices formed by the N-terminal hydrophobic domain of pilin. The central or middle layer of the fiber, formed by the bulk of the C-terminal domain, is composed of a continuous 25-stranded β-sheet. This means that a fiber cross-section would simultaneously cut through 25 β-sheets. It is

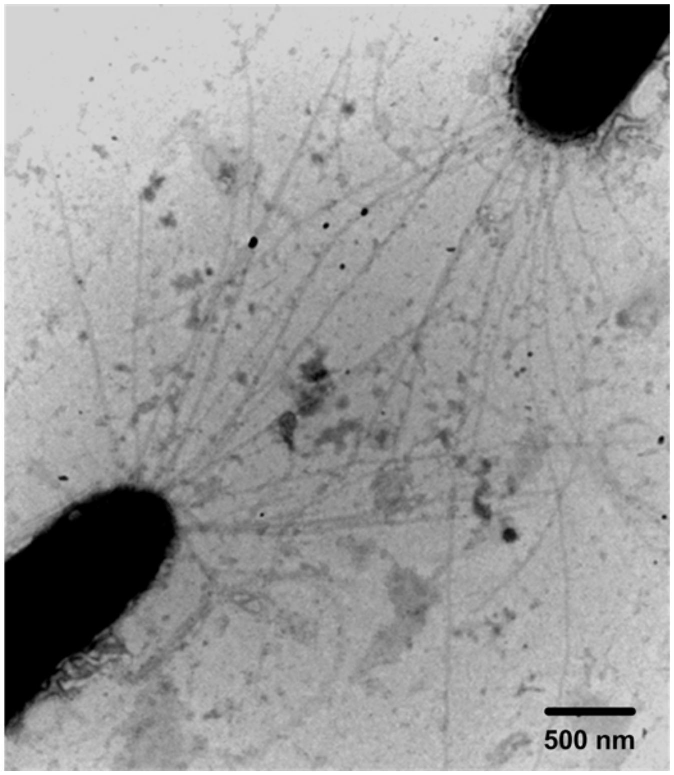

**Figure 1-2.** Electron micrograph of type IV pili.
*M*. *xanthus* cells showing polarly localized Tfp. The cells were stained with phosphotungstic acid and viewed by transmission electron microscopy.

proposed that the packed α-helices provide flexibility to the fiber and hydrogen bonding between β-sheets support the lengthwise mechanical strength. The outermost layer consists of the extreme C-terminal disulphide bridged loop and the αβ-loop region. This layer, proposed to be fully exposed, has the most sequence variation and likely provides the substrate specificities of various Tfp.

### 2. Tfp assembly and function

Less is known about the process of Tfp assembly and how Tfp are anchored to the cell. It is believed that Tfp are assembled at the base since there does not appear to be an inner channel for the subunits to pass through (180). In addition, it is known that PilA can spontaneously insert into the inner membrane. It has been hypothesized that the assembly of Tfp may be somewhat similar to that of filamentous phages (145) as both share some commonality with type II protein secretion systems (135, 145).

It is clear, however, that many genes are involved in Tfp assembly and all organisms studied thus far share a common set of proteins (Pil) for Tfp biogenesis and function (114, 115). Due to differences in nomenclature for Tfp genes in *Neisseria* sp., the remaining discussion will use the names from *P. aeruginosa* and *M. xanthus*. In *P. aeruginosa*, more than 30 genes have been implicated in Tfp biogenesis and function (114). The *M. xanthus pil* locus is composed of 17 genes and 14 of these share similarity with their *Pseudomonas* counterparts and are designated with the same names (180). PilD, a bifunctional prepilin peptidase/methylase, cleaves off the leader sequence of PilA (12, 43, 114, 180). This cleavage apparently prepares PilA for assembly into filaments, as *pilD* mutants fail to assemble Tfp. PilD also methylates PilA on the most N-terminal residue, usually a phenylalanine, after cleavage. The exact role of methylation is not clear at this time as variants containing other hydrophobic residues at this site are tolerated (114). Other core members crucial for Tfp biogenesis are PilMNOPQ (12, 43, 114, 180). PilM contains a conserved ATP binding motif and is homologous to the cell shape determinant protein MreB and the cell division protein FtsA. This homology may suggest that it is partially responsible for determining the polar location of the Tfp membrane complex. PilN and PilO, containing extensive stretches of hydrophobic residues at their N-termini, are thought to be membrane proteins that anchor other Pil proteins to the cytoplasmic membrane. Both PilQ and PilP are required for filament passage through the outer membrane. PilQ is a member of the secretin super-family and appears to form multimeric outer membrane pores that allow the passage of the assembled PilA filament. PilP, an outer-membrane lipoprotein, appears to be involved in the stabilization of the PilQ membrane complex. In *M. xanthus*, the *tgl* gene, which is not located in the *pil* gene cluster, encodes another lipoprotein that is required for PilQ assembly (128, 129, 180).

Two other components that are required for Tfp functionality are PilB and PilT. These two share homology and are predicted to have ATPase activity (43, 114). Yet, PilB and PilT have distinct and opposite functions. *pilB* mutants fail to assemble Tfp and the ATPase activity of PilB is thought to drive the assembly or polymerization of PilA subunits. PilB, therefore, is referred to as the extension motor for Tfp systems. On the other hand, *pilT* mutants assemble paralyzed or non-retractable Tfp (43, 114). So PilT appears to be the retraction motor and its ATPase activity is thought to cause the depolymerization of PilA during retraction. Tfp depolymerization has been hypothesized to occur at a rate of 1,500 subunits per second at the base (122) and the subunits appear to be redistributed back in the cytoplasmic membrane (125). *P. aeruginosa* has another protein, PilU, which is homologous to both PilB and PilT (43, 114). Although the role of PilU is not as clear, it appears more functionally similar to PilT. *pilU* mutants also display a paralyzed Tfp phenotype with non-motile but piliated cells. Recently, subcellular localization studies showed that PilT is located at both cell poles, whereas PilU is only localized at the piliated pole (46). In this study PilC, an inner membrane protein, was determined to be involved in the localization of PilB. Mutation of any gene described above leads to loss of Tfp-mediated motility (114, 180). In fact, mutations in all genes except *pilT* and *pilU*, result in the lack of a pilus filament.

In addition, there exist additional genes that encode components of regulatory systems. Both *P. aeruginosa* and *M. xanthus* possess the PilR-PilS two-component system that has been implicated in the regulation of pilin expression (180). A few chemotaxis-like systems also appear to control motility or function of Tfp (167, 177, 180). Obviously, there is a lack in the understanding of many aspects of Tfp-mediated motility including assembly, anchoring, function and regulation. Future studies should undoubtedly provide a better understanding of how, when and where Tfp assemble and retract.

### D. Review of bacterial chemotaxis

Chemotaxis is a biological phenomenon that allows cells to move toward favorable environments while avoiding or moving away from unfavorable ones (2, 3). Bacterial chemotaxis has been known for well over a century. It was first described by biologists such as Theodor Engelmann and Wilhelm Pfeffer, when they described the movement of bacteria towards certain chemicals and oxygen (3, 51). In the 1960s, a revolution in the field of bacterial chemotaxis was initiated by Julius Adler when he decided to revisit the topic with the belief that it could serve as a simple model for more complex processes such as human smell or sensory responses (3). Adler and colleagues discovered that some *Escherichia coli* mutants failed to respond to some but not all chemical stimuli, while others failed to respond to all stimuli. His seminal findings led to the hypothesis that specific receptors on the cell surface detect specific stimuli and transmit that information to a central pathway to control the chemotaxis response.

Another breakthrough took place when it was shown that bacterial chemotaxis was achieved by a biased random walk (16-18) (Fig. 1-3). Using a microscope that could track movements of single cells, Howard Berg showed that bacteria exhibited smooth runs disbursed by short tumbles (18). Straight or slightly curved runs usually last for a couple seconds and are followed by a tumble that lasts for about one tenth of a second. The bacteria would then initiate another run in a new and random direction. In the absence of a chemical gradient, it was determined that bacteria move around randomly and do not progress in any particular direction (16, 17). In a gradient of chemical attractant, bacteria were observed to increase the time between tumbles if they were moving towards higher concentration of the attractant. In other words, they swim further

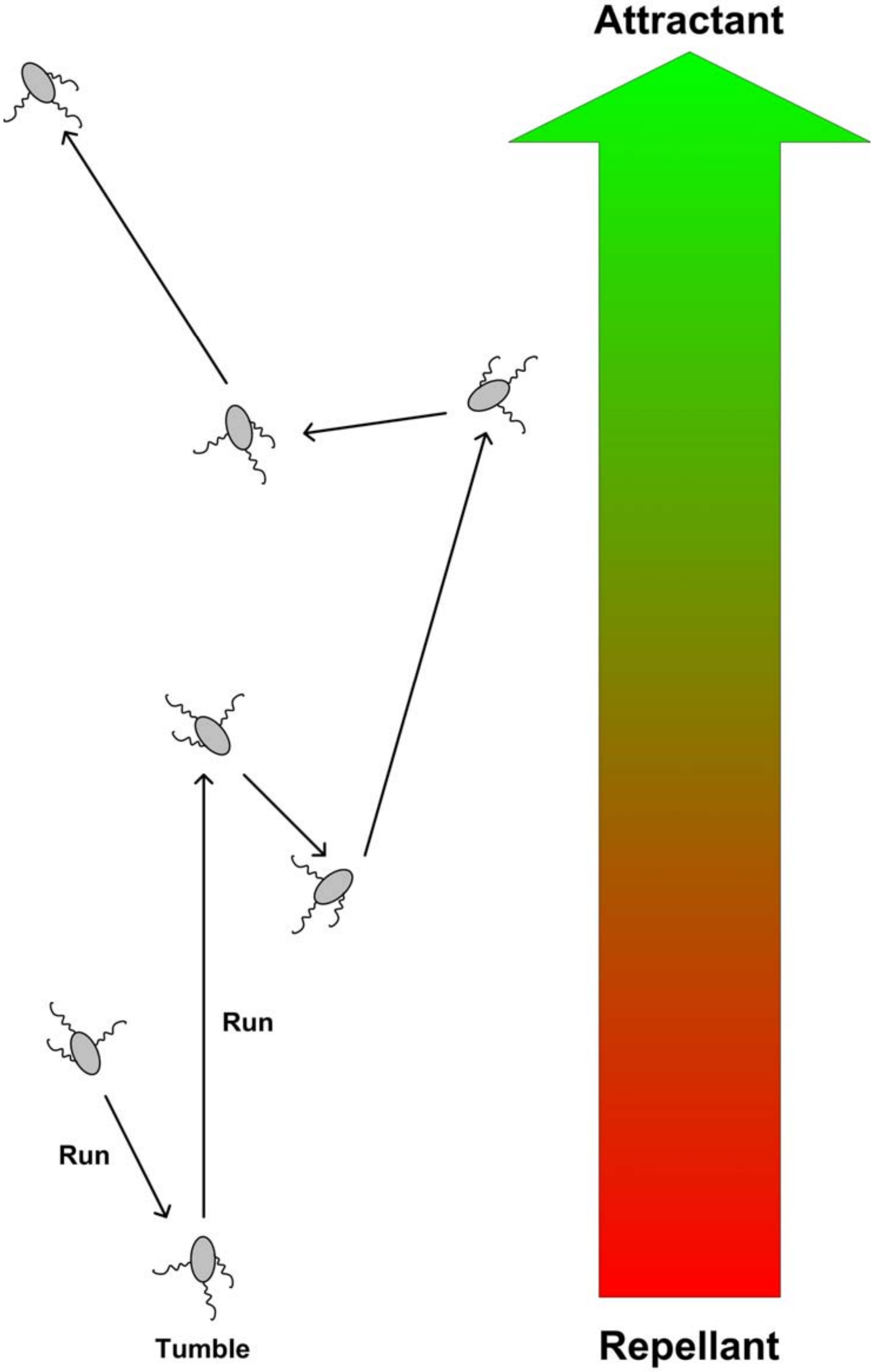
Attractant
Run
Run
Tumble
Repellant

**Figure 1-3.** Schematic of a biased random walk.
Figure based on Webre *et al*. (187).

up the attractant gradient. In contrast, if bacteria migrate down the gradient, they increase the frequency of tumbles, thus changing directions more frequently. If the new direction is unfavorable, they continue to maintain a high tumble frequency. Otherwise, they suppress tumbles and continue movement in a favorable direction. The tumbling and smooth swimming were later attributed to flagellar rotation (20). It was determined in *E. coli* that counter-clockwise (CCW) rotation resulted in smooth swimming or runs, whereas clockwise (CW) rotation resulted in tumbles (102).

## 1. The bacterial chemotaxis signal transduction pathway

The underlying molecular mechanism regulating bacterial chemotaxis involves a specialized two-component system called the chemotaxis signal transduction pathway (58). In a general sense, the classical two-component and the chemotaxis systems perceive some input signal, usually external, and subsequently process and propagate the information to the cytoplasm to regulate the output of the system. One basic difference between classical two-component signaling pathways and chemotaxis signaling pathways is that the output of chemotaxis pathways is generally the regulation of motility instead of the regulation of gene transcription (Fig. 1-4). The response by bacterial chemotaxis systems generally involves two distinct events, excitation and subsequent adaptation, both of which will be discussed in this section.

### a. Excitation

Excitation or stimulation of a chemotaxis system requires a core of proteins to detect stimuli, process the input and mediate the response, as illustrated by the

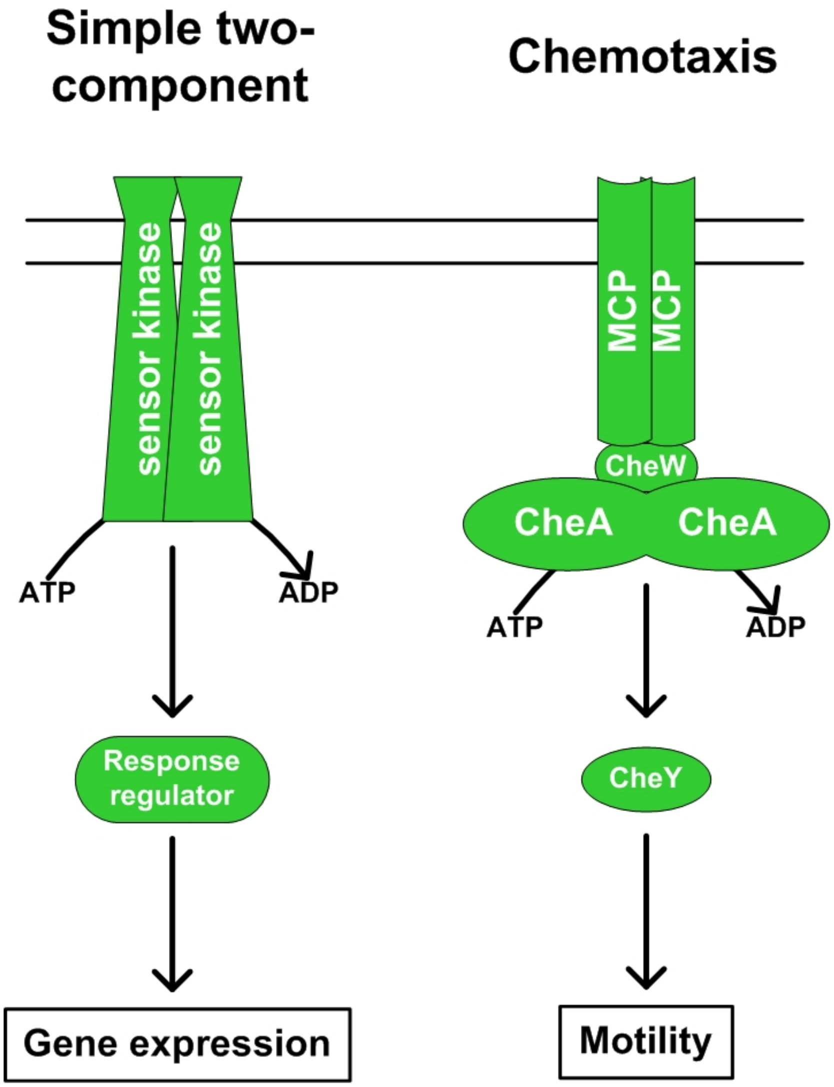
Simple two-component
Chemotaxis
sensor kinase
sensor kinase
MCP
MCP
CheW
CheA
CheA
ATP
ADP
ATP
ADP
Response regulator
CheY
Gene expression
Motility

**Figure 1-4.** Comparison of a two-component system with a chemotaxis system.

chemotaxis system in *E. coli* (32, 58, 178) (Fig. 1-5). The sensory function is carried out by methyl-accepting chemotaxis proteins (MCPs). These are generally transmembrane proteins consisting of an N-terminal periplasmic ligand binding domain and a C-terminal cytoplasmic signaling domain. Perception of signals by the sensory domain modulates the autophosphorylation of the CheA histidine kinase on a conserved histidine residue. The interaction between the MCP signaling domain and CheA is facilitated by CheW, which functions essentially as a scaffold. These three proteins form what is collectively referred to as the signaling complex. In many bacterial systems, multiple MCPs can interact with the same CheA and CheW, allowing a variety of chemical attractants and repellants to be processed through the chemotaxis signaling pathway. The output of chemotaxis systems is accomplished by CheY, a single domain response regulator. CheY catalyzes the transfer of phosphate from CheA to itself on a conserved aspartic acid residue (58, 110). Phosphorylation of CheY induces conformational changes that affect its subsequent binding to the flagellar motor complex to modulate the direction of flagella rotation (32, 58, 178). MCPs, CheW, CheA, and CheY are the common core components of all known chemotaxis pathways and mutations in any gene encoding them generally result in the loss of chemotaxis.

### b. Adaptation

Probably the most unique characteristic of chemotaxis systems is their ability to exhibit adaptation. Adaptation is the return of the cell back to a prestimulus state of runs and tumbles once the concentration of the stimulus is stable (32, 40, 80). In addition, adaptation also gives cells a memory so it can analyze a newly encountered environment

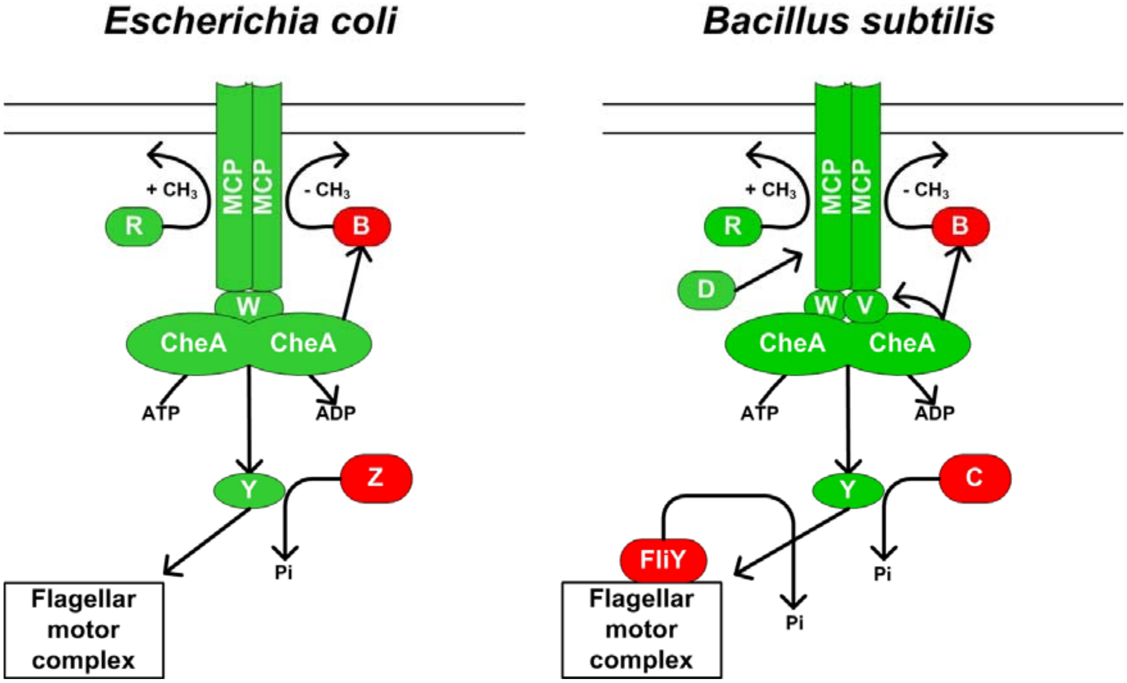

Escherichia coli
Bacillus subtilis
MCP
MCP
+ CH3
- CH3
R
B
W
CheA
CheA
ATP
ADP
Y
Z
Pi
Flagellar motor complex
MCP
MCP
+ CH3
- CH3
R
B
D
W
V
CheA
CheA
ATP
ADP
Y
C
Pi
FliY
Pi
Flagellar motor complex

**Figure 1-5.** Chemotaxis systems in *E. coli* and *B. subtilis*.
Green components represent stimulatory signaling through the pathway and red indicates inhibition or reduction of signal flow.

and compare it to the one from the previous few seconds. The chemotaxis system has been dubbed as a brain of the bacterium because of its adaptation or memory.

At the molecular level, adaptation is accomplished by covalent modification of chemoreceptors through methylation. CheR and CheB are responsible for the methylation and demethylation of MCPs (31) (Fig. 1-5), respectively. The CheR methyltransferase binds to the cytoplasmic signaling domain of MCPs and constitutively adds methyl groups to conserved glutamate residues. Methylation of these residues increases the ability of MCPs to activate the CheA kinase (32, 40). The increase in CheA kinase activity leads to the other part of the adaptation mechanism conferred by CheB. CheB possesses an N-terminal response regulator domain and a C-terminal methylesterase domain (32, 40, 80). Phosphorylation of CheB by CheA converts it to an active state to demethylate MCPs. Therefore, the activity of CheB is highly dependent on the activity of MCPs and CheA. When methylation increases, the activity of the signaling complex increases and CheB becomes activated to reset the system back to a low level of methylation or prestimulus activity. This feedback loop in the regulation of MCP methylation is an important determinant in achieving a memory of the environment and adaptation to stable concentrations of chemicals.

In addition to methylation and demethylation, there are other mechanisms for modulating the levels of phosphorylated CheY (CheY-P). The first mechanism involves the dephosphorylation of CheY-P (58). The intrinsic half-life of *E. coli* CheY-P is around 10 seconds and CheZ accelerates the dephosphorylation of CheY-P, probably enabling *E. coli* to respond to changes in an even shorter time (132, 159). CheZ had originally been described as a CheY phosphatase; however, the crystal structure of CheZ complexed with

CheY suggests that CheZ may not have the enzymatic activity of a phosphatase (204). Instead, CheZ is proposed to accelerate the autophosphatase activity of CheY by actively participating in a predestined nucleophillic attack on the phosphorylated residue in the CheY active site. Rather than a true phosphatase, CheZ appears to act more like an allosteric effector. It should be noted that CheZ homologues only exist in certain enterics and a few other proteobacteria (170). Functionally analogous to CheZ is the CheC-FliY family of CheY phosphatases (Fig. 1-5). These proteins, first described in *Bacillus subtilis*, have since been found in a variety of unrelated organisms (168-170). Although the crystal structure of CheC is structurally distinct from that of CheZ, it likely plays a similar role in the dephosphorylation of CheY-P as CheZ (131). The existence of two structurally distinct and likely independently evolved CheY-P phosphatases suggests the importance of regulating the level of CheY-P in a CheA independent fashion in bacterial chemotaxis.

The second mechanism of modulating CheY phosphorylation involves diversion of phosphate flow from CheY. In some organisms, additional CheY-like proteins can accept phosphate from CheA (148, 150, 170). These CheY-like proteins lack the ability to interact with the flagellar motor, the downstream target. These CheYs have been called phosphate sinks and essentially steal or sequester available phosphate from the true CheY that interacts with the flagellar motor. In both *Sinorhizobium meliloti* and *Rhodobacter sphaeroides*, phosphate sinks have been hypothesized as a mechanism for regulating the level of CheY-P (148, 150). Both of these organisms apparently lack homologues of CheZ or CheC.

## 2. Comparison between different chemotaxis systems

The two best studied chemotaxis systems are undoubtedly those of the enterics (namely, *E. coli* and *Salmonella typhimurium*) and that of *B. subtilis*. They share a common set of chemotaxis proteins and have similarity in behavior to attractants and repellants. However, the underlying mechanism for their chemotaxis response is quite different (170) (Fig. 1-5). For the organisms mentioned above, CCW rotation results in a smooth swimming or runs and CW rotation results in tumbles (102). In *E. coli*, the flagellar motor rotates in the CCW direction by default, that is, in the absence of CheY binding (32, 40). In response to repellants, the activity of the CheA kinase increases, resulting in increase levels of CheY-P. The binding of CheY-P at the flagellar motor causes CW rotation. In comparison, the presence of attractants leads to a decrease in both CheA kinase activity and CheY-P levels. Under these conditions flagella rotate primarily in the CCW direction. In *B. subtilis*, the flagellar motor rotates CW in the absence of CheY binding. Binding of attractant to MCPs increases CheA kinase activity and CheY-P levels. Under these conditions, binding of CheY-P to the flagellar motor results in CCW rotation. Even though these two organisms respond to stimuli by a different underlying molecular mechanism, they have the same outcome, increased flagella rotation in the CCW direction.

On the molecular side of things, *B. subtilis* contains a much more complex chemotaxis system. *B. subtilis* has a homologue of every *E. coli* chemotaxis protein except CheZ. *B. subtilis* has two components, CheC and FliY, with presumably the same function as CheZ (170). CheC and FliY share homology at their N-termini and have both been shown to have CheY-P phosphatase activity. There are two main differences between these two proteins: the extent of phosphatase activity and their location in the cell. CheC is cytoplasmic and has only ~6% of the phosphatase activity of FliY. FliY, which also shares homology with flagellar motor switch proteins, is predicted to reside within the flagellar motor complex (169). So FliY apparently functions to remove phosphate from CheY at the site of its downstream target while CheC may do the same at a slower rate in the cytoplasm. CheC has also been implicated in adaptation responses by modulation of the signaling complex as it was shown to interact with both MCPs and CheA (96). Besides CheC and FliY, *B. subtilis* has two other important chemotaxis proteins, CheV and CheD. CheV has two domains, one homologous to CheY and the other homologous to CheW (170). The CheW-like domain is believed to be important in the stabilization of the signaling complex and the CheY-like domain is implicated in adaptation (88, 141). CheD is an MCP glutamine deamidase that functions to convert glutamine to glutamate making them suitable for methylation. CheD is important for adaptation because it influences the methylation patterns of MCPs. CheD has also been implicated in enhancing the phosphatase activity of CheC (169). It was perhaps fortunate that *E. coli* was chosen as the model system for studying chemotaxis first because we now know that it is likely one of the simplest bacterial chemotaxis systems that exists in nature.

## 3. Non-conventional chemotaxis-like pathways

In recent years, it has become increasingly evident that bacterial chemotaxis systems can control a variety of cellular process other than tactic responses or the direction of motility. So far these cellular processes have fallen into two general categories: developmental or differentiation processes and the biogenesis of cell surface structures.

In both *Rhodospirillum centenum* and *Myxococcus xanthus*, chemotaxis-like systems appear to be involved in the progression into a developmental cycle (22, 97). In *R. centenum*, it was reported that mutations in the *che*$_3$ gene cluster led to either premature developmental cyst formation or the failure to produce cysts (22). Similarily, the *M. xanthus* Che3 pathway appears to regulate the timing of entry into the developmental process known as fruiting body formation (97). In *E. coli*, it was reported that the chemotaxis system itself, but not chemotaxis, is required for the differentiation of liquid swimmer cells to surface motile swarmer cells, which are hyperflagellated and have elongated cell bodies (42). It is unclear how this transformation occurs. A recent study proposed that the flagellum is sensing the “wetness” of the external environment and subsequently signals through the chemotaxis system (183).

Chemotaxis-like systems have also been implicated in the biogenesis of three different cell surface structures. In *P. aeruginosa* and *Synechocystis* sp. PCC6803, chemotaxis-like systems are implicated in the biogenesis of Tfp (23, 49). In *R. centenum*, the Che$_2$ system regulates the production of polar and lateral flagella and is perhaps responsible for the swimmer cell to swarmer cell transition in this bacterium (21). Lastly, the *M. xanthus* Dif (Che2) pathway has been implicated in regulating the production of extracellular polysaccharides (EPS), which are critical for the Tfp driven motility in this organism (15, 25, 202). Although all these non-conventional chemotaxis-like systems regulate process other than chemotaxis, they do appear to regulate the production of motility apparatuses or determinants with the exception of the Che3 pathways in *M. xanthus* and *R. centenum*.

## E. General review of *Myxococcus xanthus*

*Myxococcus xanthus* is undoubtedly the most studied myxobacterium. With a 9.2 Mb genome, *M. xanthus* encodes all the necessary components for fruiting body formation and differentiation, a variety of signal transduction systems, two surface motility systems and production of many secondary metabolites. As a single-celled prokaryotic organism, *M. xanthus* provides a great model for the studies of many interesting processes and phenomena mentioned above. The following sections will briefly discuss *M. xanthus* development and motility. Much emphasis is placed on the Dif chemotaxis-like pathway, the primary focus of this research.

### 1. Overview of *Myxococcus xanthus* development

#### a. Development and the starvation signal

The hallmark of myxobacteria is their ability to undergo multicellular development (55, 56, 84, 155). When sufficient nutrients are available, *M. xanthus* cells grow and divide like other bacteria (Fig. 1-6). However, when cells become starved for nutrients, they can aggregate to form a multicellular fruiting body containing hundreds of thousands of cells if not more. The majority of the cells in a mature fruiting body differentiate into environmentally resistant myxospores. Once conditions improve, myxospores may germinate to give rise to vegetative cells. Myxobacteria are the ultimate social creatures among prokaryotes. Not only does development of a multicellular structure require intimate and extensive cell-cell communication, it also ensures that when conditions improve, a social group of vegetative cells is reformed instantaneously.

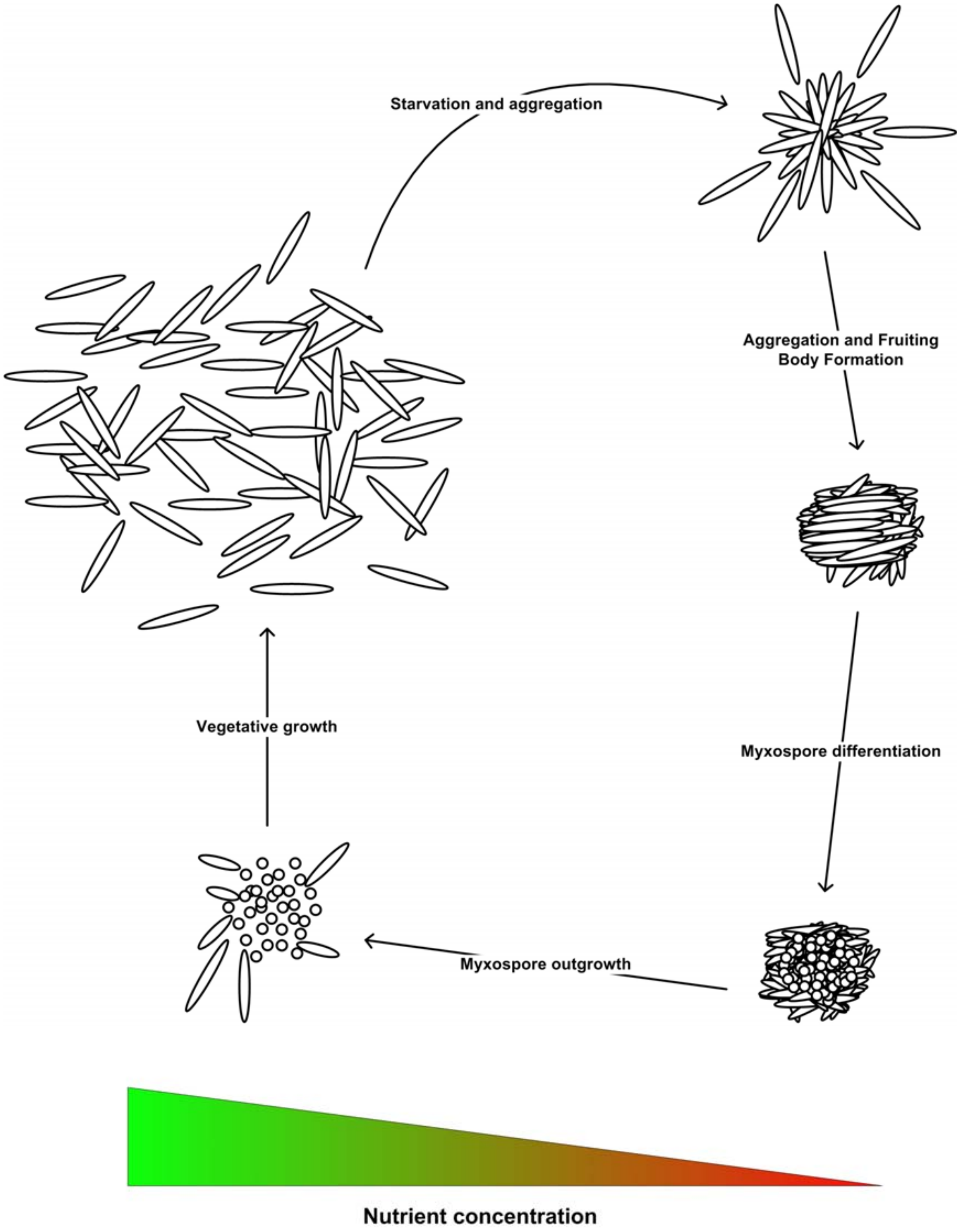
Starvation and aggregation
Aggregation and Fruiting Body Formation
Myxospore differentiation
Myxospore outgrowth
Vegetative growth
Nutrient concentration

**Figure 1-6.** Cartoon of *M. xanthus* vegetative growth and development.
Figure based on Dworkin (53). Cell size, shape and the number of cells or myxospores in each stage are not to scale.

The ultimate signal responsible for initiating the developmental cycle is starvation. Prior to developmental cell-cell signaling, the cell provides itself with an intracellular signal that begins the regulatory cascade. It has been suggested that *M. xanthus* uses its ribosomes to predict when nutrients are limiting (84). This mechanism known as the "stringent response" is found in other bacteria. It is initiated when there is a shortage of any charged tRNA, which triggers the accumulation of guanosine tetra- and penta- phosphate or (p)ppGpp (127). RelA is a ribosome associated (p)ppGpp synthetase. The *M. xanthus* RelA, named after its *E. coli* counterpart, is required to initiate both development and the developmental regulatory cascade (64, 160). In support of a role for (p)ppGpp in development, overexpression of the *E. coli* RelA in *M. xanthus* leads to the accumulation of (p)ppGpp and partial activation of the regulatory cascade for the developmental cycle in the presence of nutrients.

### b. Cell-cell communication signals during development

The *M. xanthus* developmental process requires cell-cell signaling. The cell-cell signals of *M. xanthus* have been categorized into five groups: A, B, C, D and E signals (55, 56, 84, 155). These groupings are based on extracellular complementation between different classes of developmental mutants and through the utilization of mutant strains containing Tn*5lacZ* transcriptional fusions in developmentally regulated genes. Mutants of each cell-cell signal class uniquely arrest development at specific stages as determined by developmental gene expression, suggesting an orderly progression from one signal to the next. These cell-cell signals will be briefly described in the following few paragraphs.

The first cell-cell signal utilized by *M. xanthus* appears to be the A signal, which is produced and sensed following the stringent response. Experimental evidence suggests that the A signal is the extracellular accumulation of six amino acids generated by extracellular proteolysis. It includes tryptophan, proline, phenylalanine, tyrosine, leucine, isoleucine and small peptides containing these amino acids (55, 84, 158). Many A signal mutants can be rescued simply by supplying a mixture of these amino acids. Several genetic loci are implicated in the sensing of starvation and in the production and of A signal. *asgA* and *asgD* encode histidine protein kinases containing a response regulator-like domain. Neither AsgA nor AsgD are predicted to posses apparent input or output domains, so it is unclear how they perceive and/or respond to stimuli. *asgB* and *asgC* encode a DNA binding and a sigma factor-like protein, respectively. *asgE* encodes a homologue of amidohydrolases. Since *asgABCD* mutants can be rescued for A signaling, they likely function in sensing starvation and in the production of A signal. The output of the system appears to be conferred by the SasS-SasR-SasN signal transduction pathway (87). This pathway was identified by isolation of suppressor mutants that restored A signal dependent developmental gene expression. The A signal pathway is proposed to be analogous to peptide-type quorum sensing systems (84).

C signal has undoubtedly been the most extensively studied cell-cell signal in *M. xanthus*. There is, however, some controversy and unresolved issues on how C signal actually functions. Much of the controversy has arisen due to the multiple forms of CsgA, encoded by the single *csgA* gene. They are called p17 and p25 according to their apparent molecular weights (84). One group proposes that C signal is the result of CsgA enzymatic activity (155). The large p25 version of CsgA is homologous to small-chain alcohol dehydrogenases (SCAD) and it is proposed that C signal is the product of CsgA catalyzed reactions. Two lines of evidence support this hypothesis. Over-expression of SocA, another *M. xanthus* SCAD-like protein, suppresses a *csgA* mutant and another suppressor of *csgA* was also identified as a distinct *M. xanthus* SCAD-like protein (103, 104). The other viewpoint is that the small p17 version of CsgA is itself the C signal (84). In support of this hypothesis, addition of purified p17 restored development to a *csgA* mutant. This activity of p17 was abolished when treated with protease or CsgA specific antibodies prior to the extracellular complementation assay. It was further proposed that p25 is cleaved by an extracellular serine protease at the cell surface to generate p17 (108). This model suggests that p25 is on the cell surface. Subsequent proteolytic processing cleaves off the N terminal region, allowing p17 to remain associated with the cell. Surface exposed p17 may then interact with the still hypothetical C signal receptor on an adjacent cell to ensure that a cell can not signal itself (84). Even though there are still unresolved issues regarding the two C signaling models, it is possible that pole to pole cell contact or proper cell alignment might be required for C signaling. This was demonstrated by Kim and Kaiser who scratched small channels in an agar surface and placed cells in these channels (95). Specifically, nonmotile mutant cells, normally incapable of expressing C signal dependent developmental genes, expressed C signal-regulated Tn*5lacZ* transcriptional fusions and produced refractile myxospores. Since neither of these events occurred when cells were arranged randomly on the agar surface and since the cells in the channels were found to be arranged or aligned end on end, it was concluded that both cell motility and cell alignment were important and required for proper C signaling.

Another cell-cell signal is E signal. *esg* mutants are characterized as containing mutations in either one of the two subunits of a branched-chain keto dehydrogenase. These mutants have slightly lower levels of iso-branched fatty acids in their membranes (55, 84, 155). *esg* mutants fail to undergo development, but can be rescued by extracellular complementation using *esg*$^+$ strains or by the addition of short-chain fatty acids such as isovalerate, methylbutyrate and isobutyrate. How *esg*$^-$ strains are rescued by *esg*$^+$ is still not completely understood, but may involve the minute amounts of lipid transferred between adjacent cell membranes (84, 129).

The B and D cell-cell signals have not been investigated very extensively (55, 84, 155). It is known that B signal mutations map to a single gene *bsgA*, which encodes an *E. coli* Lon-type protease. *dsg* mutants were determined to have missense mutations in translation initiation factor 3. The mechanisms of extracellular complementation of these two groups remain to be resolved or understood.

### c. Involvement of other signaling pathways in development

Besides the starvation and cell-cell developmental signals, there are a couple of other major classes of developmental regulators. One large class of developmental regulators is composed of NtrC-like activators. NtrC-like activators are enhancer elements that regulate transcription at $\sigma^{54}$ dependant promoters (195). They generally consist of a response regulator domain and a DNA binding domain and in most cases are controlled by two-component signal transduction systems. One of the *M. xanthus* chemotaxis systems, Che3, appears to use a NtrC-like activator to control the timing of entry into the developmental cycle (97). More recently, a global mutagenesis of all uncharacterized NtrC-like activators found that 12 of the previously 28 uncharacterized NtrC-like activators were required for fruiting body formation, aggregation or sporulation (44). These findings suggested that NtrC-like activators play important roles in *M. xanthus* development. Another major class of developmental regulators are those implicated in *M. xanthus* motility. The majority of developmental mutants, besides those of the A-E signaling pathways, have defects in either the A or S motility system (71, 112). This signifies the importance of motility in the coordination of aggregation in the developmental process.

## 2. *Myxococcus xanthus* motility

The first major breakthrough in understanding the mechanisms of *M. xanthus* motility was without a doubt the two tandem publications by Hodgkin and Kaiser in 1979 (70, 71). They found that *M. xanthus* actually possessed two genetically distinct gliding motility systems: the adventurous (A) and the social (S) motility systems. The first paper described the identification of mutants defective in A motility, and the second one focused on mutants defective in S motility. A motility is generally characterized as the movement of single cells while S motility refers to the movement of groups or rafts of cells. Using genetic crosses between various mutants, they were able to determine that two genetically distinct systems governed motility in *M. xanthus*. Specifically, they found that only combinations of both an A and S motility mutations would result in a non-motile strain. They identified two classes of A motility mutants, *agl* (A gliding) and *cgl* (contact gliding). The major difference between these two classes of mutants was that *cgl*, but not *agl*, could regain motility by extracellular complementation or stimulation.

Likewise, the S motility mutants were divided into two classes, *sgl* (S gliding) and *tgl* (transient gliding). Again, the difference between these mutants was that *tgl*, but not *sgl*, could be stimulated extracellularly to restore motility. The last class of motility mutants discovered were called *mgl* (mutual gliding) because they were defective in both A and S motility. By utilizing stimulation assays and genetic crosses, it was determined that at least 9 genes or loci controlled S motility and at least 21 controlled A motility. All *mgl* mutations mapped to one locus. These early experiments provided the framework for later investigations of *M. xanthus* motility.

### a. Adventurous motility

Even though many genes required for A motility have been identified, the mechanism of A motility remains obscure. Besides the early *cgl* and *agl* mutants, more recent work has identified over 30 A motility genes (203). Probably the most notable are the ones that encode homologues of the Tol and Ton-like proteins, which are parts of transport systems involved in biopolymer transport and outer-membrane stability (33, 107). The involvement of these transporter homologues is consistent with the recently proposed slime extrusion model for *M. xanthus* A motility (190). To a large extent, the slime extrusion idea came from previous studies on the gliding motility of certain cyanobacteria (see earlier discussion on gliding motility) (73, 190). Wolgemuth *et al.* showed that *M. xanthus* cells leave “slime trails” that are only apparent in A motile cells (190). As in cyanobacteria, electron microscopy revealed hundreds of nozzle-like structures at *M. xanthus* cell poles. In addition, electron and fluorescent microscopy showed the presence of ribbon-like material that appeared to be extruded from the cell poles. A mathematical model was presented to suggest that as few as 50 of the nozzle-like structures functioning simultaneously could generate the thrust required for gliding motility. It should be cautioned, however, that the nozzle-like structures were also present in the few A motility mutants that were examined (190). There are still many unresolved issues with slime secretion as the mechanism for *M. xanthus* A motility.

### b. Social motility

The mechanism of S motility is better understood in comparison to A motility. It is known that *M. xanthus* S motility requires cell proximity, Tfp, and exopolysaccharides (82). In the current model, Tfp are proposed to extend from one pole of a cell, attach to its substrate, most likely exopolysaccharides on neighboring cells, and retract resulting in cell movement (82, 105).

The requirement of Tfp for S motility was demonstrated primarily through genetic studies. In 1979, Dale Kaiser observed a correlation between the presence of Tfp and S motility (85). He found that the majority of S motility mutants, including *tgl*, lacked Tfp using electron microscopy. Importantly, he observed that *tgl* mutants, which can be stimulated extracellularly to become S-motile, produced Tfp after stimulation. Later studies indicated that 14 of the 17 genes at the *pil* locus are required for S motility (180). With the exception of *pilT*, these 14 *pil* genes are required for the assembly of Tfp. *pilT* mutants, which are $S^-$, are hyperpiliated and likely produce paralyzed or non retractable Tfp (194). The three *pil* genes not required for S motility or Tfp assembly likely encode proteins with regulatory function (180). *tgl*, a gene essential for the assembly of Tfp, is not located at the *pil* locus (71, 179, 182). As previously discussed, *tgl* mutants are unique in that they can be transiently stimulated to produce Tfp and become S motile. This stimulation can be accomplished by any strain that is genetically *tgl*$^+$ and is the result of phenotypic not genotypic complementation. Tgl, a protein with tetratricopeptide (TRP) motifs, is believed to encode an outer membrane lipoprotein that helps stabilize the PilQ pore complex, allowing Tfp to transverse the outer membrane (128). It was shown recently, that Tgl proteins can be transferred between neighboring cells providing the explanation for the observed stimulation of *tgl* mutants (129).

Exopolysaccharides (EPS) were first implicated in both S motility and development in the mid 1980s (154, 156), and their role in S motility has become more clear in recent years. Earlier work on *dsp* (dispersed) mutants, which are defective in S motility, indicated that they lacked the cellular cohesion displayed by wild-type *M. xanthus* (154). It was discovered that *dsp* mutants are defective in the production of what was known as fibrils at that time. On the other hand, these mutants still produced Tfp and were later found to be hyperpiliated (167, 202). The S motility defects of these mutants were therefore attributed to the lack of fibril production (154).

The fibrils or extracellular matrix were named so because of their rope-like appearance when viewed by scanning electron microscopy. Fibrils were described as being composed of roughly equal amounts of protein and polysaccharide based on analysis of crudely purified preparations (13). The polysaccharide portion, containing monosaccharides and amine sugars, was suggested to form the backbone which is decorated with proteins. The fibrillar appearance is likely the artifact of sample preparation. These materials likely form a dense matrix or cell covering as shown by transmission electron microscopy (94, 120). The polysaccharide in the matrix or surface covering is now known as exopolysaccharides (EPS).

The role of EPS in S motility is now better understood. Li *et al*. showed that crudely purified EPS, with or without protease treament, could reduce the amount of surface Tfp on hyperpiliated *dsp* (EPS$^-$) cells in suspension (105). It was proposed that the hyperpiliation of these cells was caused by the lack of Tfp retraction due to the lack of EPS production. In addition, they showed that the amine sugars in EPS were likely the target for Tfp attachment because chitin, a natural polymer of amine sugars, was able to precipitate isolated Tfp filaments. These findings led them to conclude that the polysaccharides or EPS may provide the anchor and trigger for Tfp retraction in *M. xanthus* S motility.

In addition to Tfp and exopolysaccharides, LPS O-antigen has been implicated in S motility (34, 200). It was demonstrated that LPS O-antigen mutants where defective in S motility by genetic crosses of known A and S motility mutations and examination of colony edges (34). Using additional genetic crosses and phenotypic assays, certain LPS O-antigen mutants were later determined to be partially defective in A motility as well (200). The exact role of LPS in *M. xanthus* motility clearly requires additional clarification.

### c. Regulation of *M. xanthus* motility

The best studied system that regulates *M. xanthus* motility is the Frz chemotaxis signal transduction pathway. The Frz genes were discovered because *frz* mutants form twisted and tangled “frizzy” filaments on developmental medium (185, 186, 205). The “frizzy” phenotype was later attributed to the involvement of the Frz system in controlling the reversal of both A and S motile cells (26, 185, 186). The proteins encoded by the *frz* genes were found to be homologous to bacterial chemotaxis proteins (118, 185, 186). Null *frz* mutants seldom reverse their direction of gliding. On average, wild-type cells reverse their direction of movement about every 7 minutes whereas *frz* mutants do so about every hour (26). Recent studies on FrzS have shed some light on how the Frz system might regulate motility. FrzS contains an N-terminal domain homologous to response regulators and a C-terminal domain predicted to possess an extended coiled-coil structure (184). FrzS was observed to oscillate between the cell poles at a rate of about 5 min/oscillation in wild type, which is similar to the reversal interval (123). This oscillation was dependent on the Frz chemotaxis system and correlated with cell reversal. FrzS oscillation was rarely observed in *frzE* mutants which rarely reverse their gliding direction. In contrast, *frzCD*$^{c}$ (constitutive signaling) hyper-reversal mutants reverse direction very frequently and FrzS oscillation always correlated with these reversals. Very importantly, it was observed that these oscillations resulted in FrzS localization. This localization also correlated with the piliated end of the cell, suggesting that FrzS may be responsible for directing the S motility engine to the proper cell end.

Another system with regulatory function in *M. xanthus* motility is related to MglA. MglA, a small Ras-like GTPase, appears to be a regulator of both A and S motility (67). *mglA* originally was identified by a non-motile *M. xanthus* mutant (70, 71). However, subsequent analysis revealed that *mglA* mutant cells are motile. The reason *mglA* mutants appear non-motile is because they reverse the direction of cell movement very frequently, roughly 3 reversals per minute. Such frequent reversals result in no net cell movement (165). The precise function of MglA in the regulation of motility is still under investigation. AglZ, a protein required for A motility, was recently found to interact with MglA (197). Interestingly, AglZ is structurally similar to FrzS in that it contains both a response regulator-like domain and a domain predicted to have an extended coiled-coil structure. Although no oscillations of AglZ have been reported, it is intriguing to imagine that similar regulation schemes might exist for both the A and S motility systems.

The Dif and the Che4 chemotaxis-like systems also regulate the motility behavior of *M. xanthus*. The Dif chemotaxis-like pathway is implicated in controlling cell reversals upon exposure to certain lipid chemoattractants (93) (see detailed discussion on Dif in later section). This regulation likely occurs at the level of A motility as dictated by the experimental setup, which observed the movement of well-isolated *M. xanthus* cells only. The Che4 chemotaxis pathway has been implicated specifically in the regulation of Tfp driven motility or S motility (177). An inverse correlation was observed between reversal rates and velocities of S motile cells. This inverse correlation means that cells exhibiting higher velocities tend to reverse direction less frequently. Phenotypic analyses of *che4* mutants indicated that they had lost the correlation between cell reversal and velocity. The Che4 pathway was hypothesized to regulate the reversal rate of S motile cells as a function of their velocity.

It is becoming obvious that the regulation of *M. xanthus* motility involves a complex network of signaling pathways. There must be cross-talk between these multiple regulatory systems. It can be noted that no specific downstream target has been identified for the response regulator (output) of any of these regulatory systems. It is also a given that the engines for A and S motility must be coordinated so that they do not work against each other. Much remains to be done to understand how A and S motility are globally and cooperatively regulated.

### 3. Review of the *Myxococcus xanthus dif* locus

The Dif chemotaxis-like pathway appears to exhibit an amazing level of complexity including apparent multiple inputs and outputs. There are possibly three distinct sensory components mediating input signals into the pathway: one for EPS production, one for dilauroyl phosphatidylethanolamine (PE), and a third for dioleoyl PE. There are at least two distinct outputs, the regulation of EPS production and the regulation of cell reversal. The identification of the Dif pathway and the current understandings of how the Dif pathway functions in the regulation of these processes will be discussed in more detail in the following subsections.

### a. Identification and characterization of the *dif* locus

The *M. xanthus dif* locus was identified by a mutant defective in fruiting body formation (199). The original transposon insertion was found in a gene now known as *difA* that encodes a homologue of bacterial MCPs (Fig. 1-7). Four of the remaining five *dif* genes also encode homologues of bacterial chemotaxis proteins. DifC, DifD, DifE, and DifG are homologous to CheW, CheY, CheA and CheC, respectively (15, 25, 199). DifB has no homology to known chemotaxis proteins.

The phenotype of the original *difA* insertion mutant included defects in fruiting body formation and S motility (199). In-frame deletions of *difA* as well as *difC* and *difE*

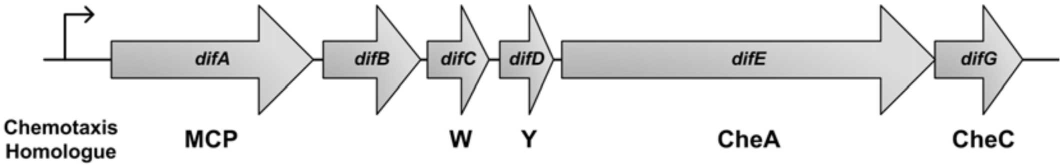
difA
difB
difC
difD
difE
difG
Chemotaxis Homologue
MCP
W
Y
CheA
CheC

**Figure 1-7.** The *M. xanthus dif* locus.
Shown is the positioning and orientation of *dif* genes and their homologies to chemotaxis-like proteins. W and Y stand for CheW and CheY respectively. Figure based on Black and Yang (25).

resulted in similar defects in development and S motility as did the *difA* insertion (15, 25, 199). Tfp and EPS, both of which are required for *M. xanthus* S motility, were examined in these mutants. The results showed that these mutants lacked EPS and were hyperpiliated (15, 202). In addition, *difA* and *difE* mutants could be rescued for fruiting body formation by the addition of crudely purified EPS from wild type (202). These findings show that the Dif pathway is required for the production of EPS and provides an explanation for the lack of S motility in these mutants.

### b. Interactions among Dif proteins

The homologies of Dif proteins with bacterial chemotaxis proteins and the similar phenotypes of *difA*, *difC*, and *difE* mutants led to the hypothesis that the Dif proteins define a chemotaxis-like signaling pathway and DifA, DifC and DifE potentially form a signaling complex. Later work using the yeast-two-hybrid (Y2H) system provided evidence for this hypothesis (201). Yang and Li found that Dif proteins interacted in a similar fashion as other known chemotaxis proteins. Specifically, DifC (CheW-like) was found to interact with DifA (MCP-like) and DifE (CheA-like). DifD (CheY-like) was found to interact with DifE. Interactions between DifA, DifC, and DifE in a modified Y2H experiment suggested that they likely formed a ternary complex. In addition, interactions were found between DifD and DifG (CheC-like), which is consistent with the finding in *B. subtilis* that CheC can function as a phosphatase of CheY-phosphate (169). Unlike the interactions shown in *B. subtilis*, no interactions were found between DifG and DifA or DifE using the Y2H system (96, 201).

### c. Signaling by DifA, the chemoreceptor homologue

The recent construction and partial characterization of a chimeric NarX-DifA receptor has provided valuable information into the regulation of the Dif pathway (196). The chimeric NarX-DifA protein, NafA, was constructed by creating a fusion between the N-terminal nitrate-sensing module of NarX with the C-terminal cytoplasmic signaling domain of DifA. It was demonstrated that the expression of *nafA* in a *difA* deletion strain restored fruiting body formation, S motility, and EPS production in a nitrate dependent manner. Interestingly, there appeared to be distinct levels of EPS required for fruiting body formation and S motility, suggesting delicate regulation of the Dif pathway during these two processes. It was unknown how DifA, without a prominent periplasmic sensory domain, could perceive and transmit signals. Nevertheless, the experiments with NafA indicated the importance of transmembrane signaling and the DifA N-terminus in the regulation of EPS production (196). More recent work also revealed that the N-terminus of DifA was more extended than previously thought (Xu and Yang, unpublished). Although this extension maintained the predicted small periplasmic region, it revealed an N-terminal cytoplasmic region that could potentially be involved in signal perception. NafA will continue to provide valuable information in the understanding of many aspects of the regulation and function of the Dif pathway.

### d. The Dif pathway and lipid chemotaxis

In addition to regulating the production of EPS, the Dif pathway has also been implicated in chemotaxis responses to certain phosphatidylethanolamine (PE) species. Kearns *et al*. reported that *M. xanthus* exhibited excitation and adaptation responses to two PE species: dilauroyl (di C12:0) PE and dioleoyl (di C18:1 ω9c) PE (92). More specifically, these two PE species resulted in the suppression of reversal rates of A motile cells. It was later found that *difE* mutants were defective in excitation to both dilauroyl and dioleoyl PE whereas *difA* was required only for excitation of dilauroyl PE (91). This suggested that there could be a separate MCP mediating responses to dioleoyl PE. Strengthening these findings, a more recent study determined that only *difD* and *difE* mutants, but not *difA* and *difC*, were defective in response to this PE species (30). These results led the authors to propose a branch point in the pathway upstream of DifE (CheA-like), which would likely require an additional MCP and CheW to sense and transduce signals to DifE and DifD (CheY-like).

Recent studies have begun to shed some light on the perception of dilauroyl PE. First, *fibA*, which encodes a protein associated with EPS, was shown to be essential for responses to dilauroyl PE but not dioleoyl PE (90). FibA is homologous to M4 zinc metalloproteases and western blot analysis indicated extensive self-proteolytic processing of FibA. Unlike the *dif* mutants, *fibA* mutants appear normal for S motility, fruiting body formation, agglutination, and synthesis of EPS. These findings led to the idea that FibA or a proteolytic product of FibA may be mediating input signals for dilauroyl PE taxis responses through the Dif pathway. The role of the Dif pathway, however, was compounded by the apparent requirement of EPS for responses to dilauroyl PE (91). Since *difA* and *difE* mutants are required for EPS production, they fail to localize FibA to the EPS (202). So it was ambiguous whether the lack of EPS (FibA) or the lack of a functional Dif pathway caused the defects of *dif* mutants in dilauroyl PE responses. For a long time, the only evidence that the Dif pathway was specifically involved in PE taxis was that the addition of purified EPS to either *difA* or *difE* mutants did not restore excitation to PE.

The most compelling data linking dilauroyl PE taxis directly to the Dif pathway was presented in a recent study using additional *dif* mutants and a NarX-DifA (NafA) chimera (30). It was shown that *difA*, *difC* and *difE* mutants were all defective in excitation to dilauroyl PE as expected from previous studies. The important finding was that *difD* (CheY-like) mutants, which produce EPS, are defective in excitation to dilauroyl PE. This showed that a component of the Dif pathway predicted to function downstream of DifE (CheA-like) was defective in PE taxis independently of EPS production. It was also determined that *difB* and *difG* mutants, both of which produce EPS, are defective in adaptation to dilauroyl PE. These observations further suggested that the Dif pathway is directly involved in responses to PE. Additional proof came from an experiment using the hybrid NarX-DifA fusion protein, NafA (196). *difA* mutant cells expressing NafA produce EPS in a nitrate dependent manner. Bonner *et al*. demonstrated that *difA* cells containing NafA respond to dilauroyl PE if they produce EPS (30). Because of the lack of the DifA N terminal transmembrane domain in NafA, it was concluded that only the cytoplasmic domain of DifA was important and thus transmembrane signaling was not required in the response to dilauroyl PE in *M. xanthus*.

### e. Research questions

There were many remaining questions as to how the Dif pathway regulates EPS production. Roles had been established for all the Dif proteins with regard to PE taxis. However, the functions of DifB, DifD and DifG in the regulation of EPS production were unknown (Fig. 1-8). Since DifD (CheY-like) interacted with DifE (CheA-like) it was expected to function downstream of the DifE in the regulation of EPS production without experimental support. The NafA experiments determined that the N terminus and transmembrane signaling of DifA were required for EPS production, but it was a mystery what the input signal for DifA was in the regulation of EPS production. Prior to this study, only the Dif proteins and two DnaK-like homologues had been implicated in EPS production. Were there other components required for EPS production? This study attempted to address a few of these issues. Specifically, it focused on understanding the function of the uncharacterized *dif* genes, determining the nature of input signals for the Dif pathway and identifying additional regulators or components involved in EPS production.

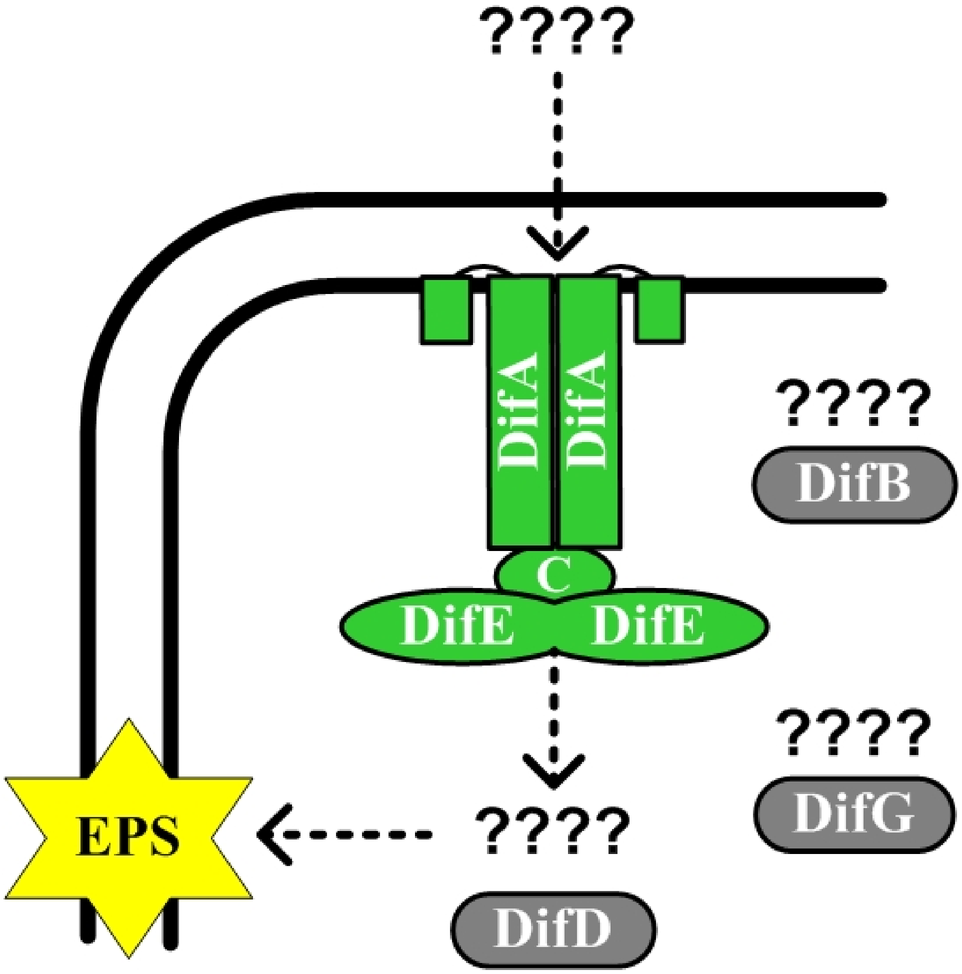
????
DifA
DifA
????
DifB
C
DifE
DifE
????
DifG
EPS
????
DifD

**Figure 1-8.** A model of the regulation of EPS production by the Dif pathway.
This is a model illustrating what was known about the regulation of EPS production by the Dif pathway prior to this study.

# CHAPTER 2

## *Myxococcus xanthus* Chemotaxis Homologs DifD and DifG Negatively Regulate Fibril Polysaccharide Production

Black, W. P. and Z. Yang. **2004**. *Myxococcus xanthus* Chemotaxis Homologs DifD and DifG Negarively Regulate Fibril Polysaccharide Production. J. Bacteriol. 186: 1001-8.

## ABSTRACT

The extracellular matrix fibrils of *Myxococcus xanthus* are essential for the social lifestyle of this unusual bacterium. These fibrils form networks linking or encasing cells and are tightly correlated with cellular cohesion, development, and social (S) gliding motility. Previous studies identified a set of bacterial chemotaxis homologs encoded by the *dif* locus. It was determined that *difA*, *difC*, and *difE*, encoding respective homologs of a methyl-accepting chemotaxis protein, CheW, and CheA, are required for fibril production and therefore S motility and development. Here we report the studies of three additional genes residing at the *dif* locus, *difB*, *difD*, and *difG*. *difD* and *difG* encode homologs of chemotaxis proteins CheY and CheC, respectively. *difB* encodes a positively charged protein with limited homology at its N terminus to conserved bacterial proteins with unknown functions. Unlike the previously characterized *dif* genes, none of these three newly studied *dif* genes are essential for fibril production, S motility, or development. The *difB* mutant showed no obvious defects in any of the processes examined. In contrast, the *difD* and the *difG* mutants were observed to overproduce fibril polysaccharides in comparison with production by the wild type. The observation that DifD and DifG negatively regulate fibril polysaccharide production strengthens our hypothesis that the *M. xanthus dif* genes define a chemotaxis-like signal transduction pathway which regulates fibril biogenesis. To our knowledge, this is the first report of functional studies of a CheC homolog in proteobacteria. In addition, during this study, we slightly modified previously developed assays to easily quantify fibril polysaccharide production in *M. xanthus*.

## INTRODUCTION

*Myxococcus xanthus* is a gram-negative bacterium with a lifestyle that is unusual for a prokaryote. Like other bacteria, *M. xanthus* cells grow and divide as vegetative cells when nutrients are abundant. During vegetative growth, cells utilize their gliding motility to move over surfaces in search of more favorable or less adverse environments (151, 186). The gliding movement of *M. xanthus* cells often occurs in large cell groups in a coordinated manner (67, 180). Since *M. xanthus* preys on other organisms, translocation in large groups is advantageous because more antimicrobial compounds and hydrolytic enzymes can be released collectively, allowing more effective killing and feeding (52). In addition to the vegetative cell cycle, *M. xanthus* cells can undergo a developmental cycle upon nutrient limitation (53). During the developmental cycle, hundreds of thousands of preexisting cells coordinate their movement to allow the orderly and timely aggregation necessary for fruiting body formation. *M. xanthus* cells eventually differentiate into environmentally resistant myxospores within mature fruiting bodies. As a unicellular organism, *M. xanthus* provides one of the simplest systems for studying social behaviors and cell-cell interactions during both its vegetative and developmental cycles.

The gliding motility of *M. xanthus* is controlled by two distinct motility systems, the adventurous (A) and the social (S) gliding motility systems (70, 71). Genetic analysis indicates that these two systems function independently in the sense that cells with a mutation in one system are still motile due to the activities of the remaining system; however, cells with mutations in both systems are rendered nonmotile. S motility is manifested by the movement of cell groups or rafts of cells, whereas A motility enables the movement of well-isolated cells. The gliding motility of *M. xanthus* is essential for both the wolf-pack-like feeding during vegetative growth and the organization of aggregation during the developmental cycle (52, 86). Experimental evidence reveals a tight correlation between S motility and fruiting body formation, as most mutants of the S motility system are defective in development to various extents (71, 112).

Due to its importance for the lifestyle of *M. xanthus*, S motility has been the focus of extensive scientific research. It has become evident that two cell surface components, the polarly localized type IV pili (85, 192) and the peritrichous extracellular matrix fibrils (9, 15, 154, 188, 202), are critical for functional S motility. Recent advances suggest that *M. xanthus* S motility resembles twitching motility mechanistically in that both forms of motility require the presence of type IV pili and close cell proximity (114, 140). It is believed that both twitching and S motilities are powered by the retraction of type IV pili (81, 122, 161, 167). The peritrichous extracellular matrix fibrils, the other structure crucial for *M. xanthus* S motility, constitute the extracellular matrix that connects adjacent cells (9, 14). The fibrils are composed of polysaccharides with roughly equivalent amounts of associated proteins; the polysaccharides appear to form the backbone of the structure (13). Although the role of fibrils in S motility is not fully understood, a recent study proposed that the fibril polysaccharide may provide the anchor for retracting pili (105). Lipopolysaccharides have also been implicated in *M. xanthus* gliding motility and development (34, 200), but the function of lipopolysaccharides in these processes remains to be elucidated.

In *M. xanthus*, both pili and fibrils appear to be controlled by two separate chemotaxis-like pathways. Strains with mutations in *frz* ("frizzy") chemotaxis gene have defects in cell reversal rates (26), and it has been suggested that the Frz pathway may partially control the type IV-pilus-mediated S motility (151, 167). On the other hand, the production of fibrils is controlled, at least in part, by the *dif* (defective in fruiting and fibrils) chemotaxis pathway (15, 199, 202). It was previously shown that three genes at the *dif* locus, *difA*, *difC*, and *difE*, are required for S motility, fruiting body formation, and fibril biogenesis (15, 199, 202). *difA* encodes a methyl-accepting chemoreceptor protein (MCP), *difC* encodes a CheW homolog, and *difE* encodes a CheA homolog (15, 199). Based on these results, the *dif* genes were hypothesized to define a chemotaxis-like signal transduction pathway that regulates the biogenesis of fibrils. The defects of the *dif* mutants in development and S motility may be attributed to their defects in fibril production.

Here we report studies of three additional genes at the *M. xanthus dif* locus, *difB*, *difD*, and *difG*. Sequence analysis indicates that DifD is homologous to CheY and DifG is homologous to CheC, a chemotaxis protein present in *Bacillus subtilis* and some other bacteria but absent in the enteric bacteria (96). DifB shows homology to a conserved family of hypothetical bacterial proteins with unknown function. We constructed and studied strains with in-frame deletions in each of these three genes. Unlike *difA*, *difC*, and *difE*, the three remaining genes at the *dif* locus, *difB*, *difD*, and *difG*, are not absolutely required for *M. xanthus* S motility, fruiting body formation, or fibril biogenesis. Surprisingly, we discovered that both *difD* and *difG* mutants overproduce fibril polysaccharides in comparison with production by the wild type. Therefore, rather than being positive regulators like DifA, DifC, and DifE, DifD and DifG negatively regulate the production of fibril polysaccharides in *M. xanthus*. In addition, during the course of this study, we slightly modified previously described dye binding assays to easily quantify the production of fibril polysaccharides in *M. xanthus*.

## MATERIALS AND METHODS

**Bacterial strains and growth conditions.** The *M. xanthus* strains and plasmid constructs used in this study are listed in Table 2-1. *M. xanthus* was grown at 32°C on Casitone-yeast extract (CYE) agar plates or in CYE liquid medium (45). Clone-fruiting (CF) agar plates were used as the development-inducing medium for *M. xanthus* (63). XL1-Blue (Stratagene), the *Escherichia coli* strain used for plasmid construction, was grown and maintained at 37°C on Luria-Bertani agar plates or in Luria-Bertani liquid medium (124). Unless noted otherwise, agar plates contained 1.5% agar. Kanamycin was added to media at 100 µg/ml for selection purposes when appropriate.

**Construction of *dif* locus mutants.** Mutants with in-frame deletions at the *dif* locus were constructed by a two-step homologous recombination gene replacement protocol by using a modified positive-negative kanamycin/galactose (KG) cassette selection method (176). DNA fragments with an internal in-frame deletion were generated by a two-step, overlap PCR procedure (146) by using *PfuTurbo* DNA polymerase (Stratagene). The fragments with appropriate deletions were blunt-end ligated into the *Sma*I site of pBJ113 (79) to create plasmids pWB117 through pWB120 (Table 2-1). The deletion plasmid constructs were electroporated (89) into DK1622, a wild-type *M. xanthus* strain (85). Kanamycin-resistant transformants were subsequently plated on CYE agar plates supplemented with 1% galactose. Deletion mutants were identified by a galactose-resistant and kanamycin-sensitive phenotype and by PCR and Southern

**Table 2-1.** *M. xanthus* strains and plasmids.

| *M. xanthus* strain or plasmid | Relevant genotype or description | Source or reference |
|---|---|---|
| **Strains** | | |
| DK1622 | Wild type | (85) |
| YZ602 | Δ*difB* | This study |
| YZ603 | Δ*difE* | This study |
| YZ604 | Δ*difG* | This study |
| YZ613 | Δ*difD* | This study |
| **Plasmids** | | |
| pBJ113 | Gene replacement vector with KG cassette; Kan$^r$ | (79) |
| pWB117 | *difB* in-frame deletion in pBJ113 | This study |
| pWB118 | *difE* in-frame deletion in pBJ113 | This study |
| pWB119 | *difG* in-frame deletion in pBJ113 | This study |
| pWB120 | *difD* in-frame deletion in pBJ113 | This study |

analyses of chromosomal DNA (146, 176). Double mutants were constructed by Mx4-mediated generalized transduction (130).

**Motility assays.** Motility on hard-agar plates was examined by spotting 5 µl of a cell suspension of approximately 5 x $10^9$ cells/ml onto the center of a standard CYE agar plate. After 2 days of incubation at 32°C, overall colony morphology, colony expansion, and colony edge morphology were examined and documented macroscopically and microscopically. Motility on low-percentage- or soft-agar surfaces was examined as previously described (152). Briefly, 5 µl of cells at the concentration described above was spotted onto the center of a CYE plate containing 0.4% agar and incubated at 32°C for 5 days before documentation.

**Assessment of fruiting body development.** To examine fruiting body formation, exponentially growing cells from overnight cultures were harvested and resuspended in MOPS (morpholinepropanesulfonic acid) buffer (10 mM MOPS [pH 7.6], 2 mM $MgSO_4$) at approximately 5 x $10^9$ cells/ml. Five microliters of this cell suspension was spotted in triplicate onto the surface of CF agar plates. Development was examined and documented after 5 days of incubation at 32°C.

**Analysis of cellular cohesion.** The agglutination assay described by Wu et al. (194) was used to determine the cellular cohesion of various *M. xanthus* strains. Exponentially growing overnight cultures of *M. xanthus* were harvested and resuspended to approximately 2.5 x $10^8$ cells/ml in CYE medium, and the optical density (OD) at 600 nm was recorded every 10 min for a total of 2 h. Agglutination is expressed as relative absorbance for each time point, which was calculated by dividing the OD at each time point by the initial OD for each strain.

**Examination of fibril production.** To detect fibril-specific protein antigens, whole-cell lysates were prepared from 5 x $10^7$ cells. Cell lysates were then separated by sodium dodecyl sulfate-10% polyacrylamide gel electrophoresis and analyzed by immunoblot analysis by using standard protocols (146). Monoclonal antibody (MAb) 2105, a MAb against the fibril protein FibA, was used as the primary antibody (61, 90).

To examine the polysaccharide portion of the fibrils, two different assays were performed. The first was a plate assay to determine the binding of the fluorescent dye calcofluor white, as described previously (48, 137). Briefly, cells from overnight cultures were pelleted and resuspended in MOPS buffer at approximately 5 x $10^9$ cells/ml, and 5-µl volumes of these suspensions were spotted on the surface of CYE agar plates impregnated with 50 µg of calcofluor white/ml. The plates were incubated at 32°C for 6 days before they were examined and photographed under the illumination of a handheld long-wavelength (365-nm) UV light source.

The second assay was a liquid colorimetric assay to measure the binding of Congo red and trypan blue. The liquid assay, adapted from that of Arnold and Shimkets (10), was used to quantitatively determine the relative level of fibril polysaccharide production. All strains tested were harvested at near-identical culture densities (approximately 3.5 x $10^8$ cells/ml), washed, and resuspended to approximately 2.8 x $10^8$ cells/ml in MOPS buffer. Stock solutions of the dyes were prepared in deionized distilled water at 150 µg/ml for Congo red and 100 µg/ml for trypan blue. A total of 900 µl of the cell suspension was mixed with 100 µl of a dye stock solution to give final concentrations of 2.5 x $10^8$ cells/ml and either 15 µg of Congo red/ml or 10 µg of trypan blue/ml. Control samples containing each dye in MOPS buffer only were included, and triplicate assays were performed for all samples. All samples were vortexed briefly and incubated undisturbed in the dark at room temperature for 30 min. The cell suspensions were then pelleted at 16,000 x *g* in a benchtop centrifuge for 5 min, and the absorbances of the supernatants were measured at 490 and 585 nm for Congo red and trypan blue, respectively. The reported percentage of dye bound by each sample was calculated from the quotient obtained by dividing the absorbance of each sample by the absorbance of the control.

**Nucleotide sequence accession numbers.** The nucleotide sequences of the genes studied here have been deposited in GenBank under the accession numbers AF076485 and AY327119.

## RESULTS

**Sequence analysis of *difB*, *difD*, and *difG*.** It was previously reported that five open reading frames existed at the *dif* locus (199). We recognized later that an additional gene, *difG*, lies immediately downstream of *difE* (Fig. 2-1). The last two nucleotides of the predicted start codon for *difG*, a GTG rather than an ATG, overlap with the first two nucleotides of the stop codon of *difE*, a TGA. *difG* is predicted to encode a protein of 200 amino acids with 27% identity to the CheC chemotaxis protein of *B. subtilis* (Fig. 2-2A). The homology is extended over the entire length of both proteins, and a conserved-domain search identified DifG as a CheC homolog with high confidence (5). DifD shows a very high degree of homology to several CheY proteins (199); the highest is 62% identity to CheY of *B. subtilis* (Fig. 2-2B). As previously reported, *difA*, *difC,* and *difE* encode homologs of the chemotaxis proteins MCP, CheW, and CheA, respectively (199). DifB encodes a positively charged protein of 222 amino acids with 27 lysine (K) and 14

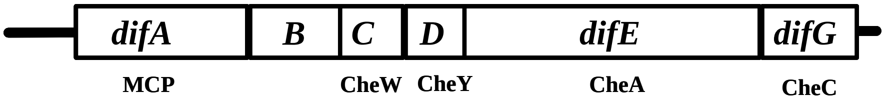
difA
B
C
D
difE
difG
MCP
CheW
CheY
CheA
CheC

**Figure 2-1.** The *M*. *xanthus dif* locus and homology.
All of the *dif* genes read from left to right. The homology of the encoded polypeptides to chemotaxis proteins is indicated below the relevant genes.

**A:**

```
Mx_DifG MS-QPLHSDAQLDALREVANIGCGHAANALSRLMGGRKVDLSIPRVLLTGPSDAAELLGG 59
Bs_CheC MSIFNGIKEEQMDILREVGNIGAGHSASAMAQLL-NRKIDMEVPFAKLLSFDELVDFFGG 59

Mx_DifG A-APVVSGWLGIQGGLRGALLLVLP--QQDGAALEALLLEGQP--AIHQTERD-SVMAET 113
Bs_CheC ADVPVASIFLRMEGDLTGSMFFIMPFFQAEQFIRELIGNPDFDIEDLGEDHMSSSALHEL 119

Mx_DifG ANIVASACLSAMGRLTGWKLVPTVPTVRRGRARDVVSDAVGQVEGDASSVVVLEAR-FLA 172
Bs_CheC GNILAGSYLTALADLTKLQLYPSVPEVSLDMFGAVISEGLMELSQVGEHAIVVDTSIFDQ 179

Mx_DifG TAAPPVGGQLLLVLARDSIRDLLARLG--V 200
Bs_CheC SHQQELKAHMFMLPDYDSFEKLFVALGASL 209
```

**B:**

```
Mx_DifD MAKRVLVVDDAIFMRNMIKDIFASGGFEVVGEAANGLEAVEKYKELKPDLTTMDIVMPFK 60
Bs_CheY MAHRILIVDDAAFMRMMIKDILVKNGFEVVAEAENGAQAVEKYKEHSPDLVTMDITMPEM 60

Mx_DifD SGIEATREIIKADSSAVVIMCSALGQESLVMEAIEAGASDFIVKPFRAEDVLAVVKKVL 119
Bs_CheY DGITALKEIKQIDAQARIIMCSAMGQQSMVIDAIQAGAKDFIVKPFQADRVLEAINKTL 119
```

**Figure 2-2.** Homology of DifG and DifD to CheC and CheY.
Homology of *M. xanthus* DifG (Mx_DifG) to *Bacillus subtilis* CheC (Bs_CheC) (A) and DifD (Mx_DifD) to *B. subtilis* CheY (Bs_CheY) (B). DifG shares 27% identity with *B. subtilis* CheC. DifD shares 62% identity with *B. subtilis* CheY. Identical residues are shaded in black and the sequences shown comprise the entire proteins.

arginine (R) residues and a total of 31 net positive charges (data not shown). The N terminus of DifB shows limited similarity to a conserved but uncharacterized family of hypothetical bacterial proteins (data not shown).

**Construction of mutants with in-frame deletions in *difB*, *difD*, *difE*, and *difG*.** In previous studies, mutants with in-frame deletions in *difA* and *difC* were constructed and examined, but the *difE* mutations had been insertions only (15, 100, 199, 202). Since *difG* is immediately downstream of *difE*, it was not clear whether the defects of the *difE* insertion mutant were the result of *difE* disruption or polar effects on *difG* or other genes downstream. Similarly, a *difB* insertion mutant was reported to have a *dsp* (dispersed growth) phenotype, but the defects could be the result of a polar effect by the insertion (100). To examine the functions of *difB*, *difD*, *difE*, and *difG*, we constructed mutants with in-frame deletions of these four genes as described in Materials and Methods. In strain YZ602, amino acid residues 4 through 219 were deleted from DifB; in YZ613, amino acids 26 through 99 of DifD were deleted; YZ603 contains a deletion of amino acid residues 4 to 840 of DifE; and YZ604 contains a deletion of amino acids 4 to 199 of DifG.

**Examination of motility of the new *dif* mutants.** It was shown previously that DifA and DifC are essential for S motility (15, 199). To determine if any of the new *dif* deletion mutants were defective in S motility, these mutants were examined on both hard (1.5%)- and soft (0.4%)-agar plates as described in Materials and Methods. Microscopically, the colony edges of all mutants on hard agar, except for YZ603 (*difE*), consisted of both single cells and cell groups, suggesting that both motility systems were present (Fig. 2-3A). Among these mutants, the colony morphology of YZ602 (*difB*)

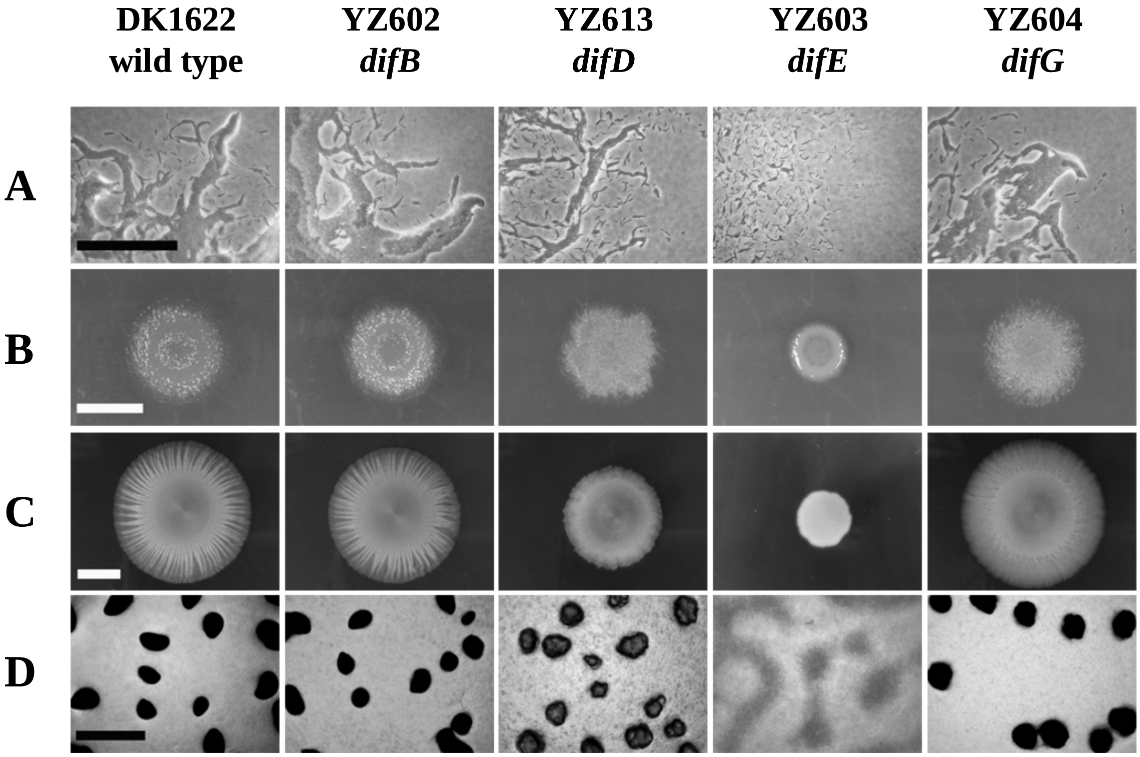
DK1622
wild type
YZ602
*difB*
YZ613
*difD*
YZ603
*difE*
YZ604
*difG*
A
B
C
D

**Figure 2-3.** Phenotypic analysis of *dif* mutants.
Colony edge morphology, colony spreading, and fruiting body formation. The strains and their genotypes are indicated above each column. (A) Colony edge morphology on hard agar; scale bar, 100 μm. (B) Colony expansion on hard (1.5%) agar; scale bar, 1 cm. (C) Colony expansion on soft (0.4%) agar; scale bar, 1 cm. (D) Development on CF media, scale bar, 500μm.

appeared the most similar to that of the wild type on hard and soft agar. The colonies of both the wild type and YZ602 displayed slightly glossy centers with rough and dry-looking edges on hard agar (Fig. 2-3B); on soft agar, they exhibited comparable colony patterns and levels of spreading (Fig. 2-3C). The colony morphologies of YZ613 (*difD*) and YZ604 (*difG*) appeared somewhat similar to each other on hard agar, since both had an extremely dry and rough appearance over the entire colony. Of these two, YZ613 (*difD*) deviated most significantly in colony morphology from that of the wild type on both surfaces: it displayed a considerable reduction in spreading on soft agar and irregular colony edges on both agar surfaces. YZ604 (*difG*) appeared similar to the wild type with respect to the degree or level of colony expansion, indicating little if any defects in motility. YZ603 (*difE*) appeared glossy over the entire colony and spread substantially less than did the wild-type strain on both hard- and soft-agar surfaces; however, it must have retained A motility due to the many single cells observed at its advancing colony edges on hard agar.

The above results suggested that the *difE* mutant lacked S motility but that the mutants of *difB*, *difD*, and *difG* possessed both A and S motilities. To confirm the motility status for each strain, secondary mutations in each motility system were introduced into each of the *dif* deletion mutants. Colony expansion of the double mutants was examined on hard-agar surfaces. Except for YZ603 (*difE*), which lost motility in a background lacking A motility, all mutants retained motility regardless of the mutant background (data not shown). These results indicated that the *difB*, *difD*, and *difG* genes are not absolutely required for either motility system. Since YZ603 (*difE*) exhibited the same defects as the previously described *difE* insertion mutant ((199, 202); see also sections below), it may therefore be considered an internal negative control for this study.

**Characterization of development.** Since the *difA* and the *difC* mutants were previously shown to be defective in fruiting body formation (15, 199), the new *dif* deletion mutants were examined for development as described in Materials and Methods. On CF media, all mutants with the exception of YZ603 (*difE*) formed obvious fruiting bodies or aggregates (Fig. 2-3D). However, obvious developmental defects were observed for YZ613 (*difD*), which formed aggregates that were translucent and irregularly shaped. The fruiting bodies of YZ604 (*difG*) appeared slightly bigger or less compact than those of the wild type. Similar results were obtained when development was examined on TPM (10 mM Tris, pH 7.6; 8mM MgSO4; 1 mM $KH_2PO4$) medium (99), and the defects observed for YZ613 (*difD*) were even more pronounced than those on CF (data not shown). In the process of this study, we noticed that both YZ613 and YZ604 consistently formed fruiting bodies and aggregates that were more resistant to dispersion by sonication, suggesting alterations in cell-cell interaction and/or the architecture of the aggregates.

**Assessment of cellular cohesion.** Cellular cohesion or agglutination is closely associated with S motility and requires the presence of both extracellular fibrils and pili (9, 15, 85, 154, 188, 192, 202). Since some of the new mutants displayed defects or abnormalities in both colony expansion and development, and because the previously characterized *dif* mutants were defective in agglutination (15, 202), the cellular cohesion of these new mutants was examined by the agglutination assay described in Materials and Methods. The agglutination assay is based on the ability of cells to clump and sediment out of suspension, which in time drastically reduces the apparent OD. As shown in Fig. 2-4, all of the new *dif* mutants, except YZ603 (*difE*), have agglutination patterns comparable to that of the wild-type strain, suggesting that the *difB*, *difD*, and *difG* mutants produce both fibrils and pili. To confirm that these strains were not defective in the production of type IV pili, the mutants were subjected to immunoblot analysis by using polyclonal antibodies against *M. xanthus* PilA (193). Both surface pili and pili from whole-cell lysates were examined as described previously (182, 193). The results confirmed that all of the *dif* mutants were capable of producing surface pili (data not shown).

**Examination of extracellular fibril production.** Previous studies demonstrated that both *difA* and *difC* mutants are defective in fibril production (15, 202). One of the fibril proteins, FibA, a metalloprotease (90), was found missing from the cell surfaces of *difA* and *difC* mutants (15, 202). Even though the *fibA* mutant could agglutinate properly, it formed less-organized fruiting bodies (90), somewhat reminiscent of the phenotypes displayed by the *difD* and *difG* mutants. Furthermore, the difficulty of disrupting or dispersing the aggregates formed by the *difD* and *difG* mutants might indicate changes in cell surface properties. The new *dif* mutants were therefore examined for fibril biogenesis. First, the presence of FibA was examined by immunoblot analysis using MAb 2105, as described in Materials and Methods. All of the new *dif* mutants, with the exception of YZ603 (*difE*), showed levels of reactivity with MAb 2105 comparable to those of the wild type (Fig. 2-5), suggesting that the *difB*, *difD*, and *difG* mutants are not defective in the production of FibA, which is associated with the extracellular fibrils.

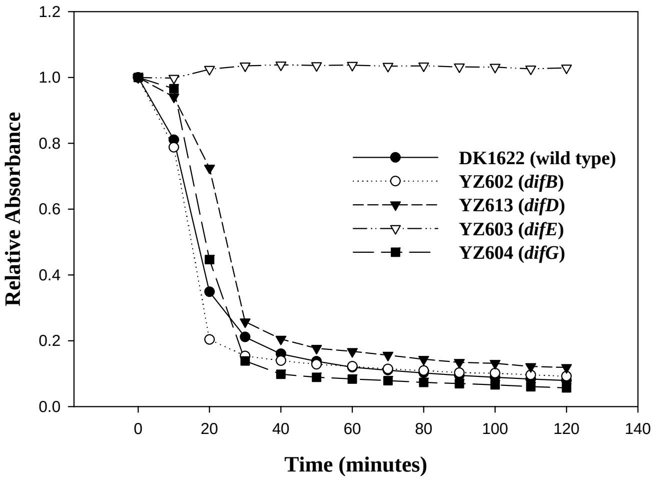

**Figure 2-4.** Agglutination assay of *dif* mutants.

Agglutination and cellular cohesion assays. Cells were grown overnight in CYE medium, and the OD at 600nm was adjusted to approximately 0.5 with CYE medium. Absorbance was measured every 10 min for 2 h. Relative absorbance was obtained by dividing the absorbance at each time point by the initial absorbance for each strain. The graph represents the data from one of many experiments with similar results.

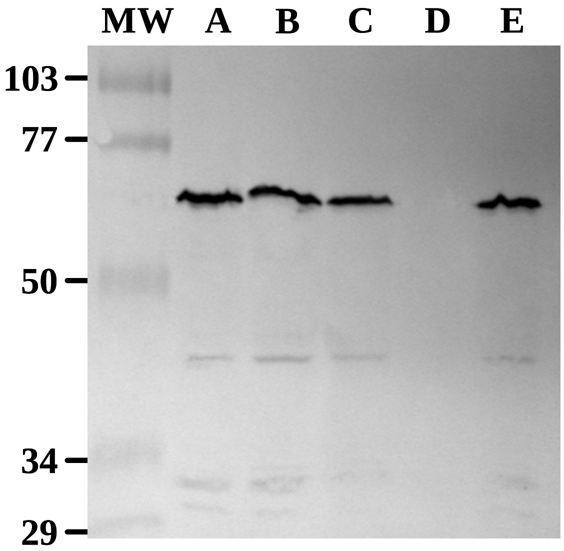

**Figure 2-5.** Immunoblot analysis of the fibril protein FibA.

Whole cell lysates were prepared from 5 × $10^8$ cells, separated by sodium dodecyl sulfate-polyacrylamide gel electrophoresis, and probed with the anti-FibA MAb 2105. Lanes: MW, molecular weight standards in thousands; A, DK1622 (wild type); B, YZ602 (*difB*); C, YZ613 (*difD*); D, YZ603 (*difE*); E, YZ604 (*difG*). The most predominate band is at a molecular weight of ca. 66,000. The multiple banding patterns are consistent with previous reports and likely reflect self-processing of FibA, an M4 metalloprotease (90).

Next, the production of fibril polysaccharide was examined by the binding of the fluorescent dye calcofluor white (Fig. 2-6). The binding of the dye, visualized by fluorescence under the illumination of UV light, demonstrates the production of fibril polysaccharides (48, 137, 202). The wild-type strain fluoresced when illuminated by UV light, whereas the *difE* deletion mutant exhibited no fluorescence, indicating undetectable levels of binding to the fluorescent dye. The *difB* mutant fluoresced at a level comparable to that of the wild type. Surprisingly, YZ613 (*difD*) and YZ604 (*difG*) showed substantially increased intensities of fluorescence, suggesting an overproduction of fibril polysaccharides.

Fibril polysaccharide production was analyzed more quantitatively by the binding of two separate dyes in colorimetric assays. Previous studies identified Congo red and trypan blue as dyes capable of binding to cells with fibrils (10, 48). By using a slightly modified version of the procedure of Arnold and Shimkets (10) as described in Materials and Methods, the relative levels of fibril polysaccharide production by each new *dif* mutant were determined by the amount of dye bound by the cells (Table 2-2). Under our assay conditions, the wild type bound 40.0 and 14.8% of Congo red and trypan blue, respectively. Consistent with the results from the calcofluor white binding assay, YZ602 (*difB*) exhibited levels of binding of Congo red and trypan blue comparable to those of the wild-type strain. In contrast, the *difD* and *difG* mutants bound significantly more of both dyes. YZ613 (*difD*) bound 87.1 and 51.5% and YZ604 (*difG*) bound 69.7 and 36.4% of Congo red and trypan blue, respectively. These results further demonstrate that both the *difD* and *difG* mutants overproduce *M. xanthus* fibril polysaccharides.

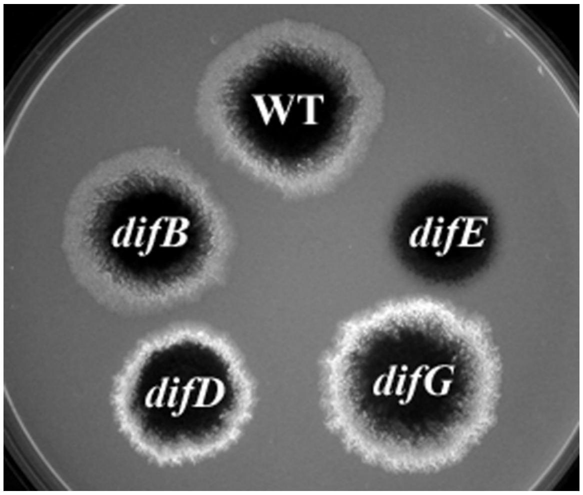

**Figure 2-6.** Binding of calcofluor white.
Five microliters of cells at approximately $5 \times 10^9$ cells/ml was spotted onto CYE plates containing 50 μg of Calcofluor white/ml. After incubation for 6 days at 32°C, the plates were photographed under the illumination of long-wave-length (365-nm) UV light. The diameter of the plate shown is 9 cm. WT, wild type.

**Table 2-2.** Binding of Congo red and Trypan blue.

| **Strain** | **Congo Red**[a] | **Trypan Blue**[a] |
|---|---|---|
| DK1622 (wild type) | 40 ± 0.8 | 14.8 ± 0.2 |
| YZ602 (*difB*) | 37.4 ± 0.4 | 15.7 ± 0.8 |
| YZ613 (*difD*) | 87.1 ± 0.2 | 51.5 ± 0.4 |
| YZ603 (*difE*) | 13.3 ± 0.6 | 1.4 ± 1.9 |
| YZ604 (*difG*) | 69.7 ± 0.6 | 36.4 ± 0.7 |

[a] All values reflect a percentage of dye bound in a suspension of $2.5 \times 10^8$ cells/ml with either 15µg/ml of Congo red or 10µg/ml of Trypan blue. Details of the experiment are described in Materials and Methods.

## DISCUSSION

We report here studies of three additional genes at the *dif* locus in *M. xanthus* (Fig. 2-1). Further sequence analysis indicated that *difG*, which is immediately downstream of *difE*, encodes a homolog of the CheC chemotaxis protein from *B. subtilis* (Fig. 2-2A). *difD*, which is immediately upstream of *difE*, encodes a CheY homolog (Fig. 2-2B). *difB*, which is further upstream of *difD* (Fig. 2-1), encodes a positively charged protein with limited homology at its N terminus to a conserved but uncharacterized family of hypothetical bacterial proteins. Due to complications of possible polar effects from insertion mutations, we constructed and analyzed in-frame deletions of *difB*, *difD*, *difE*, and *difG*. The *difE* deletion resulted in defects similar to those of a previously described *difE* insertion (199, 202), confirming the requirement of *difE* for the biogenesis of fibrils, and thus S motility and development, in *M. xanthus*. On the other hand, none of the *difB*, *difD*, or *difG* mutants exhibited phenotypes similar to those of the *difA*, *difC*, and *difE* mutants. We observed no obvious defects in the *difB* mutant under our study conditions. *difD* and *difG* mutants showed slight defects in development and altered colony morphology or colony expansion patterns. However, through qualitative and quantitative analyses, we showed that both *difD* and *difG* mutants overproduced fibril polysaccharides (Fig. 2-6 and Table 2-2). By using a colorimetric assay which measured the binding of trypan blue, the *difD* and *difG* mutants were found to produce as much as three and two times the amount of fibril polysaccharides produced by the wild type, respectively (Table 2-2). Considering that fibril-associated proteins do not appear to significantly impact the structure of fibrils and that the fibril polysaccharides may form the backbone of fibrils (13, 90, 105), the overproduction of fibril polysaccharides in *difD* and *difG* mutants may possibly represent an overproduction of fibrils. However, because no obvious FibA overproduction was detected in our experiments, the possibility remains that it is simply the fibril polysaccharide that is overproduced in these two mutants and not the fibrils themselves. Although there is a distinction between the fibril and the fibril polysaccharide, these two terms are used interchangeably in the rest of the discussion for convenience.

The finding that the *difD* deletion mutant overproduced fibril polysaccharides was unexpected and intriguing. In enteric bacteria, four major players, MCPs, CheW, CheA, and CheY, constitute the central chemotaxis pathway (32, 58). Mutations in a particular MCP gene in enteric bacteria generally cause defects in chemotaxis to the specific attractants or repellents sensed by the mutated chemoreceptor. Mutations in the genes for the other three components, CheW, CheA, and CheY, result in the same chemotaxis defects: the complete elimination of a chemotaxis response. Although it is not known what signals regulate the Dif pathway in *M. xanthus*, we had expected a *difD* mutant to have the same defects as those previously described for the *difA*, *difC*, and *difE* mutants. The present data may be explained by two working models (Fig. 2-7). The first model, depicted in Fig. 2-7A, proposes that, instead of the usual stimulatory or positive effects of CheA on CheY as seen in bacterial chemotaxis, DifE (CheA-like) inhibits the activity of DifD (CheY-like), which in turn negatively regulates fibril biogenesis. If this model is correct and since DifD is predicted to be a single-domain protein like CheY, it is reasonable to assume that there are additional components between DifD and the direct regulation of fibril polysaccharides. In the second model (Fig. 2-7B), DifX, a hypothetical interacting partner or substrate for the putative DifE kinase, is proposed. DifX could be a

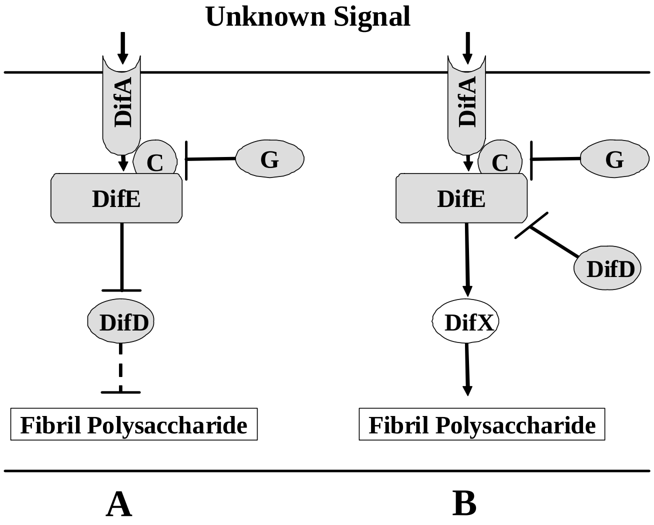
Unknown Signal
DifA
C
G
DifE
DifD
Fibril Polysaccharide
A
DifA
C
G
DifE
DifD
DifX
Fibril Polysaccharide
B

**Figure 2-7.** Two models for the Dif pathway.

Two working models for the regulation of fibril polysaccharides by the Dif pathway. Arrows indicate positive or stimulatory effects, and bars represent negative or inhibitory effects. (A), A model proposing that DifE negatively effects DifD, and that DifD in turn has an inhibitory effect on the production of fibril polysaccharides. The dashed line indicates the possible involvement of multiple components downstream of DifD. (B) A model proposing that an additional response regulator, DifX, positively regulates fibril polysaccharide production. It is further proposed that DifE stimulates the function of DifX and DifD inhibits the stimulatory effects of DifE on DifX. In both models, DifG is proposed to have an inhibitory effect on fibril polysaccharide production by interacting with the signaling complex of DifA, DifC, and DifE.

response regulator capable of positively regulating the expression of genes involved in fibril biogenesis, or it could be an enzyme or a group of enzymes catalyzing the synthesis of fibril polysaccharides. In this model, we propose that DifD inhibits the activity of DifE to stimulate DifX, perhaps by diverting the phosphate flow from DifX to itself, as does CheY1 in *Sinorhizobium meliloti* chemotaxis (148). In this context, it is perhaps relevant that preliminary results with the yeast two-hybrid system indicated direct interactions between DifE and DifD (Z. Li and Z. Yang, unpublished results). In both models, DifG is proposed to have an inhibitory effect on fibril biogenesis based on the observation that the *difG* mutant overproduced fibril polysaccharides. We tentatively placed DifG on the pathway as interacting with the putative complexes formed by DifA, DifC, and DifE. The formation of complexes by DifA, DifC, and DifE is extrapolated from the knowledge that the chemoreceptors, CheW, and CheA exist as multimolecular ternary complexes in enteric bacteria (58). The speculation that DifG interacts with the presumed complexes of DifA, DifC, and DifE is based primarily on the studies of CheC in *B. subtilis* (96). It was proposed that *B. subtilis* CheC, which shares homology with flagellar switch proteins, may interact with the flagellar switch and the chemoreceptor-CheW-CheA complex to bring about the adaptation in chemotactic responses (96). *cheC* mutants of *B. subtilis* have increased levels of MCP methylation and appear to promote the activity of the CheA kinase (142). Our findings are consistent with the model proposed for the function of CheC in *B. subtilis*.

As far as we are aware, DifG is the first CheC homolog to be identified and studied in proteobacteria. It was reported previously that the *B. subtilis* CheC protein interacted the strongest with CheD in the yeast two-hybrid analysis and that CheD homologs existed in all prokaryotic species in which CheC was present (96). In most of the bacterial and archaeal species with both CheC and CheD homologs, the genes that encode these homologs are located in the same operon. *M. xanthus* appears to be the exception in that there are no CheD homologs in the vicinity of *difG*. In fact, BLAST searches revealed no CheD homologs in the nearly completed *M. xanthus* genome sequence (Z. Yang, unpublished results). This finding is consistent with the conclusion that CheC in *B. subtilis* plays a role in chemotaxis adaptation that is independent from CheD (96). We prefer the model shown in Fig. 2-7B for two reasons. First, in most bacterial signal transduction pathways, kinases usually stimulate the functions or activities of their cognate response regulators that are responsible for regulating the downstream processes, whether transcriptional or otherwise. The model proposed in Fig. 2-7A goes against this well-known dogma. Second, preliminary genetic analysis indicated that a *difD difE* double mutant displayed a phenotype similar to the parental *difE* mutant (our unpublished results). This suggests that *difE* is epistatic to *difD* and that DifD is therefore unlikely to function downstream of DifE in the pathway.

While the working models are consistent with our data, we recognize that they are speculative and not comprehensive with regard to the regulation of fibril biogenesis and that the interactions among the Dif proteins predicted by the models remain to be examined. In addition to the *dif* locus, there are two other loci with apparent regulatory functions in fibril biogenesis. At the *sglK* locus, *fibR* and *sglK* were found to have somewhat opposite effects (188). Mutations in *sglK*, like mutations in *difA*, *difC*, and *difE*, lead to defects in fibril biogenesis, S motility, and development (188, 202). SglK is therefore a positive regulator of fibril production. On the other hand, mutations in *fibR* were found to produce increased amounts of the fibril protein FibA (90, 188). FibR therefore appears to be a negative regulator of FibA and possibly other fibril proteins. The *stk* gene was identified by transposon insertion mutations that resulted in a more cohesive or stickier phenotype (48). *stk* mutations were found to restore group motility to certain S motility mutants and led to increased production of fibrils. Stk therefore appears to be a negative regulator of fibril production. Interestingly, both Stk and SglK were found to be homologs of DnaK, a chaperone in the HSP70 family (188). How the Dif pathway may interact with SglK, FibR, and Stk is yet to be investigated. The difference between the *fibR* mutant and the *difD* and *difG* mutants should be noted. Using immunoblotting, we did not observe an obvious overproduction of FibA (Fig. 2-5). The overproduction of fibrils in *stk* mutants was observed by using scanning electron microscopy (48). Since polysaccharides form the backbones of fibrils, it is probably safe to assume that *stk* mutants overproduce fibril polysaccharides. The level of FibA production in *stk* mutants remains to be examined. In addition, our current models have not yet taken into account that *difA*, *difE*, and *fibA* are all implicated in the chemotactic response of *M. xanthus* cells to phosphatidylethanolamine attractants (90, 91).

During this study, we made slight modifications to previously described assays for quantifying the production of fibril polysaccharides in *M. xanthus*. A dye binding assay was reported previously for the determination of the kinetic parameters of Congo red binding to *M. xanthus* cells (10). In addition, it was reported that the binding of both Congo red and trypan blue, analyzed by plate assays, correlated with the amount of fibrils on the cell surface as examined by scanning electron microscopy (48). Using the absorbance at the wavelengths with peak absorbance (490 nm for Congo red and 585 nm for trypan blue), we determined that there is a linear relationship between the absorbance value and the amount of dye in a solution over a wide range (data not shown). It is therefore feasible to determine the amount of dye bound by *M. xanthus* cells by measuring the amount of unbound dye in a colorimetric assay, as noted previously (10). The wide range of possible working concentrations of the dye affords the flexibility to allow the measurements of various levels of fibril polysaccharide production. Our results indicate that compared to Congo red, trypan blue has a substantially reduced background level of binding to fibril-deficient strains. In general, we observed little if any binding of trypan blue to cells defective in fibril production. On the other hand, fibril-defective mutants still showed significant binding to Congo red in our assay. This is consistent with previous findings that, in addition to fibrils, there is an additional receptor on *M. xanthus* cells for Congo red (10, 188). Based on these observations, we suggest that trypan blue provides the more sensitive and effective measurement for the relative amount of fibril polysaccharide production in *M. xanthus*. The ability to quantify fibril polysaccharide production in various mutants should greatly facilitate the studies of the regulation of fibrils in *M. xanthus*.

## ACKNOWLEDGEMENTS

We are grateful to Jill Sible for granting access to her microscope facilities. We thank Larry Shimkets and John Kirby for helpful discussions. We thank the laboratories of Heidi Kaplan and Dale Kaiser for generously providing antibodies, plasmids, and/or protocols. We thank Wenyuan Shi for his support and encouragement.

This work was supported by grant MCB-0135434 from the National Science Foundation to Z. Yang.

# CHAPTER 3

# Type IV Pili Function as Remote Sensors for the Dif Chemotaxis Pathway in *Myxococcus xanthus* EPS Regulation

## ABSTRACT

The developmental bacterium *Myxococcus xanthus* utilizes gliding motility to aggregate during the formation of multicellular fruiting bodies. The social (S) component of *M. xanthus* gliding motility requires at least two extracellular surface structures, type IV pili (Tfp) and the fibril polysaccharide or exopolysaccharide (EPS). Retraction of Tfp is proposed to power S motility and EPS from neighboring cells is suggested to provide an anchor and trigger for Tfp retraction. The production of EPS in *M. xanthus* is regulated in part by the Dif chemotaxis-like pathway; however, the input signal for the Dif pathway in EPS regulation remains to be uncovered. Using a genetic approach combined with quantitative and qualitative analysis, we demonstrate here that Tfp function upstream of the Dif proteins in regulating EPS production. The requirement of Tfp for the production of EPS was verified using various classes of Tfp mutants. Construction and examination of double and triple mutants indicated that mutations in *dif* are epistatic to those in *pil*. Furthermore, extracellular complementation between various Tfp and *dif* mutants suggests that Tfp, instead of being signals, may constitute the sensor or part of the sensor responsible for mediating signal input into the Dif pathway. These results suggest a regulatory loop coupling EPS production to Tfp function and vice versa in *M. xanthus*. We propose that Tfp, as extracellular and polarly localized protein filaments, act in essence as sensors to detect cells in their vicinity to regulate EPS production through the Dif chemotaxis-like signaling pathway in *M. xanthus*.

## INTRODUCTION

All organisms, large or small, multicellular or unicellular, respond to their environment using signal transduction pathways, the best understood of which is probably the bacterial chemotaxis pathway (8, 32, 40). Signals detected by bacterial chemotaxis systems are frequently soluble chemicals which, upon entry into the periplasmic space, interact with and result in conformational changes of transmembrane chemoreceptors known as methyl-accepting chemotaxis proteins (MCPs). The conformational change in MCP is coupled to the modulation of the downstream CheA kinase activity by the CheW protein. The CheA autokinase transfers phosphate to the CheY response regulator, which in its phosphorylated form effects changes in bacterial motility behavior to achieve chemotaxis.

Studies in recent years have considerably expanded both the signals perceived and the processes regulated by bacterial chemotaxis and chemotaxis-like pathways. Such pathways, for example, have been shown to mediate tactic responses to light (phototaxis) (23) and oxygen (aerotaxis) (170). The signals for such tactic responses are either intracellular or they can readily reach the cell surface and intimately interact with transmembrane receptors directly or indirectly. In addition to the regulation of taxis, chemotaxis and its homologous systems have now been implicated in the regulation of diverse processes including pili production (24), flagella biosynthesis (21), cyst formation (22), swarm cell differentiation (42), and developmental gene regulation in *Myxococcus xanthus* (96). However, the signals for the regulation of these less conventional processes are mostly unknown.

The *M. xanthus* Dif chemotaxis-like pathway regulates the production of fibril exopolysaccharides (EPS) (15, 25, 201), a cell surface component essential for multicellular differentiation and social (S) gliding motility of this developmental bacterium. Under nutrient limitation, *M. xanthus* cells aggregate on surfaces using their gliding motility to form multicellular fruiting bodies. Increasing evidence indicates that *M. xanthus* S motility, as well as bacterial twitching, is powered by the retraction of type IV pili (Tfp) (81, 121, 160). EPS is proposed to be the anchor and trigger for pilus retraction in *M. xanthus* (104). The Dif chemotaxis-like proteins have been shown to form part of a signal transduction pathway that regulates EPS production (15, 25, 201). DifA, an MCP homologue lacking a prominent periplasmic domain, likely does not bind extracellular ligands directly as do many other MCPs, however. It is unknown what signals are detected by the Dif pathway to regulate EPS production in *M. xanthus*.

In this study, we show that Tfp, the S motility apparatus, likely function as a sensor or part of a sensor that mediates signal input into the Dif pathway. We first confirmed previous findings (48) that genes required for Tfp biogenesis are required for the production of EPS. Using reciprocal genetic epistasis tests, we provide evidence that Tfp function upstream of the Dif pathway to positively regulate EPS production. In addition, the Dif pathway likely uses DifD, a CheY homolog, as a phosphate sink to divert phosphate from the central Dif pathway in EPS regulation. Extracellular complementation experiments support the hypothesis that Tfp serves in the capacity of a sensor instead of an extracellular or exogenous signal for the Dif pathway. These results suggest that *M. xanthus* Tfp not only power S motility but also act as a remote sensor for the detection of cells at a distance to regulate EPS production through a chemotaxis-like pathway. We propose that S motility involves a regulatory loop in which EPS triggers Tfp retraction and Tfp provides proximity signals to the Dif pathway to modulate EPS production.

## MATERIALS AND METHODS

**Growth Conditions and Construction of *M. xanthus* Strains.** *M. xanthus* strains were grown and maintained at 32°C on Casitone-yeast extract (CYE) agar plates or in CYE liquid medium (45). XL1-Blue (Stratagene), the *Escherichia coli* strain used for plasmid construction, was grown and maintained at 37°C on Luria-Bertani (LB) agar plates or in LB liquid medium (123). Unless noted otherwise, agar plates contained 1.5% agar. When applicable, kanamycin and oxytetracycline were supplemented to media for selection at 100 μg/ml and 15 μg/ml, respectively.

DK1622 (85) was used as the wild-type and parental strain for all mutants used in this study. DK3473 (*pilR*), DK10405 (*tgl*), DK10407 (*pilA*), DK10409 (*pilT*), DK10415 (*pilS*), DK10416 (*pilB*), YZ601 (*difA*), YZ603 (*difE*), YZ604 (*difG*), and YZ613 (*difD*) have been described elsewhere (25, 181, 193, 195). The *difD difG* double deletion mutant, YZ641, was constructed from YZ613 using pWB119, which contains a *difG* in-frame deletion and a kanamycin-*galK* (KG) cassette used for gene replacement (25, 175). The double and triple deletion mutants YZ656 (*difDE*), YZ657 (*difEG*), and YZ658 (*difDEG*) were constructed similarly using *dif* deletion fragments in pBJ113 (79). The *pilA* mutation in DK10407 was transferred into the recipient strains YZ613, YZ603, YZ604, YZ641, and YZ601 by Mx4 mediated generalized transduction (129) to create strains YZ643 (*difD pilA*), YZ644 (*difE pilA*), YZ645 (*difG pilA*), YZ646 (*difDG pilA*), and YZ648 (*difA pilA*), respectively. YZ662 (*pilT tgl*) and YZ1602 (*pilS tgl*) were constructed by Mx4 transduction of the *tgl* mutation from DK10405 into DK10409 (*pilT*) and DK10415 (*pilS*), respectively. YZ642 (*difE pilT*) and YZ679 (*difE tgl*) were generated by homologous integration of a *difE* insertion vector, pYG402 (198), into DK10409 (*pilT*) and DK10405 (*tgl*), respectively. YZ680 (*tgl*) and YZ681 (*pilA tgl*) were generated by homologous integration of pWB520, which contains an internal *tgl* fragment in pZErO-2 (Invitrogen), into DK1622 and DK10407 (*pilA*), respectively. YZ729, the strain expressing the NarX-DifA (NafA) chimera, was constructed from YZ648 by integration of pXQ719, the *nafA* expressing construct (195), at the Mx8 *attB* site. All newly constructed mutant strains were verified by polymerase chain reaction (PCR), Southern blot (145), and/or phenotypic analyses.

**Examination of EPS Production.** Two methods were used to examine EPS production. The qualitative method was performed using plate assays as described previously (25, 48). Briefly, strains to be tested were harvested in exponential phase and resuspended in MOPS (morpholinepropanesulfonic acid) buffer (10 mM MOPS [pH7.6], 2 mM $MgSO_4$) at $5 \times 10^9$ cells/ml. 5 μl of this cell suspension was spotted onto CYE or CTT (85) plates containing Calcofluor white at a concentration of 50 μg/ml. Plates were incubated for 5 days at 32°C before documentation under long-wavelength (365 nm) UV light. Quantitative analysis of EPS production was performed using the previously described liquid dye binding assay (25) with slight modifications. All strains tested were harvested at similar culture densities (approximately $3.5 \times 10^8$ cells/ml), washed and resuspended to $2.8 \times 10^8$ cells/ml in MOPS buffer containing 1 mM $CaCl_2$. A 10× stock solution of Trypan blue at 50 μg/ml was prepared in deionized distilled water. Cells and the dye stock were mixed to give final concentrations of $2.5 \times 10^8$ cells/ml and 5 μg/ml Trypan blue. The remaining procedure was identical to that previously described (25). EPS production of all strains was normalized to that of the wild-type strain, which was arbitrarily set as 1.

**Mixing or Extracellular Complementation Experiments.** EPS mutants to be tested for stimulation of EPS production by mixing with other EPS mutants were grown overnight, harvested, and resuspended to approximately $5 \times 10^9$ cells/ml in MOPS buffer. Cell suspensions of two experimental strains were mixed at a 1:1 ratio (181). 5 μl of the cell mixture were spotted onto CYE plates containing Trypan blue (40 μg/ml). Plates were incubated for 5 days at 32°C before scoring for EPS production.

## RESULTS

**Tfp Regulate EPS Production.** Dana and Shimkets (48) observed that many *M. xanthus* S motility mutants failed to bind dyes specific for *M. xanthus* fibril EPS. Some of these mutants are now known to harbor mutations in Tfp biogenesis genes (191), suggesting that Tfp could be essential for EPS production in *M. xanthus*. Examination of various known Tfp mutants confirmed an apparent association between the presence of Tfp and EPS production (Fig. 3-1A). All mutants (*pilA*, *pilB*, *pilR*, and *tgl*) that have no pili (138, 191, 193) were defective in EPS production. In contrast, *pilS* and *pilT* mutants, both of which assemble pili (192, 193), still produced EPS. The *pilT* mutant, which is hyperpiliated presumably because it produces non-retractable pili, overproduced EPS when compared to the wild type.

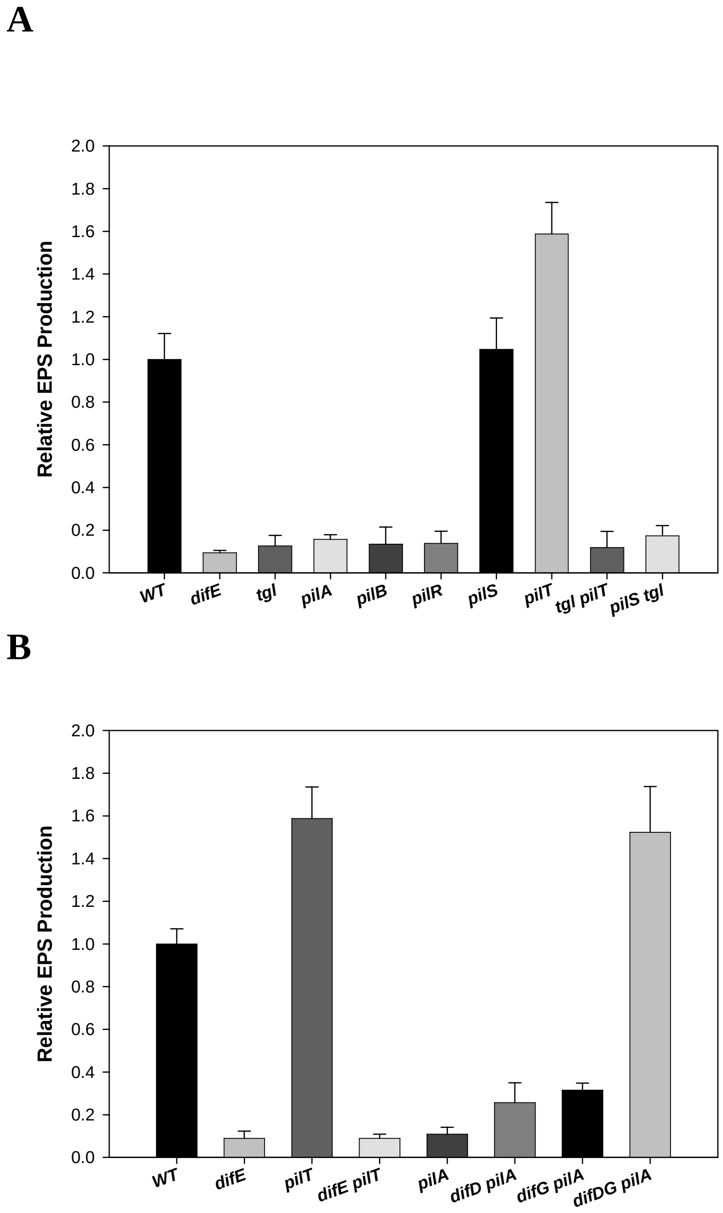

**Figure 3-1.** Quantitative analysis of EPS production.

The amount of dye bound was used as a measurement of EPS production. Values for all strains were normalized to the wild type (see *Material and Methods*). (*A*) WT (DK1622), *difE* (YZ603), *tgl* (DK10405), *pilA* (DK10407), *pilB* (DK10416), *pilR* (DK3473), *pilS* (DK10415), *pilT* (DK10409), *pilT tgl* (YZ662), and *pilS tgl* (YZ1602). (*B*) WT (DK1622), *difE* (YZ603), *pilT* (DK10409), *difE pilT* (YZ642), *pilA* (DK10407), *difD pilA* (YZ643), *difG pilA* (YZ645), *difDG pilA* (YZ646). The data represents three independent experiments, each of which was performed using triplicate samples.

The overproduction of EPS by the *pilT* mutant could be explained by either hyperpiliation or the lack of the PilT protein itself instead of hyperpiliation. A *tgl pilT* double mutant was created to differentiate these two possibilities. Tgl is an outer membrane lipoprotein that is required for Tfp to transverse the outer membrane (127, 128). The *tgl pilT* double mutant, which lacked Tfp as expected (data not shown), was defective in EPS production (Fig. 3-1A). This suggests that it is the hyperpiliation, not the loss of PilT per se, that is responsible for the observed overproduction of EPS by the *pilT* mutant (Fig. 3-1A). Likewise, a *tgl pilS* double mutant exhibited the same defects in EPS production as the *tgl* mutant (Fig. 3-1A). These observations demonstrate that the presence of Tfp structure, although not necessarily functional or retractable Tfp, is required for EPS production in *M. xanthus*.

**Tfp Function Upstream of Dif Proteins.** Since the *dif* genes play central roles in regulating EPS production, the finding that Tfp are required for EPS production indicates that Tfp functionally interact with the Dif pathway. Various double and triple mutants were constructed and analyzed for EPS production to examine the genetic epistatic relationship between *pil* and *dif* mutations (Fig. 3-1B). A *difE pilT* double mutant showed similar defects in EPS production as the *difE* parental strain, indicating that DifE is likely downstream of Tfp. Although, the defect of a *pilA* mutation in EPS production was only partially and minimally suppressed by the deletion of either *difD* or *difG*, a *difD difG pilA* triple mutant produced 1.5 times the EPS as that of the wild type, indicating a *difD difG* double mutation can fully suppress *pilA* mutations with regard to EPS production. These reciprocal genetic epistatic relationships demonstrated to relative certainty that Tfp function upstream of Dif proteins in the regulation of EPS production.

**Neither DifD nor DifG Function in the Central Dif Pathway.** The observation that a *pilA* deletion was fully suppressed only by a *difD difG* double mutation, but not by a *difD* or *difG* single mutation (Fig. 3-1B) could be explained if DifD and DifG function as modulators of the central Dif pathway instead of directly downstream of DifE as in one of the two previously proposed models (25). Additional genetic epistasis experiments were performed to examine the functional relationships among DifD, DifE, and DifG. As shown in Figure 3-2A and Figure 3-3, neither a *difD* or a *difG* single mutation nor a *difD difG* double mutation was able to suppress a *difE* mutation. Similarly, previous results had showed that a *difA* deletion could not be suppressed by the deletion of *difD* or *difG* alone or both (195). In addition, a *difD difG* double mutant was found to produce more EPS than either the *difD* or the *difG* single parental strain as analyzed by the binding of Calcofluor white (Fig. 3-2A) and by a quantitative assay (Fig. 3-3), indicating some additive effects by DifD and DifG, both of which were known negative regulators of EPS production (25). All the above results are consistent with a model in which DifD and DifG function as ancillary modulators of the central Dif pathway instead of directly downstream of DifE  (25).

**Artificial Activation of the Dif Pathway Bypasses the Requirement for Tfp.** The interpretation of the epistatic analysis involving *difD* and *difG* mutations (Fig. 3-1B) became somewhat ambiguous by the above finding that neither DifD nor DifG function as central members of the Dif pathway. The suppression of the defect in EPS production resulting from a *pilA* mutation by mutations in a central component of the Dif pathway would provide more direct evidence for the proposed functional relationship between Tfp and Dif proteins. A NarX-DifA (NafA) chimera was recently constructed and shown to

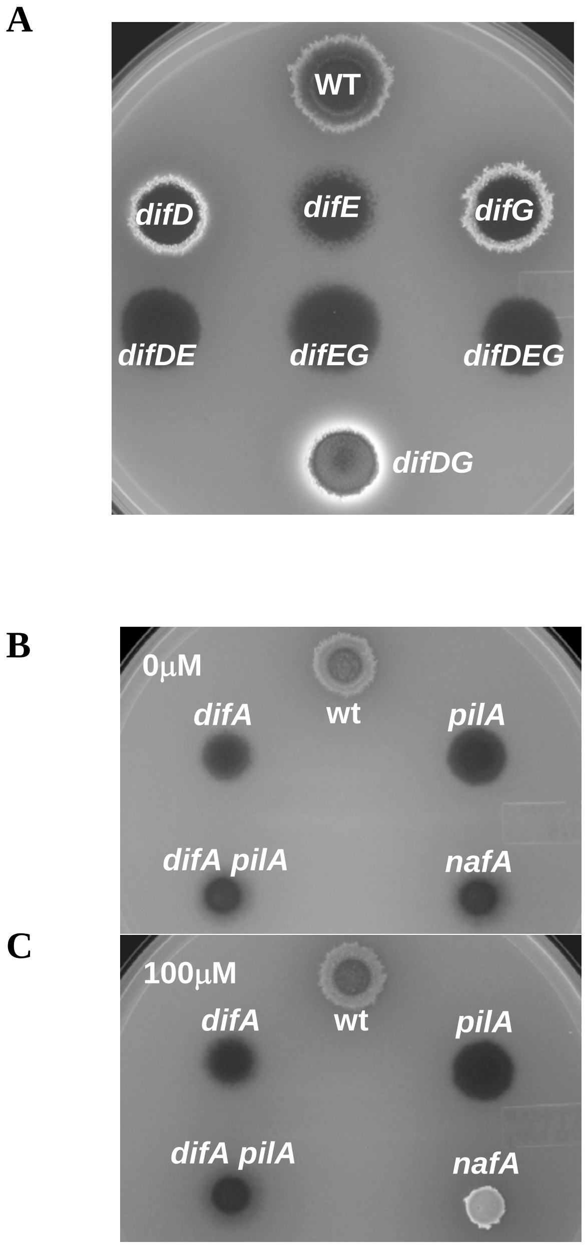
A
WT
difD
difE
difG
difDE
difEG
difDEG
difDG
B
0μM
difA
wt
pilA
difA pilA
nafA
C
100μM
difA
wt
pilA
difA pilA
nafA

**Figure 3-2.** Qualitative analysis of EPS production.
Analysis of EPS production by the binding of the fluorescent dye Calcofluor white. Experiments were preformed as described in *Materials and Methods*. (*A*) Indicated strains were spotted on CYE supplemented with Calcofluor white. WT (DK1622), *difD* (YZ613), *difE* (YZ603), *difG* (YZ604), *difDE* (YZ656), *difEG* (YZ657), *difDEG* (YZ658), and *difDG* (YZ641). (*B* and *C*) CTT plates supplemented with Calcofluor white without nitrate (*B*) or with 100 μM nitrate (*C*). WT (DK1622), *difA* (YZ601), *difA pilA* (YZ648), and *nafA* (YZ729).

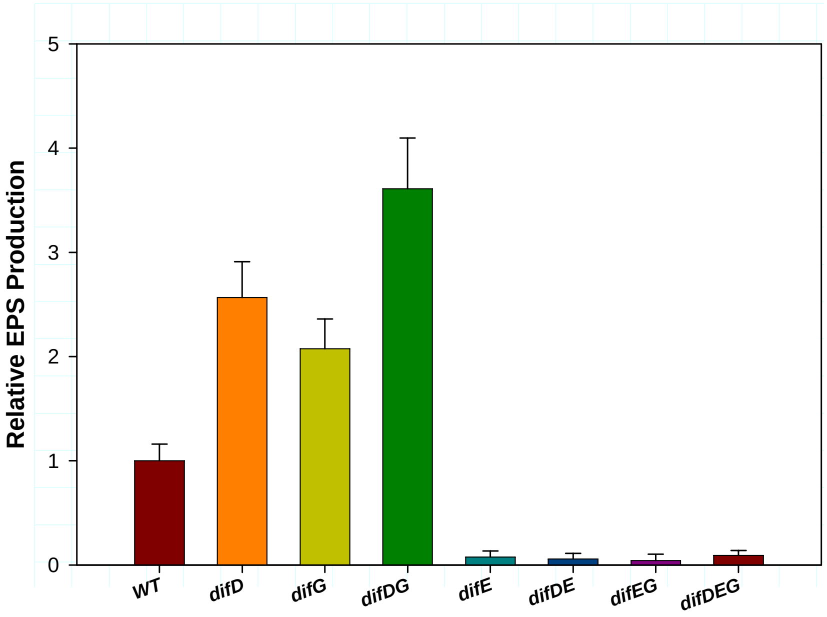

**Figure 3-3.** Quantitative analysis of EPS production.
Quantitative assay on the mutants shown in Fig. 3-2A. Assay performed as described for Fig. 3-1.

activate the Dif pathway in a nitrate dependent manner (195). If Tfp are upstream of Dif in regulating EPS production, the artificial activation of the Dif pathway using NafA and nitrate would be predicted to bypass the requirement of Tfp. Assays using plates containing Calcofluor white revealed that in the absence of nitrate, YZ729, a *difA pilA* double mutant containing a *nafA* construct, produced no detectable levels of EPS (Fig. 3-2B); however, in the presence of 100 μM nitrate, the same strain clearly produced EPS at levels equivalent to or greater than the wild type (Fig. 3-2C). These results provided more direct evidence that Tfp function upstream of the Dif pathway in the regulation of EPS production in *M. xanthus*.

A feasible and perhaps trivial explanation for the observed epistasis between *dif* and *pil* genes is that Tfp may either down regulate the expression of positive EPS regulators such as DifA or up regulate negative regulators such as DifD. DifA and DifD protein levels in *pil* mutants were examined by immunoblotting and showed no obvious differences from the wild type (Fig. 3-4). Therefore, the functional interactions between Tfp and the Dif pathway are propagated through signal transduction instead of regulation of *dif* gene expression.

**Tfp Functions as a Sensor for the Dif Pathway.** Tfp is a polymeric protein filament protruding from *M. xanthus* cell poles. The absence of regulation of Dif expression by Tfp suggests that Tfp may operate either as extracellular signals of the Dif pathway or as a sensory apparatus mediating signal input into the pathway. To examine these possibilities, mixing or extracellular complementation experiments were performed using plates containing Trypan blue (48), another dye capable of binding to *M. xanthus* EPS. Mixing of *difE* and *pilA* mutant cells did not result in EPS production as indicated

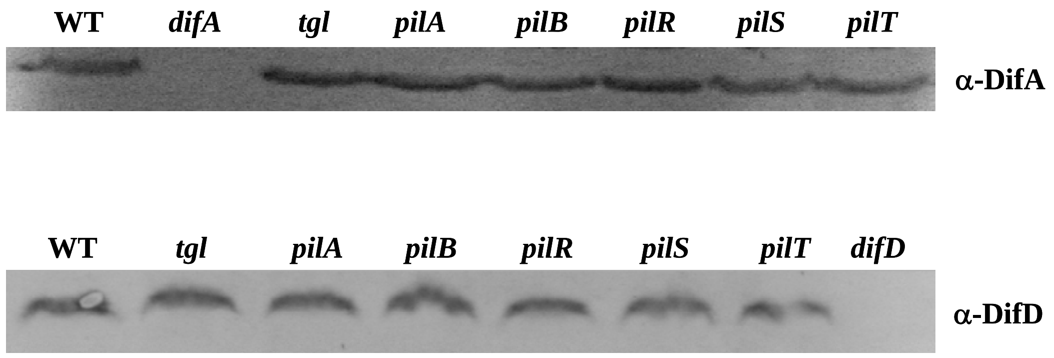
WT
difA
tgl
pilA
pilB
pilR
pilS
pilT
α-DifA
WT
tgl
pilA
pilB
pilR
pilS
pilT
difD
α-DifD

**Figure 3-4.** Immunoblot of Dif proteins in *pil* mutants.
Immunoblot analysis of all *pil* mutants that were tested for EPS production. Whole cell lysates were prepared from 5 × $10^8$ cells, separated by sodium dodecyl sulfate-polyacrylamide gel electrophoresis and probed with antibodies against DifA (195) and DifD.

by the lack of Trypan blue binding (Fig. 3-5 and Fig. 3-6). The *difE* mutant, while lacking a functional Dif pathway, is hyperpiliated (15, 104) whereas the *pilA* mutant lacks Tfp yet possesses a full complement of *dif* genes. If Tfp acted solely as external signals to the Dif pathway, *difE* mutant cells would have provided the signal to the *pilA* mutant cells and stimulated EPS production in the mixed cell population. The lack of EPS production by the mixture of *difE* and *pilA* mutant cells suggests that Tfp do not act merely as extracellular signals to the Dif pathway.

By contrast, if Tfp functions as a sensor or part of a sensor for the Dif pathway, it is conceivable that EPS production could be restored to a Tfp$^-$ mutant that is extracellularly complemented to assemble Tfp. It is known that Tgl$^-$ cells, which lack Tfp, can be stimulated to transiently assemble Tfp by close contact with Tgl$^+$ cells (178, 181). When *tgl*$^-$ cells were mixed with either *difE* or *pilA* mutant cells, the mixed population formed bluish-green colonies (Fig. 3-5 and Fig. 3-6), indicating the restoration of EPS production. A few lines of evidence support our conclusion that it was the Tgl$^-$ cells in the mixed population that produced EPS. First, the mixture containing a *difE tgl* double mutant with either a *difE* or a *pilA* mutant failed to produce EPS (Fig. 3-5), indicating the importance of an intact Dif pathway in Tgl$^-$ cells in the extracellular complementation. On the other hand, the mixed population of the *difE pilA* double mutant with the *tgl* single mutant produced EPS similarly as the mixture of *pilA* and *tgl* mutants (Fig. 3-5), indicating that an intact Dif pathway is not necessary in the *pilA* mutant in this experiment. Second, it has been shown that pilin, therefore the *pilA* gene, from the Tgl$^-$ recipient cells but not from the Tgl$^+$ donor cells is required for the stimulation of Tgl$^-$ cells (181). The mixture of *difE* with *pilA tgl* double mutant cells in

|  | ***difE*** | ***pilA*** | ***tgl*** |
|---|---|---|---|
| ***difE*** | **na** | **-** | **+** |
| ***pilA*** | **-** | **na** | **+** |
| ***tgl*** | **+** | **+** | **na** |
| ***difE tgl*** | **-** | **-** | **-** |
| ***difE pilA*** | **-** | **-** | **+** |
| ***pilA tgl*** | **-** | **nd** | **nd** |
| ***tgl pilT*** | **+** | **+** | **nd** |

**Figure 3-5.** Extracellular complementation experiment.

Summary of the mixing experiments or extracellular complementation experiments. Cells of the strains listed on the top were mixed with cells of the strains listed on the left and examined for the binding of Trypan blue, an indicator of EPS production. +, EPS produced; -, EPS not produced; na, not applicable; nd, not determined. *difE* (YZ603), *pilA* (DK10407), *tgl* (DK10405), *difE tgl* (YZ679), *difE pilA* (YZ644), *pilA tgl* (YZ681), and *pilT tgl* (YZ662).

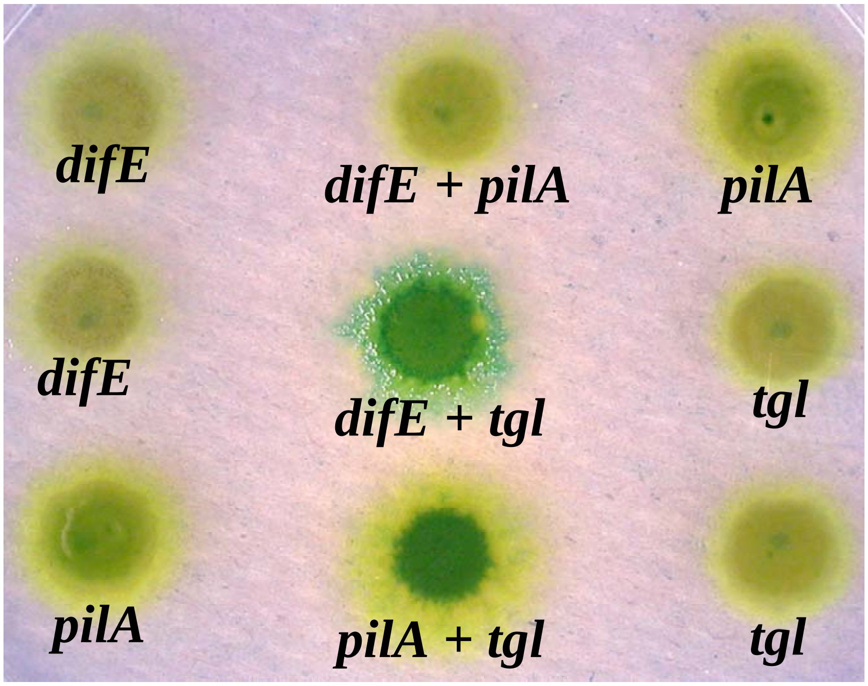
difE
difE + pilA
pilA
difE
difE + tgl
tgl
pilA
pilA + tgl
tgl

**Figure 3-6.** Extracellular complementation assay.
This is a visual example of the results from the mixing experiments or extracellular complementation assay shown in Fig. 3-5. Single mutants (left and right columns) or an equal mixture of the indicated mutants (middle column) were spotted on CYE plates containing Trypan blue as described in Materials and Methods.

our experiment did not produce EPS, indicating that the Tgl$^-$ recipient must have a wild-type *pilA* gene. Lastly, it had been shown previously that adventurous or A motility is essential for the stimulation of Tgl$^-$ cells to assembly Tfp (178). Our results indicated that the introduction of an A motility mutation into a *difE*, *pilA*, or *tgl* mutant background abolished EPS production in the extracellular complementation experiments (data not shown). These results are consistent with the interpretation that Tgl$^-$ cells but not *difE* or *pilA* mutant cells were stimulated to produce EPS when mixed with the appropriate cells. The inference from these results is that the assembly of Tfp by the otherwise Tfp$^-$ cells of the *tgl* mutant reconstituted a functional sensor for the Dif pathway. This sensor could then detect and transmit signals to the intact Dif pathway downstream leading to EPS production. The observation here also served as a proof of principle for the mixing or extracellular complementation experiments for the examination of EPS production.

The extracellular complementation experiments (Fig. 3-5) also provided further support for a few conclusions reached earlier. First, the stimulation of *tgl* by either the *pilA* or the *difE pilA* double mutant indicates that external Tfp or lack thereof from the donor cells are not important for EPS production, strengthening the notion that Tfp do not function as external signals for the Dif pathway. Second, we have shown that the *difE tgl* double mutant was stimulated to assembly surface pili when mixed with *pilA* mutants (data not shown). The lack of EPS production by this mutant in the presence of *pilA* mutant cells (Fig. 3-5) further validate the conclusion that Dif proteins function downstream of Tfp in EPS regulation. Lastly, a *pilT tgl* double mutant retained the ability to produce EPS when stimulated by either *difE* or *pilA* mutant cells (Fig. 3-5). This observation coincides with the ability of a *pilT* mutant to produce EPS and indicates that non-retractable or paralyzed Tfp are sufficient to stimulate the Dif pathway for the regulation of EPS production.

## DISCUSSION

In this study, we demonstrated a correlation between the presence of Tfp and the production of EPS in *M. xanthus*. All mutants that fail to assemble pili were found to be defective in EPS production (Fig. 3-1A) whereas those (*pilS* and *pilT*) that still possess Tfp filaments produced EPS at levels equivalent to or greater than the wild-type strain. Genetic epistasis provided evidence that Tfp function upstream of the Dif chemotaxis-like pathway to positively regulate EPS production (Fig. 3-1B). Mixing or extracellular complementation experiments indicated that Tfp from adjacent cells could not restore EPS production to Tfp$^-$ mutant cells (Fig. 3-5 and Fig. 3-6). On the other hand, *tgl* mutants, which can be stimulated extracellularly to produce Tfp transiently (181), do produce EPS when mixed with Tgl$^+$ but EPS$^-$ cells. In addition, studies of various double mutants showed that DifD (CheY-like) does not function downstream of DifE (CheA-like) in EPS regulation and that DifD and DifG exhibit additive effects as negative regulators of EPS production (Fig. 3-2A and Fig. 3-3).

**A working model.** Based on current and previous studies, a working model is presented in Fig. 3-7 to describe the regulation of EPS production by the Dif pathway. Tfp are proposed to be at the top of the regulatory cascade and act to mediate signal input into the pathway. The signal is then transmitted to a signaling complex composed of DifA (MCP-like), DifC (CheW-like) and DifE. The DifE putative kinase in this ternary complex is proposed to regulate EPS production in a phosphorylation-dependent manner

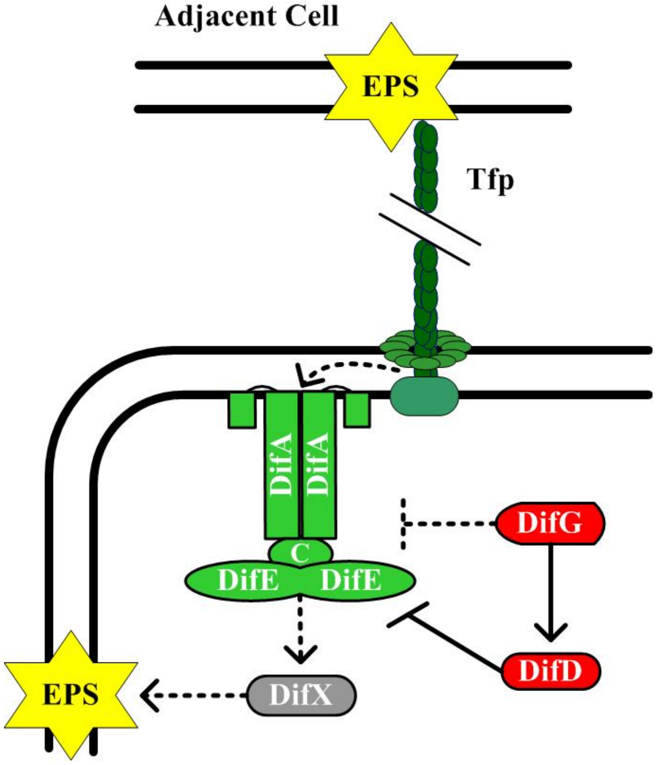
Adjacent Cell
EPS
Tfp
DifA
DifA
C
DifE
DifE
DifG
DifD
DifX
EPS

**Figure 3-7.** Model of Tfp-Dif regulation of EPS.
Model depicting the regulation of EPS production in *M. xanthus* by TFP and the Dif pathway. Demonstrated interactions are indicated by solid lines and proposed interactions by dashed lines. Arrows and bars indicate positive and negative regulation, respectively. See text for details of the model.

by transmitting signals downstream to yet unidentified components represented collectively by DifX. DifD directly interacts with DifE as a phosphate sink to negatively regulate EPS production. DifG directly interacts with DifD, presumably as a phosphatase of DifD-phosphate (DifD-P), to promote the inhibitory effect of DifD on EPS production. DifG is additionally hypothesized to interact with the DifACE complex to negatively regulate the output of the pathway.

This model (Fig. 3-7) is consistent with and supported by the currently available data. DifA, DifC, DifE and Tfp all positively regulate EPS production, and DifD as well as DifG do so negatively (15, 25, 201) (Fig. 3-1). In addition to the epistasis presented is this study, previous studies by the same lab indicated that *difD* and *difG* mutations failed to suppress *difA* mutations in EPS production (195). The formation of a DifACE ternary complex was demonstrated using a modified yeast 2-hybrid system, as was the interaction between DifD and DifG (200). The proposed function of a phosphate sink for DifD, which is supported by genetic epistasis and by the EPS-overproducing phenotype of *difD* mutants, mirrors the function of CheY2 in *Rhizobium meliloti* chemotaxis (161, 162).

DifG must have at least two points of contact with the central pathway. *Bacillus subtilis* CheC, which DifG is homologous to, has been shown to have CheY-P phosphatase activity (168). Similarly, DifG could simply function as a phosphatase of DifD-P in the Dif pathway in *M. xanthus*; however, this fails to explain the additive effects of *difD* and *difG* mutations on EPS production (Fig. 3-2A and Fig. 3-3). Since *B. subtilis* CheC was observed to interact with both CheA and McpB in Y2H experiments (95), we hypothesize that there are additional interactions between DifG and the DifACE ternary complex. The proposed DifACE-DifG interactions are further supported by studies of chemotactic responses of *M. xanthus* to phosphatidylethanolamine (PE). It is known that *difA* and *difC* are essential only for responses to 16:1 PE while *difE* and *difD* are required for responses to both 18:1 and 16:1 PE species (30). Therefore, it appears that multiple upstream pathways responsible for PE tactic responses converge at the point of the DifE kinase. Since *difG* is required for chemotactic adaptation to 16:1 but not 18:1 PE (30), the interactions of DifG with the pathway should be restricted to DifA, DifC, and other upstream components specific to the 16:1 response.

**Complex signaling network.** *M. xanthus* Dif pathway is part of a complex signaling network with multiple inputs, distinct outputs, and possible cross-talks with other signaling pathways. There are other known EPS regulators in *M. xanthus* besides the ones depicted in Fig. 3-7. SglK and Stk, two DnaK homologs, have opposing effects on EPS production (48, 187, 197). SglK is a positive regulator of EPS production whereas Stk is a negative one. Some of the 30 plus genes at the *eps* locus clearly encode regulatory proteins rather than biosynthetic ones (108). The Dif proteins must somehow interact functionally with these EPS regulators to effect the function of the EPS biosynthetic genes, some of which undoubtedly reside at the *eps* locus (108). The Dif pathway is also involved in chemotactic responses to at least two PE species as eluded to earlier (30). In contrast to its role in EPS regulation (Fig. 3-7), DifD likely functions downstream of DifE in the excitation response to these PE molecules (30). FibA, a protein essential for mediating responses to 16:1 PE, does not appear to interfere with the production of fibril EPS (89). On the other hand, the best known and studied chemotaxis system in *M. xanthus* is encoded by the *frz* genes (185). The Dif pathway should interact with the Frz proteins at some level to regulate *M. xanthus* motility behavior. In addition, while EPS production can be readily analyzed under nutrient-rich conditions, starvation is a prerequisite to analyze responses to PE in *M. xanthus* (89). It is not known how nutrient conditions influence the function of the Dif pathway. Regardless of the answers to many of these questions, it is clear that the Dif signaling proteins are involved in multiple processes in a complex regulatory network.

**The type IV pilus as a remote sensor upstream of a chemotaxis-like pathway.** Why are Tfp required for the regulation of EPS production by the Dif pathway? One possibility is that pilin, the subunit of Tfp, could function as exogenous or endogenous signals for the Dif pathway. The results from extracellular complementation experiments (Fig. 3-5) are not consistent with pilins from neighboring cells being exogenous signals. We argue that pilins are unlikely endogenous signals based on the EPS$^-$ phenotypes of the *pilQ* (data not shown) and *tgl* mutants (Fig. 3-1A). Both Tgl and PilQ are required for the formation of secretin oligomers/channels for the Tfp filaments to traverse the outer membrane (127, 128). *tgl* and *pilQ* mutations were not expected to influence the endogenous pool of pilins. Indeed, *tgl* and *pilQ* mutants contained endogenous pilins indistinguishable in amount and molecular weight from those of the wild type as analyzed by immunoblotting of cell lysates prepared from bacteria with their pilus filaments sheared off (127, 180) (data not shown). Pilus retraction is apparently not required for EPS production (Fig. 3-1A and Fig. 3-5), excluding the possibility that retracted pilins could function as endogenous signals. We instead propose that Tfp is the sensor or part of a sensory apparatus that detects and transmits signals to the Dif pathway (Fig. 3-7). It was suggested that the distal ends of Tfp may interact with EPS to initiate pilus retraction in *M. xanthus* (104). We propose that *M. xanthus* utilizes the distal ends of Tfp to sense the presence of other cells by interacting with EPS on their cell surfaces, and such signals of cell proximity are subsequently relayed to a chemotaxis-like signaling pathway for the regulation of EPS production in this social bacterium.

It appears therefore that not only can Tfp be triggered to retract by EPS, the interactions between these two cell surface structures can also lead to the stimulation of EPS production in *M. xanthus*. Such a regulatory feedback loop makes perfect biological sense considering that *M. xanthus* S motility requires Tfp and EPS as well as cell proximity. There would be no pilus retraction and S motility if there are no adjacent cells to provide EPS within the reach of a pilus; there would be no stimulation of EPS production unless there are nearby cells that can take advantage of these surface molecules. This is perhaps a perfect example of the mutualistic existence of this well known social creature. *M. xanthus* cells not only exploit their neighborly brethren, but also provide timely help once a friend is within an arm's reach.

**Bacterial protein filaments as environmental sensors.** Many bacteria possess cell surface protein filaments that certainly have the potential to function as remote sensors or antennas to monitor their surrounding environment. In the past, these structures had more or less been regarded as the targets of regulation by or as passive participants of signal transduction pathways. Bacterial flagella, the best known motility apparatus, have been extensively studied as the target of transcriptional regulation and chemotaxis signaling pathways, for example (19, 110). However, flagella have also been suspected to be a sensor of surfaces or viscosity in regulating swarmer cell differentiation for sometime (65, 118). It was shown recently that flagella have the ability to effect the switch in response to changes at its distal end (57). This suggests that the flagellar filament can transmit signals from the tip to the base or the cytoplasm, whatever mechanism it may use. It has been suggested more recently that the flagellum acts as a sensor of environmental wetness in regulating flagella-based swarming motility (182). Similarly, the type three secretion (T3S) needle, a structure related to flagella, may transmit signals of host contact for triggering the secretion and expression of T3S effector proteins (27, 68).

Besides the proposed sensor function in *M. xanthus* by this study, Tfp have been suspected to function in signal transduction in a few other scenarios. It is known that Tfp play critical roles in the colonization of epithelial cells by pathogenic *Neisseria* (97, 125) and enteropathogenic *Escherichia coli* (EPEC) (62). In both cases, microcolonies that initially formed on host surfaces eventually disperse into a single cell layer during later stages of the infection (120, 135, 174). This dispersal coincides with the disappearance of Tfp and appears to require pilus retraction. The signal for dispersal is possibly provided by contact between Tfp and epithelial cells (188). It was recently reported that the transcription of Tfp genes in *Actinobacillus pleuropneumoniae* is regulated by contact with host cells (28). In all of these cases, Tfp may function as sensors for contact with host cells for the regulation of downstream events. We report here for the first time that Tfp can signal through a chemotaxis-like signal transduction pathway possibly by acting as sensors of cell proximity. Although it is unclear how the protein filaments in the other cases may regulate their downstream events, the adoption of such filamentous protein protrusions as environmental sensors by bacteria is likely more widespread than previously thought.

# CHAPTER 4

## A Mutation in *cheW7* Suppresses *difA* Deletion in *Myxococcus xanthus*

## ABSTRACT

*Myxococcus xanthus* is a Gram-negative soil bacterium that undergoes multicellular differentiation or development when nutrients become limiting. Aggregation, which is part of the developmental process, requires the surface gliding motility of this bacterium. One component of *M. xanthus* motility, the social (S) gliding motility, enables the movement of cells in groups. Previous studies demonstrated that the cell surface associated exopolysaccharides (EPS) were required for *M. xanthus* S motility. *difA*, which encodes a homologue of methyl-accepting chemotaxis proteins (MCP), is required for EPS production and thus S motility and development. In this study, a suppressor of *difA* was isolated in order to identify additional regulators of EPS production. The suppressor mutation was found to reside at the *M. xanthus che7* chemotaxis gene cluster and the suppression was the result of a frame-shift mutation in *cheW7*. Further examination indicated that inactivation of *cheW7* may lead to the interaction of Mcp7 with DifC and DifE to reconstruct a functional Dif pathway in the regulation of EPS production. Our results may suggest that there are cross-talks between the Che7 and the Dif pathways under certain environmental conditions.

## INTRODUCTION

*Myxococcus xanthus* is a Gram-negative rod-shaped bacterium with a developmental cycle and surface motility known as gliding (53, 158). When nutrients are abundant, *M. xanthus* cells grow and divide as vegetative cells. Gliding enables cells to move and expand to new territories during the vegetative cell cycle. When nutrients become limiting, hundreds of thousands of cells can aggregate and organize into multicellular structures called fruiting bodies. Within fruiting bodies, cells undergo differentiation to form environmentally resistant myxospores. Gliding motility is essential for the aggregation and organization of the fruiting bodies during the developmental process.

*M*. *xanthus* possesses two genetically distinct forms of gliding motility: the adventurous (A) and the social (S) gliding motility systems (70, 71). A motility is described as the movement of well isolated cells whereas S motility is the movement of large cell groups. The proposed mechanism for A motility is slime secretion through nozzles localized at the cell poles (190). S motility, which is analogous to bacterial twitching motility, requires the extension and retraction of type IV pili (Tfp) (122, 149, 161, 167). In addition to Tfp, cell surface structures called exopolysaccharides (EPS) are also required for *M*. *xanthus* S motility and are proposed to function as triggers and anchors for Tfp retraction (105, 154, 157, 202).

The production of EPS in *M*. *xanthus* is known to be regulated by the Dif chemotaxis-like pathway (15, 25, 199, 202). *difA* encodes a homologue of methyl-accepting chemotaxis proteins (MCP), *difC* a homologue of CheW and *difE* a homologue of CheA (15, 199). DifA, DifC and DifE are proposed to form a ternary signaling complex required for EPS production, and thus are considered positive regulators. This proposal is based primarily on their similarities to known chemotaxis proteins, demonstrated protein-protein interactions and phenotypic analyses of mutant strains (15, 25, 199, 201, 202). Two other components of the Dif pathway, DifD and DifG, are homologous to CheY and CheC, respectively, and appear to function as negative regulators of signal flow through the core Dif pathway in regard to EPS production.

Many questions remain regarding how the Dif proteins regulate EPS production. To identify additional EPS regulators, a *difA* suppressor was isolated and characterized in this study. The suppressor mutation restored EPS production, as well as agglutination, S motility and development to a *difA* mutant. This suppression required both *difC* and *difE*. The suppressor mutation was mapped to the uncharacterized *M. xanthus che7* locus. More specifically, the mutation was found to be a frame-shift in *cheW7*, which extends the *cheW7* reading frame into the downstream gene. Our results suggest that elimination of *cheW7* may force Mcp7 to interact with and activate the Dif chemotaxis-like pathway.

## MATERIALS AND METHODS

**Bacterial strains and growth conditions.** *M. xanthus* strains and plasmids used in this study are listed in Table 4-1. *M. xanthus* was grown and maintained at 32°C on casitone-yeast extract (CYE) agar plates or in CYE liquid medium (45). Clone-fruiting (CF) agar plates were used to induce *M. xanthus* development (63). The *Escherichia coli* strains used in this study, XL1-Blue (Stratagene), DB3.1 (Invitrogen), and DH5α λ*pir* (144) were grown and maintained at 37°C on Luria-Burtani (LB) agar plates or in LB

Table 4-1. ***M. xanthus* strains and plasmids used in this study.**

| *M. xanthus* strains and plasmids | Relevant genotype or description | Source or reference |
|---|---|---|
| **Strains:** | | |
| DK1622 | Wild type | (85) |
| LS308 | Tn*5*$\Omega$1407 | (156) |
| YZ504 | $\Delta$*difA* | (199) |
| YZ101 | $\Delta$*difA cheW7-1* | This study |
| YZ601 | $\Delta$*difA* | (196) |
| YZ615 | $\Delta$*difE cheW7-1* | This study |
| YZ617 | $\Delta$*difC cheW7-1* | This study |
| YZ651 | $\Delta$*difA cheW7-1*, kan$^r$ | This study |
| YZ666 | $\Delta$*difA cheW7-1* | This study |
| YZ684 | $\Delta$*difA cheW7-1che7*::kan$^r$-linkage | This study |
| YZ687 | $\Delta$*difA che7*::kan$^r$-linkage | This study |
| YZ688 | $\Delta$*difA* + pWB515 | This study |
| YZ697 | $\Delta$*difA* + pWB530 | This study |
| YZ1600 | $\Delta$*difA* + pWB531 | This study |
| YZ1601 | $\Delta$*difA* $\Delta$*cheW7* | This study |
| YZ1604 | $\Delta$*difA* $\Delta$*cheW7* $\Delta$*mcp7* | This study |
| YZ1605 | $\Delta$*difA* $\Delta$*cheW7* $\Delta$*mcp7* att::pWB426 | This study |
| YZ1612 | $\Delta$*difA* $\Delta$*cheW7* $\Delta$*mcp7* att::pWB433 | This study |
| YZ1613 | $\Delta$*difA cheW7-1* $\Delta$*mcp7* | This study |
| YZ1615 | $\Delta$*difA* $\Delta$*cheW7* att::pWB435 | This study |
| YZ1616 | $\Delta$*difA* $\Delta$*cheW7* $\Delta$*mcp7* att::pWB435 | This study |
| YZ1617 | $\Delta$*difA cheW7-1* $\Delta$*mcp7* att::pWB433 | This study |
| BY132 | *magellan4*::*che7*, kan$^r$ | This study |
| | | |
| **Plasmids:** | | |
| pZErO-2 | Cloning vector, kan$^r$ | Invitrogen |
| pMycoMar | *magellan4* mutagenesis vector | (144) |
| pBR322 | Cloning vector, amp$^r$, tet$^r$ | (29) |
| pBJ113 | Cloning vector, kan$^r$, *galK* | (79) |
| pBY132 | *magellan4* isolated from BY132, kan$^r$ | This study |
| pWB116 | $\Delta$*difA* in-frame deletion, pBJ113 | (196) |
| pWB200 | Cloning vector, kan$^r$, *intP* (Mx8 att) | (196) |
| pWB300 | Cloning vector, tet$^r$, *intP* (Mx8 att) | This study |
| pWB410 | Cloning vector, tet$^r$, kan$^r$, *intP* (Mx8 att) | This study |
| pWB425 | Expression vector, kan$^r$, *intP* (Mx8 att) | This study |
| pWB426 | *Sac*I-*Not*I *che7* fragement in pWB425 | This study |
| pWB433 | *mcp7* PCR fragment in pWB425 | This study |
| pWB435 | *cheW7-1* PCR fragment in pWB425 | This study |
| pWB513 | PCR-2.5Mb from *che7* in pZErO-2 | This study |
| pWB515 | *Sac*I-*Not*I *che7* fragement in pZErO-2 | This study |
| pWB521 | PCR-downstream of *che7* in pZErO-2 | This study |
| pWB530 | *Sac*I-*Pst*I *che7* fragement in pZErO-2 | This study |
| pWB531 | *Cla*I-*Not*I *che7* fragement in pZErO-2 | This study |
| pWB534 | $\Delta$*cheW7mcp7* in-frame deletion in pBJ113 | This study |
| pWB552 | $\Delta$*cheW7* in-frame deletion in pBJ113 | This study |
| pWB553 | $\Delta$*mcp7* in-frame deletion in pBJ113 | This study |

[a] *cheW7-1* is the *difA* suppressor allele, see Results for more details.

liquid medium (124). Unless otherwise noted, agar plates contained 1.5% agar. When necessary, kanamycin was added to media at 100 μg/ml for selection purposes.

**Transposon mutagenesis.** *M*. *xanthus* cells were mutagenized by the *mariner* based transposon *magellan4* as previously described (144, 203). Approximately of 500 ng of pMycoMar, a plasmid harboring the transposon, was electroporated into *M*. *xanthus* strains (89). Mutagenized cells were recovered at 32°C and plated on CYE agar plates supplemented with kanamycin.

The site of transposon insertions was determined as previously described (203). Briefly, 1 μg of genomic DNA was digested with *Sac*II, an enzyme that does not cut within the *magellan4* sequence. The resulting DNA was used for self-ligation at a final concentration of 40 ng/μl. 5 μl of the ligation was electroporated into DH5α λ*pir*, an *E. coli* strain capable of propagating oriR6Kγ based plasmids. Plasmids were recovered from the transformants and sequenced using the primers MarR1 and/or MarL1 (203). The sequence was then compared with the *M*. *xanthus* genomic database at TIGR.

**Plasmid construction.** In order to make pWB425, the *M*. *xanthus* expression vector, pWB300 and pWB410 needed to be constructed first. To replace the kan$^r$ cassette in pWB200 with tet$^r$ (196), pWB200 was digested with *Bgl*II and *Rsr*II to release the kan$^r$ fragment. A *Bam*HI/*Ava*I fragment containing the tet$^r$ cassette was obtained from pBR322. Both the vector and the tet$^r$ fragment were blunt-ended with T4 DNA polymerase and ligated to generate pWB300. To construct pWB410, pWB300 was cut with *Ase*I, which removes part of the *lac* promoter, and treated with T4 DNA polymerase. The pWB300 backbone was ligated to a *Bsp*HI/*Apo*I kan$^r$ fragment from pZErO-2 (Invitrogen) treated with T4 DNA polymerase to create pWB410. pWB410 was constructed such that the kan$^r$ cassette and the selectable *lacZα-ccdB* lethal fusion would be driven off the kan$^r$ promoter. This plasmid was propagated in the *E. coli* strain, DB3.1 (Invitrogen), which is resistant to the toxic effects of CcdB. To construct pWB425, pWB410 was digested with *Bsp*HI, which released the origin of replication, the kan$^r$ backbone, and the tet$^r$ cassette. The origin of replication was ligated to the kan$^r$ backbone to create pWB425, a *M. xanthus* expression vector driven by the kan$^r$ promoter.

The plasmids used to create antibiotic linkages, pWB521 and pWB513, were constructed by PCR amplifying fragments in intergenic regions downstream of the *che7* locus or 2.5 Mb away from the *che7* locus, respectively, and cloning into the *Eco*RV site of pZErO-2. To create *cheW7*, *mcp7*, and *cheW7 mcp7* in-frame deletion plasmids, fragments containing both upstream and downstream sequences of *cheW7* and/or *mcp7* were generated PCR. The relevant fragments were joined by a two-step overlap PCR reaction and were cloned into pBJ113 (79). The resulting plasmids pWB552 (Δ*cheW7*), pWB553 (Δ*mcp7*), and pWB534 (Δ*cheW7* Δ*mcp7*) were used to delete specific portions of the *che7* locus as described below.

Plasmids containing different portions of *cheW7* and/or *mcp7* were constructed as follows (Fig. 4-3). pBY132 was constructed by digestion of genomic DNA from BY132 with *SphI* and self-ligation. The resulting plasmid contained *magellan4* and the full length *cheW7* and *mcp7*. The *Sac*I/*Not*I fragment from pBY132 was cloned into the same sites in pZErO-2 to construct pWB515. The *Sac*I/*Pst*I fragment from pWB515 was cloned into the same sites of pZErO-2 to generate pWB530. pWB531 was created by digesting pWB515 with *Hin*DIII and *Cla*I, treating with T4 DNA polymerase and religating. pWB426 was created by inserting the *Sac*I/*Not*I fragment from pWB515 into the same sites of pWB425. pWB433 and pWB435 were created by PCR amplification of fragments containing either *mcp7* or the mutant version of *cheW7* (*cheW7-1*), respectively, and cloning into the *Eco*RV site of pWB425.

***M*. *xanthus* strain construction.** All in-frame deletions were created in the *difA* suppressor strain (YZ101) or the *difA* deletion strain (YZ601). The deletion constructs pWB116, pWB552, pWB553, and pWB534 were electroporated into the relevant strains to create the deletion mutants YZ666 (*cheW7-1* Δ*difA*-full), YZ1601 (Δ*difA* Δ*cheW7*), YZ1604 (Δ*difA* Δ*cheW7* Δ*mcp7*), and YZ1613 (Δ*difA* *cheW7-1* Δ*mcp7*), respectively, using a kanamycin/galactokinase (KG) cassette as previously described (Table 4-1) (25, 79, 176). Mutant strains were verified by PCR and/or Southern blotting (146).

Linkages to the *che7* locus or 2.5 MB away from *che7* were accomplished by electroporation of pWB521 into YZ101 and YZ601, and pWB513 into YZ101 to create strains YZ684, YZ687, and YZ651, respectively. The transfer of existing mutations or the transfer of loci linked to an antibiotic marker from one strain to another strain was performed using genomic DNA transformations as previously described (177). Briefly, 3-5 µg of donor genomic DNA was electroporated into the recipient strain. After recovery, the transformed cells were concentrated and plated on selective medium.

Strains with various *che7* fragments integrated at the *che7* locus were constructed by electroporation of pWB515, pWB530, pWB531 into the relevant strains to create YZ688, YZ697, and YZ1600, respectively (Table 4-1 and Fig. 4-3). Strains ectopically expressing various *che7* fragments were constructed by electroporation of pWB426, pWB433, and pWB435 and allowing integration at the Mx8 attachment site of YZ1604 creating strains YZ1605, YZ1612, and YZ1616, respectively (Table 4-1 and Fig. 4-3).

**Assessment of development, S motility, and EPS production.** Strains to be tested were grown in CYE liquid medium and harvested during exponential growth. 5 µl of cells at of $5 \times 10^9$ cells/ml was spotted onto CYE plates containing 0.4% agar for analysis of S motility or on CF plates for development. Plates were incubated at 32°C for 5 days before documentation. Plates containing Congo red or Calcofluor white were used to examine EPS production. Briefly, 5 µl of cells at $5\times10^9$ cells/ml was spotted onto CYE plates supplemented with either Congo red (30 µg/ml) or Calcofluor white (50 µg/ml). Plates were incubated at 32°C for 5 days before documentation. Strains producing EPS appear as reddish-orange colored colonies as opposed to the yellow colonies formed by non-EPS producers on Congo red plates. On Calcofluor white plates, strains binding this dye, which is indicative of EPS production, can be visualized by fluorescent intensity when exposed to long-wave-length (365 nm) UV light.

## RESULTS

**Isolation of a *difA* suppressor in S motility.** The *difA* deletion mutant SW504 (199) was used as the parental strain for the isolation of *difA* suppressors. *difA* mutants, which are defective in S motility and EPS production, do not agglutinate or clump in liquid medium (199, 202). To enrich for spontaneous *difA* suppressors, SW504 cells were cultured in test tubes in liquid medium and incubated at 32°C for five days without agitation. 5 µl aliquots from the bottom of the test tubes were spotted on CYE plates containing 0.4% agar and incubated at 32°C for 5-7 days. *difA* mutants form compact colonies on soft agar plates due to the lack of S motility (152). Only cells that regained S motility would be expected to move away from the origin of inoculation. Cells from motile flares were purified as potential *difA* suppressors for further study (data not shown).

**A *difA* suppressor exhibits S motility, development and produces EPS.** A potential *difA* suppressor, designated YZ101, was examined for the suppression of *difA* in S motility, development, and EPS production. When examined macroscopically, the colonies of wild type are rough and dry on hard (1.5%) agar plates, whereas the colonies of *difA* mutants are smooth and glossy. The colonies of YZ101 appeared similar to that of the wild type, but not to those of *difA* mutants (data not shown). S motility was examined on soft (0.4%) agar plates as shown in Fig. 4-1. The nearly identical colony sizes of YZ101 and the wild-type strain suggested that S motility was restored in the suppressor. Likewise, YZ101 produced distinct fruiting bodies on CF medium as did the wild type (Fig. 4-1B). It was noted that the fruiting bodies of YZ101 distributed somewhat differently and formed predominately at the perimeter of the inoculation site.

In addition, the suppressor strain agglutinated (data not shown) and produced EPS (Fig. 4-2) similar to the wild type. The agglutination of YZ101 (data not shown), suggested that YZ101 produces EPS. EPS production was examined by the binding of Calcofluor white, see Materials and Methods (Fig. 4-2). YZ101, like the wild-type strain, fluoresced on these plates after exposure to UV light, indicating that YZ101 produces EPS (Fig. 4-2). These results confirmed the restoration of EPS production in the *difA* suppressor strain.

**The *difA* suppressor is not located at the *dif* locus.** The *difA* suppressor was expected to have resulted from a single mutation since it was isolated without mutagenesis. Several genetic experiments were conducted to examine if the suppressor

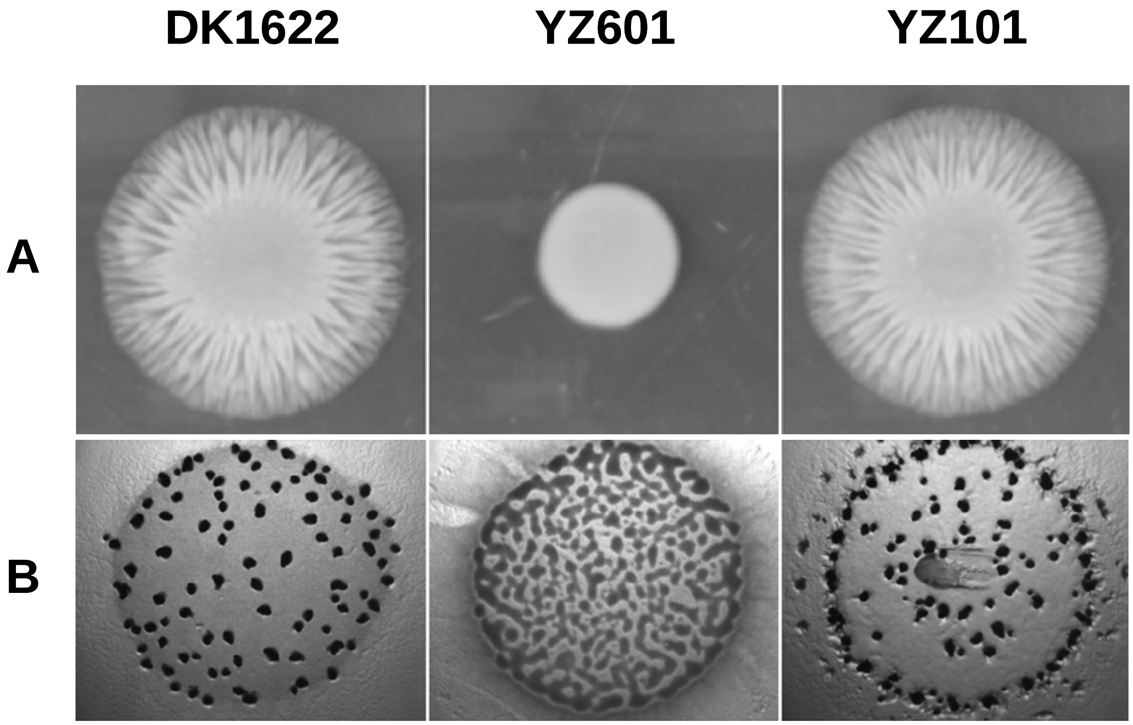

**Figure 4-1.** Analysis of S motility and development.

Analysis of S motility and development of *M. xanthus* strains. Five microliters of cells at a concentration of approximately 5 × $10^9$ cells/ml were spotted onto 0.4% CYE plates (A) or CF starvation agar plates (B) and incubated for 5 days at 32°C. DK1622, wild type; YZ601, Δ*difA*; YZ101, *difA* suppressor strain.

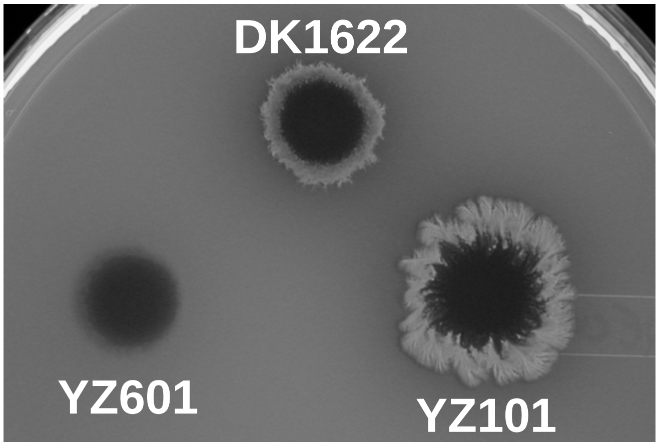

**Figure 4-2.** Analysis of EPS production.

Analysis of EPS production of *M. xanthus* strains. Five microliters of cells at a concentration of approximately 5 × $10^9$ cells/ml were spotted onto CYE agar plates supplemented with Calcofluor white (50 µg/ml) and incubated for 5 days at 32°C. DK1622, wild type; YZ601, Δ*difA*; YZ101, *difA* suppressor strain.

mutation resides at the *dif* locus. LS308, containing the Tn*5* insertion Ω1407 linked to the *dif* locus (100, 156, 202) was used as the donor for transductions of the suppressor, YZ101. The resulting transductants that lacked the *difA* gene were identified by immunoblotting with α-DifA antibodies. These transductants were found to display S motility and fruiting body development (data not shown) suggesting that the suppressor may not be linked to the *dif* locus. These experiments indicate that the suppression was not the result of a mutation at the *dif* locus.

**The suppression requires *difC* and *difE*.** *difC* or *difE* were deleted from YZ101 to determine if they were required for the suppression. The resulting mutants, YZ615 and YZ617, were found to lack development, S motility and EPS production (data not shown). These results indicated that *difC* and *difE* are required for the suppression in YZ101, and the suppressor likely functions upstream of DifC and DifE. One concern about the parental strain of the suppressor mutant was that the *difA* allele contained a deletion of only the C-terminus of DifA (199). The N-terminal transmembrane region is intact and could be involved in the suppression. To examine this possibility, we deleted the entire *difA* coding region using the previously constructed Δ*difA* plasmid, pWB116 (196). This deletion strain, YZ666, was indistinguishable from YZ101 in S motility, development and EPS production (data not shown). These finding indicate that YZ101 harbors a *difA* bypass suppressor that requires DifC and DifE for the suppression.

**The *difA* suppressor mutation is linked to the *M. xanthus che7* locus.** To identify the suppressor mutation, YZ101 was mutagenized with the *mariner* based transposon *magellan4* (144) and plated on CYE plates containing Congo red and kanamycin. EPS$^-$ transformants were identified by the lack of binding of Congo red. The insertion sites in these mutants were identified by cloning and sequencing. Seven of these insertions occurred at the *dif* locus in either *difC* or *difE*, confirming that *difC* and *difE* are required for the suppression. More importantly, five insertions occurred at the *M. xanthus che7* locus (Fig. 4-3), suggesting that the suppressor mutation in YZ101 may reside at the *che7* locus. These five *che7* transposon insertions were introduced into both the wild-type strain DK1622, and the original *difA* suppressor strain YZ101 by genomic DNA transformations (177). All five insertions in the YZ101 background were defective in Congo red binding, but the same insertions in the DK1622 background retained the ability to bind the dye. These findings suggest that the suppression in YZ101 is likely affiliated with the *che7* locus.

To determine if the suppressor mutation was located at the *che7* locus, a kanamycin resistance marker was inserted downstream of the *che7* cluster in an intergenic region as described in Materials and Methods (Table 4-2). The strains YZ687 and YZ684, contained insertions in the wild type and suppressor backgrounds, respectively, and maintained an EPS$^+$ phenotype. Genomic DNA isolated from YZ687 and YZ684 was used to transform YZ101 and YZ601, respectively. The transformants were analyzed for EPS production by the binding of Congo red. As shown in Table 4-2, among the 155 transformants from YZ101, 32 lost the ability to produce EPS. Among the 178 transformants from YZ601, 55 gained the ability to produce EPS. As a control, a kanamycin resistance marker was inserted ~2.5 Mb away from the *che7* locusin YZ101 to generate YZ651. When the genomic DNA from YZ651 was transformed into YZ601, all 108 transformants were EPS$^-$ (Table 4-2). Based on these results, it was concluded that the suppressor allele was located near the *che7* gene cluster.

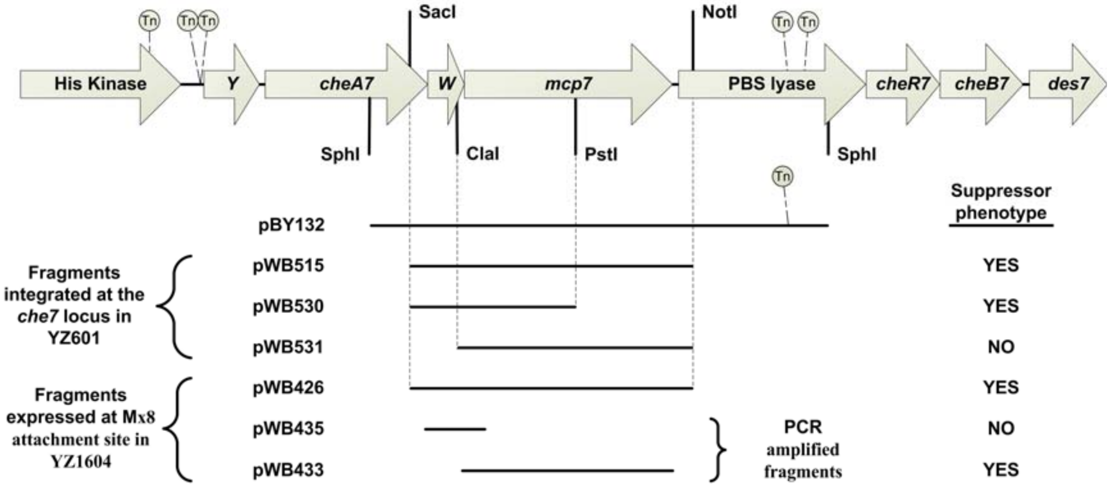
Tn
Tn
Tn
SacI
NotI
Tn
Tn
His Kinase
Y
cheA7
W
mcp7
PBS lyase
cheR7
cheB7
des7
SphI
ClaI
PstI
SphI
Tn
Suppressor phenotype
pBY132
Fragments integrated at the che7 locus in YZ601
pWB515
YES
pWB530
YES
pWB531
NO
Fragments expressed at Mx8 attachment site in YZ1604
pWB426
YES
pWB435
NO
pWB433
YES
PCR amplified fragments

**Figure 4-3.** Schematic of the *M. xanthus che7* locus.
The *che7* locus is approximately 13 kb and the gene lengths, transposon insertion sites, and restriction sites are all drawn to scale. Suppressor phenotype was determined by the ability to bind Congo red dye in plate assays. See the text for details on plasmids and strains.

**Table 4-2.** Cotransformation frequencies of kan$^{r}$ and *che7*.
Below details the cotransformation experiments of the suppressor phenotype with kan$^{r}$. Lower portion depicts how we established the kanamycin linkage to the *che7* locus.

| Donor Strain DNA | Recipient Strain | EPS$^{+}$ Transformants | EPS$^{-}$ Transformants | % Cotransformation |
|---|---|---|---|---|
| **YZ687** | **YZ101** | **123** | **32** | **20.6** |
| **YZ684** | **YZ601** | **55** | **123** | **30.8** |
| **YZ651** | **YZ601** | **0** | **108** | **0** |

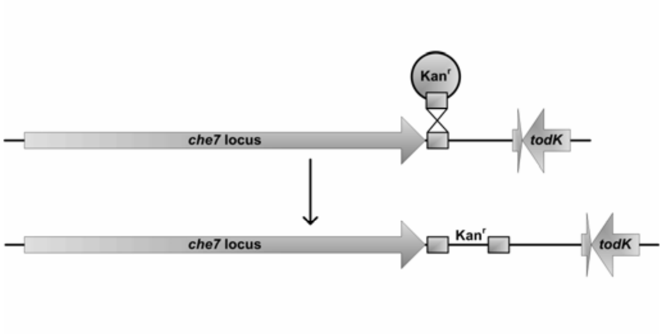

**The suppressor allele is located in *cheW7*.** Based on the understanding of the Dif pathway and the requirement of *difC* and *difE* for the suppression, it was reasoned that the suppressor mutation might have occurred in either *cheW7* or *mcp7*. To further define the location of the suppressor mutation, different DNA fragments from the *che7* locus (Fig. 4-3) were cloned from the suppressor strain YZ101 and analyzed for the suppression of the full *difA* deletion in YZ601. These constructs were transformed into YZ601, and the transformants were tested for EPS production. Only pWB515 and pWB530 were able to support the suppressor phenotype when integrated at the *che7* locus in YZ601 (Table 4-1 and Fig. 4-3). Since the fragment in pWB515 retained suppressor activity, it was sequenced to identify the suppressor mutation. One single insertion of a cytosine-guanine base pair was identified in *cheW7* and the suppressor mutation was therefore designated *cheW7-1*. CheW7 is predicted to have 148 amino acids, and this insertion created a polypeptide with 228 amino acids. The N-terminal 107 amino acids of the mutant CheW7-1 protein are from CheW7, while the rest has no homology to known proteins. The *cheW7-1* allele extended the *cheW7* open reading frame 256 base pairs into *mcp7*, the gene immediately downstream.

**Mechanism of the suppressor mutation.** The frame-shift mutation in *cheW7* suggested that a loss of function mutation in *cheW7* might be responsible for the suppression of *difA*. The entire *cheW7* coding region was deleted from the *difA* deletion mutant YZ601 to examine this possibility. The resulting strain, YZ1601, lacked EPS production (data not shown), suggesting that this may not be the mechanism of suppression. To examine the possibility that *cheW7-1* was a gain of function mutation the *cheW7-1* allele in pWB435 was expressed in the *difA cheW7* double deletion mutant, YZ1601 (data not shown) and the *difA cheW7 mcp7* triple deletion mutant, YZ1604 (Fig. 4-3). Both resulting strains, YZ1615 and YZ1616, were EPS$^-$ suggesting that this was not the mechanism of suppression either.

It is possible that the inactivation of *cheW7* together as well as the expression of *mcp7* is responsible for the observed suppression. Perhaps the *cheW7* deletion in YZ1601 may have somehow affected *mcp7* expression. In support of this idea, YZ1613, which contains a *mcp7* deletion in YZ101, was found to be defective in EPS production (data not shown). To examine this possibility, pWB433 was used to express Mcp7 in the *difA cheW7 mcp7* triple deletion strain, YZ1604, and in YZ1613. The resulting strains YZ1612 and YZ1617 produced EPS as examined by Congo red binding (Fig. 4-3). On the other hand, expression of Mcp7 in the *difA* deletion strain, YZ601, resulted in a strain that was EPS$^-$ (data not shown). These results are consistent with the proposal that the inactivation of CheW7 and the simultaneous expression of Mcp7 is responsible for the suppression of *difA* in YZ101.

## DISCUSSION

Here we report the identification of a *cheW7* frame-shift mutation as a *difA* (MCP-like) suppressor. Our results suggest that inactivation of *cheW7* mediates the interaction of Mcp7 with DifC (CheW-like) and DifE (CheA-like) to recreate a functional Dif pathway with regard to EPS production and thus restores development and S motility. Our results might indicate possible cross-talks between the Che7 and the Dif pathways under certain environmental conditions. On the other hand, preliminary yeast-two-hybrid

(Y2H) analysis failed to detect interactions between Mcp7 with either DifC or DifE (data not shown), suggesting that the proposed interactions, if exist, may be relatively weak.

There is apparent cross-talk between a few of the eight predicted *M*. *xanthus* Che pathways. It was thought initially that the multiple chemotaxis systems of *M*. *xanthus* controlled different cellular processes by the regulation of distinct outputs. Later discoveries revealed that some of the different *M*. *xanthus* Che systems may regulate the same or similar processes. For instance, the Frz chemotaxis pathway regulates the reversal frequency of both A and S motile cells (185). The *M*. *xanthus* Che4 system was recently reported to regulate the reversal frequency of S motile cells (177). Therefore, it appears that both the Frz and Che4 systems control cell reversals mediated by S motility. Likewise, both the Dif and Frz systems appear to regulate cell reversal of A motile cells. Besides EPS production, the Dif pathway has been implicated in excitation responses to distinct phosphatidylethanolamine (PE) species by increasing the time between cell reversals (30, 93). The experimental design of the PE excitation assay is based on monitoring A motile cells, so the Dif pathway is projected to control A motility based cell reversals. Furthermore, the Dif system appears to mediate the excitation aspect of PE taxis while the Frz system appears to mediate at least part of the PE adaptation response (91, 92). Collectively, these observations strongly suggest common points of contact, possibly the output targets, between the Frz and Che4 pathways for S motility and between the Dif and Frz pathways for A motility.

This particular *difA* suppressor mutation also helped to validate a previous hypothesis. Our previous observations suggested that Tfp function upstream of the Dif chemotaxis-like pathway to regulate the production of EPS (see Chapter 3). In support of that finding, we found that the *cheW7-1* mutation also suppressed the EPS production defects of *pilA* mutants (data not shown). In the suppressor strain, EPS production (the Dif pathway) is likely controlled by the input signals that regulate the activity of Mcp7. Even though the input signal for Mcp7 is unknown, the signal is not expected to be shared with DifA. This is consistent with our finding that the suppressor mutation also suppresses the EPS defects of *pilA* mutants if Tfp function as sensors of signals for the Dif pathway as we proposed. In support of Mcp7 and DifA sensing different inputs, the phenotypes of YZ101 were slightly different from the wild-type strain. Even though both development and EPS production were restored to YZ101, there were some obvious differences in the way they were restored (Fig. 4-1 and Fig. 4-2). This was most obvious in the Calcofluor white binding assay. YZ101 showed both increases in both colony size and level of dye binding. These differences in development and EPS production could be attributed to differences in signal inputs and/or regulation schemes of the Che7 and Dif pathways.

In addition, the identification of *cheW7-1* as a suppressor of *difA* suggests that *M. xanthus* may integrate the input signals of Mcp7 into the Dif pathway. It is also possible that the inactivation of *cheW7* may have created an artificial interaction between Mcp7 and the Dif pathway as a result of homologies between chemotaxis systems. Further investigation is undoubtedly necessary to distinguish between these possibilities.

# CHAPTER 5

## Identification of Additional Genes Involved in *Mycococcus xanthus* EPS Production

## INTRODUCTION

*Myxococcus xanthus* is a Gram-negative rod shaped social bacterium. When environmental conditions are favorable, *M. xanthus* cells grow and divide vegetatively as do other bacteria (55, 158). These cells glide over surfaces coordinating their movements as microbial wolf-packs, which are constantly in search of prey microorganisms as food sources. If the environmental conditions worsen, hundreds of thousands of preexisting *M. xanthus* cells have the capacity to aggregate and organize into multicellular structures called fruiting bodies. Within these developmental structures, cells can differentiate into environmentally resistant myxospores, which can germinate when conditions improve and reenter vegetative growth. The developmental process of *M. xanthus* is highly dependent on surface gliding motility.

In *M. xanthus* two genetically distinct motility systems drive the surface gliding of this bacterium (70, 71). Adventurous (A) motility is defined as the movement of single and well isolated cells. It was recently proposed that the mechanism that powers A motility is through the secretion of slime from the cell poles (190). The mechanism of social (S) motility or the movement of cell groups, is much better established. Both motility systems are critical for the *M. xanthus* developmental cycle, as most motility mutants are defective in development to varying degrees (71, 112).

S motility, mechanistically similar to bacterial twitching motility, is driven by the extension and retraction of type IV pili (Tfp) (122, 149, 161, 167). In *M. xanthus*, two cell surface structures are absolutely required for functional S motility, polarly localized Tfp and exopolysaccharides (EPS) (154, 192, 194, 202). EPS has been proposed to act as both the anchor and trigger for Tfp retraction (105). LPS O-antigen, another cell surface component, has been implicated in *M. xanthus* S motility (34, 200), but the role of LPS O-antigen in S motility is not clear.

Previous studies identified several genetic loci involved in the production of EPS in *M. xanthus*: the *dif* locus, *sglK*, *stk*, and the recently described *eps* and *eas* loci (48, 109, 188, 199, 202). In this study, genetic screens were carried out to identify additional genes involved in EPS production in *M. xanthus*. Using the fairly non-specific *mariner*-like transposon, *magellan4*, we identified mutants that were defective in EPS production and mutants that overproduced EPS. All of the loci expected to be identified in these screens were represented. More than 25 genes previously not known to be implicated in *M. xanthus* S motility or EPS production were identified. The characterization of these newly identified genes may facilitate the understanding of the regulation of EPS production and S motility in *M. xanthus*.

## MATERIALS AND METHODS

**Bacterial strains and plasmids used in this study.** The *M. xanthus* strains, DK10407 and YZ101, used and those generated in this study are isogenic derivatives of DK1622, a wild-type strain (85, 179) (for YZ101, see Chapter 4). *M. xanthus* strains were grown and maintained in casitone-yeast extract (CYE) liquid medium or on CYE agar plates at 32°C (45). The *Escherichia coli* strains used in this study, XL1-Blue (Stratagene) and DH5α λ*pir* (144), were grown and maintained in Luria-Burtani (LB) liquid medium or on LB agar plates (124). Agar plates contained 1.5% agar unless noted otherwise. Kanamycin (100 µg/ml) and oxytetracycline (15 µg/ml) were used for selection purposes when necessary.

**Generation and identification of EPS mutant strains.** The *mariner*-based transposon *magellan4* was used for the genetic screens. The *magellan4* element contains a kanamycin resistance cassette, the conditional oriR6Kγ origin of replication and the flanking sequences required for transposition (144). Approximately 500 ng of pMycoMar (containing *magellan4*) (144) was electroporated (89) into YZ101, DK1622, or DK10407. Electroporated cells were recovered for 4 hours in CYE medium at 32°C before plating on appropriate antibiotic-selective CYE plates containing the dye Congo red (30 µg/ml) (48).

**Identification of *magellan4* insertion sites in the *M. xanthus* chromosome.** The sequence around transposon insertions was determined as previously described (203). Briefly, 1 µg of genomic DNA was digested with *Sac*II or *Bss*HI, neither digest the *magellan4* sequence. The resulting DNA was self-ligated at a final concentration of 40 ng/µl. 5 µl of the ligation was transformed into DH5α λ*pir*, an *E. coli* strain capable of propagating plasmids with the oriR6Kγ origin of replication. Plasmids recovered from these transformants were sequenced using MarR1 and/or MarL1 as sequencing primers (203). The sequence was compared against the *M. xanthus* genomic database (TIGR).

**Transfer of *magellan4* linked mutations.** The transfer of *magellan4* linked mutations from one strain to another was performed using genomic DNA transformations as previously described (177). Briefly, 3-5 µg of genomic DNA from a donor strain was electroporated into two recipient strains, DK1622 and YZ101. After recovery, the transformed cells were concentrated and plated on selective media with Congo red.

## RESULTS

**Transposon mutagenesis to identify mutants defective in EPS production.** Previous results and observations by us and other investigators have delineated the importance of Tfp in the regulation of EPS production (see Chapter 3). In particular, *pil* mutants that fail to assemble intact Tfp are defective in the production of EPS. Our previous results indicated that a *difA* suppressor mutation mapping to the *M. xanthus che7* locus, suppresses the EPS production defects in *pilA* mutants and likely all other *pil* mutants (see Chapter 4 discussion). To circumvent and eliminate the background of *pil* gene insertions in our genetic screen for mutants defective in EPS production, we carried out transposon mutagenesis using the *difA* suppressor strain, YZ101 (see Chapter 4 for details on YZ101). This screen did not identify any of the known *pil* genes and in retrospect served two-goals, one to identify the suppressor allele and the other to identify unknown regulators of EPS production.

To identify additional genes required for EPS production, the *difA* suppressor strain YZ101 was mutagenized with the transposon *magellan4* (144) and plated on CYE plates with Congo red and kanamycin as describe in Materials and Methods. Strains defective in EPS production fail to bind the dye Congo red and appear as yellowish-orange colonies while those that produce EPS can bind Congo red and appear as reddish-orange colonies (48). Mutants that are defective in EPS production were identified by the lack of Congo red binding on selective plates (Fig. 5-1). These mutants in the YZ101 background were purified and numbered in order beginning with BY101. Of approximately 20,000 *magellan4* insertions obtained in this genetic screen, around 70 such mutants were isolated as defective in EPS production due to the lack of Congo red

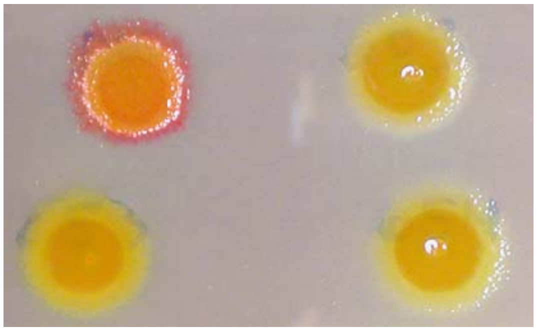

**Figure 5-1.** Example of *M. xanthus* binding Congo red.
Upper left, DK1622 (wild type); other strains, various EPS defective mutants.

binding. Some of these mutants were later found to be phase variant tan strains, and were still kept and might be evaluated at a later time.

**Identification of *magellan4* insertions in mutants defective in EPS production.** The location of *magellan4* insertions were identified as described in Material and Methods. All mutants had duplications of a TA dinucleotide flanking the transposon as expected (144), except BY121, in which *magellan4* is flanked by the duplication of a TCA trinucleotide. Among the mutants, only one strain was found to have two transposon insertions. Only one of two insertions was found to result in an EPS$^-$ phenotype when reintroduced into the suppressor background. Table 5-1 lists the mutants harboring insertions in the *che7* locus and in genes that are known to be involved in EPS production in *M. xanthus*. Insertions in the *che7* locus were EPS$^+$ when transferred into the wild-type strain and led to the identification of the *difA* suppressor allele (see Chapter 4 for details).

As expected, insertions occurred at both the *dif* and *eps* loci. Eight insertions were located in *difC* or *difE*, and 7 of these 8 were independent insertions (Table 5-1). The *eps* locus comprised the largest group of insertions. 10 of the 26 *eps* genes were disrupted 15 times in our screen. The *eps* locus was co-published from the results of several labs (109). Of particular significance was that 5 additional insertions at the *eps* locus occurred in two predicted open reading frames, ORF06786 and ORFC00825, that were not considered *eps* genes previously (109) and show no homology with known EPS biosynthesis proteins.

**Table 5-1.** Selected *magellan4* insertions causing defects in EPS production.

| Strain | 5'[a] | ORF[a] | Gene[b] |
|---|---|---|---|
| BY156 | 5805979 | ORF01351 | *rfbB* (O-antigen export) |
| BY105 | 5806193 | ORF01351 | *rfbB* (O-antigen export) |
| BY155 | 8232744 | ORF07676 | *difE* |
| BY145 | 8233503 | ORF07676 | *difE* |
| BY141 | 8233561 | ORF07676 | *difE* |
| BY167 | 8234665 | ORF07673/4 | intergenic between *difC* and *difD* |
| BY133 | 8234721 | ORF07673 | *difC* |
| BY151 | 8234848 | ORF07673 | *difC* |
| BY152 | 8234848 | ORF07673 | *difC* |
| BY139 | 8234968 | ORF07673 | *difC* |
| BY134 | 8517992 | ORF07364 | PBS lyase-like (*che7* locus) |
| BY132 | 8518169 | ORF07364 | PBS lyase-like (*che7* locus) |
| BY124 | 8525031 | ORF07361 | *cheY7* (upstream insertion) |
| BY115 | 8525031 | ORF07357 | *cheY7* (upstream insertion) |
| BY121 | 8525650 | ORF07356 | Histidine kinase (*che7* locus) |
| BY106 | 9039256 | ORF06813 | *epsZ* |
| BY142 | 9039673 | ORF06813 | *epsZ* |
| BY138 | 9040355 | ORF06813 | *epsZ* |
| BY127 | 9040370 | ORF06813 | *epsZ* |
| BY109 | 9040681 | ORF06812 | *epsY* |
| BY113 | 9040681 | ORF06812 | *epsY* |
| BY112 | 9042245 | ORF06810 | *epsY* |
| BY144 | 9043224 | ORFC00825 | hypothetical |
| BY114 | 9043437 | ORFC00825 | hypothetical |
| BY110 | 9045036 | ORF06805 | *epsV* |
| BY120 | 9046888 | ORF06804 | *epsU* |
| BY126 | 9047860 | ORF06803 | *epsT* |
| BY107 | 9049828 | ORFB07664 | transposase *orfB*, IS5 family (*epsP*) |
| BY147 | 9063915 | ORF06785 | *epsH* |
| BY135 | 9065368 | ORF06786 | putative membrane |
| BY102 | 9065413 | ORF06786 | putative membrane |
| BY101 | 9066088 | ORF06786 | putative membrane |
| BY104 | 9072872 | ORF06776 | *epsC* |
| BY123 | 9072910 | ORF06776 | *epsC* |
| BY157 | 9074392 | ORF06774 | *epsB* |
| BY137 | 9075610 | ORFA00949 | *epsA* |

[a] The 5’ gene coordinate of the insertion site and designated ORF number as obtained from the *M. xanthus* genomic database (TIGR).
[b] The known gene name or the predicted function or homology to known proteins.

Unexpectedly, our screen also identified two insertions at the *sasA* or *rfb* locus (Table 5-1). It is known that the *rfb* locus is involved in the production of LPS O-antigen (34). *magellan4* insertions in *rfbB* in a YZ101 background were observed to have a lower level of Congo red binding (data not shown), possibly indicating partial EPS production defects in this strain. On the other hand, *M. xanthus* has previously been predicted to have multiple Congo red binding sites on its cell surface (48). Decreased Congo red binding of an LPS O-antigen mutant might suggest that LPS O-antigen is the second target for Congo red binding. A Congo red dye binding assay using either a double *rfbB dif* mutant or *rfbB eps* mutant could be used to resolve this issue. These *rfbB* insertions have not been tested in a DK1622 background in regard to EPS production, which could provide additional details.

The remaining 25 genes identified in this screen were not previously implicated in EPS production in *M. xanthus*. All of these insertions will be transferred into the wild-type background to ensure their role in EPS production and will be the subject of future investigation. To clarify the naming of strains, *magellan4* back-crossed mutations are numbered with consistency for ease of future identification, for example: BY101 donor DNA transformed into YZ101 recipient cells yields BY901, whereas BY101 donor DNA transformed into DK1622 recipient cells yields strain BY1101.

**Transposon mutagenesis to isolate mutants overproducing EPS.** In addition to the genetic screen for mutants defective in EPS production, a screen was also initiated to identify EPS overproducers. Both DK1622 (wild type) and DK10407 (*pilA*) were mutagenized by *magellan4* in this screen. Our previous results suggested that *pil* mutants were defective in EPS production and could be suppressed by certain secondary loss of function mutations in other genes (see Chapters 3 and 4). For the negative regulator screens, the phenotype of DK10407 provided for an easier screen, the gain of EPS production, compared to an increase in EPS production, which would be observed in a wild-type DK1622 background. These strains are named as follows: potential overproducers in the DK1622 background are numbered beginning with BY601 while those in the DK10407 background begin with BY801.

**Identification of *magellan4* insertions in the putative overproducing EPS mutant strains.** The DNA sequence surrounding the sites of *magellan4* insertions was identified as described in Materials and Methods. All of these insertions had the typical *mariner*-type insertion. Of the two mutations identified in the DK10407 background, one of the insertions occurred in *stk*, a gene previously known to negatively regulate EPS production (48). *stk* encodes a homologue of DnaK, a member of the Hsp70 family. The results of a previous study using genetic epistasis with the *stk* allele and other S motility mutants suggested that a *stk* mutation might suppress a *pilA* mutation (48). The results from this study are consistent with that prediction. In total, eight insertion mutants were isolated as putative EPS overproducers from both the wild-type and DK10407 backgrounds. However, the potential involvement of the genes disrupted by *magellan4* in these strains, with the exception of the *stk* insertion, remains unclear. None of these genes encode homologues of proteins known to be involved in the regulation of EPS production. These remaining insertions will be characterized further and will be the focus of future investigation.

## DISCUSSION

Here we report the use of genetic screens to identify unknown gene involved in the production of EPS in *M. xanthus*. Prior to our screens, only three genetic loci had been implicated in EPS production, *dif*, *sglK*, and *stk* (15, 25, 48, 188, 199, 202). Our screens identified both the *dif* locus and *stk*, which validated the results obtained in our screens. We did not expect to hit *sglK* in our screen because genetic epistasis experiments indicate that the EPS defects of *sglK* mutants can be suppressed by the *difA* suppressor mutation (Black and Yang, unpublished data).

In addition to the loci known to be involved in EPS production our screen identified other previously unknown genes and loci. First, the majority of the genes identified in our screens were located in the *eps* biosynthetic locus, which was identified simultaneously by other labs (109). The remaining insertions, 25 in genes required for EPS production and 7 in genes that negatively regulate EPS, will be investigated in future studies.

# REFERENCES

1. **Adams, D. G., D. Ashworth, and B. Nelmes.** 1999. Fibrillar array in the cell wall of a gliding filamentous cyanobacterium. J. Bacteriol. **181:**884-92.

2. **Adler, J.** 1966. Chemotaxis in bacteria. Science **153:**708-16.

3. **Adler, J.** 1976. The sensing of chemicals by bacteria. Sci. Am. **234:**40-7.

4. **Agarwal, S., D. W. Hunnicutt, and M. J. McBride.** 1997. Cloning and characterization of the *Flavobacterium johnsoniae* (*Cytophaga johnsonae*) gliding motility gene, *gldA*. Proc. Natl. Acad. Sci. USA **94:**12139-44.

5. **Altschul, S. F., T. L. Madden, A. A. Schaffer, J. Zhang, Z. Zhang, W. Miller, and D. J. Lipman.** 1997. Gapped BLAST and PSI-BLAST: a new generation of protein database search programs. Nucleic Acids Res. **25:**3389-402.

6. **Anderson, K. L., and A. A. Salyers.** 1989. Biochemical evidence that starch breakdown by *Bacteroides thetaiotaomicron* involves outer membrane starch-binding sites and periplasmic starch-degrading enzymes. J. Bacteriol. **171:**3192-8.

7. **Anderson, K. L., and A. A. Salyers.** 1989. Genetic evidence that outer membrane binding of starch is required for starch utilization by *Bacteroides thetaiotaomicron*. J. Bacteriol. **171:**3199-204.

8. **Armitage, J. P., I. B. Holland, U. Jenal, and B. Kenny.** 2005. "Neural networks" in bacteria: making connections. J. Bacteriol. **187:**26-36.

9. **Arnold, J. W., and L. J. Shimkets.** 1988. Cell surface properties correlated with cohesion in *Myxococcus xanthus*. J. Bacteriol. **170:**5771-7.

10. **Arnold, J. W., and L. J. Shimkets.** 1988. Inhibition of cell-cell interactions in *Myxococcus xanthus* by congo red. J. Bacteriol. **170:**5765-70.

11. **Atsumi, T., L. McCarter, and Y. Imae.** 1992. Polar and lateral flagellar motors of marine Vibrio are driven by different ion-motive forces. Nature **355:**182-4.

12. **Bardy, S. L., S. Y. Ng, and K. F. Jarrell.** 2003. Prokaryotic motility structures. Microbiology **149:**295-304.

13. **Behmlander, R. M., and M. Dworkin.** 1994. Biochemical and structural analyses of the extracellular matrix fibrils of *Myxococcus xanthus*. J. Bacteriol. **176:**6295-303.

14. **Behmlander, R. M., and M. Dworkin.** 1991. Extracellular fibrils and contact-mediated cell interactions in *Myxococcus xanthus*. J. Bacteriol. **173:**7810-21.

15. **Bellenger, K., X. Ma, W. Shi, and Z. Yang.** 2002. A CheW homologue is required for *Myxococcus xanthus* fruiting body development, social gliding motility, and fibril biogenesis. J. Bacteriol. **184:**5654-60.

16. **Berg, H. C.** 1975. Bacterial behaviour. Nature **254:**389-92.

17. **Berg, H. C.** 1975. Chemotaxis in bacteria. Annu. Rev. Biophys. Bioeng. **4:**119-36.

18. **Berg, H. C.** 1971. How to track bacteria. Rev. Sci. Instrum. **42:**868-71.

19. **Berg, H. C.** 2003. The rotary motor of bacterial flagella. Annu. Rev. Biochem. **72:**19-54.

20. **Berg, H. C., and R. A. Anderson.** 1973. Bacteria swim by rotating their flagellar filaments. Nature **245:**380-2.

21. **Berleman, J. E., and C. E. Bauer.** 2005. A *che*-like signal transduction cascade involved in controlling flagella biosynthesis in *Rhodospirillum centenum*. Mol. Microbiol. **55:**1390-402.

22. **Berleman, J. E., and C. E. Bauer.** 2005. Involvement of a Che-like signal transduction cascade in regulating cyst cell development in *Rhodospirillum centenum*. Mol. Microbiol. **56:**1457-66.

23. **Bhaya, D.** 2004. Light matters: phototaxis and signal transduction in unicellular cyanobacteria. Mol. Microbiol. **53:**745-54.

24. **Bhaya, D., A. Takahashi, and A. R. Grossman.** 2001. Light regulation of type IV pilus-dependent motility by chemosensor-like elements in *Synechocystis* PCC6803. Proc. Natl. Acad. Sci. USA **98:**7540-5.

25. **Black, W. P., and Z. Yang.** 2004. *Myxococcus xanthus* chemotaxis homologs DifD and DifG negatively regulate fibril polysaccharide production. J. Bacteriol. **186:**1001-8.

26. **Blackhart, B. D., and D. R. Zusman.** 1985. "Frizzy" genes of *Myxococcus xanthus* are involved in control of frequency of reversal of gliding motility. Proc. Natl. Acad. Sci. USA **82:**8767-70.

27. **Blocker, A., K. Komoriya, and S. Aizawa.** 2003. Type III secretion systems and bacterial flagella: insights into their function from structural similarities. Proc. Natl. Acad. Sci. USA **100:**3027-30.

28. **Boekema, B. K., J. P. Van Putten, N. Stockhofe-Zurwieden, and H. E. Smith.** 2004. Host cell contact-induced transcription of the type IV fimbria gene cluster of *Actinobacillus pleuropneumoniae*. Infect. Immun. **72:**691-700.

29. **Bolivar, F., R. L. Rodriguez, P. J. Greene, M. C. Betlach, H. L. Heyneker, and H. W. Boyer.** 1977. Construction and characterization of new cloning vehicles. II. A multipurpose cloning system. Gene **2:**95-113.

30. **Bonner, P. J., Q. Xu, W. P. Black, Z. Li, Z. Yang, and L. J. Shimkets.** 2005. The Dif chemosensory pathway is directly involved in phosphatidylethanolamine sensory transduction in *Myxococcus xanthus*. Mol. Microbiol. **57:**1499-508.

31. **Borkovich, K. A., L. A. Alex, and M. I. Simon.** 1992. Attenuation of sensory receptor signaling by covalent modification. Proc. Natl. Acad. Sci. USA **89:**6756-60.

32. **Bourret, R. B., and A. M. Stock.** 2002. Molecular information processing: lessons from bacterial chemotaxis. J. Biol. Chem. **277:**9625-8.

33. **Bouveret, E., L. Journet, A. Walburger, E. Cascales, H. Benedetti, and R. Lloubes.** 2002. Analysis of the *Escherichia coli* Tol-Pal and TonB systems by periplasmic production of Tol, TonB, colicin, or phage capsid soluble domains. Biochimie. **84:**413-21.

34. **Bowden, M. G., and H. B. Kaplan.** 1998. The *Myxococcus xanthus* lipopolysaccharide O-antigen is required for social motility and multicellular development. Mol. Microbiol. **30:**275-84.

35. **Bradley, D. E.** 1974. The adsorption of *Pseudomonas aeruginosa* pilus-dependent bacteriophages to a host mutant with nonretractile pili. Virology **58:**149-63.

36. **Bradley, D. E.** 1980. A function of *Pseudomonas aeruginosa* PAO polar pili: twitching motility. Can. J. Microbiol. **26:**146-54.

37. **Bradley, D. E.** 1972. Shortening of *Pseudomonas aeruginosa* pili after RNA-phage adsorption. J. Gen. Microbiol. **72:**303-19.

38. **Braun, T. F., M. K. Khubbar, D. A. Saffarini, and M. J. McBride.** 2005. *Flavobacterium johnsoniae* gliding motility genes identified by *mariner* mutagenesis. J. Bacteriol. **187:**6943-52.

39. **Braun, T. F., and M. J. McBride.** 2005. *Flavobacterium johnsoniae* GldJ is a lipoprotein that is required for gliding motility. J. Bacteriol. **187:**2628-37.

40. **Bren, A., and M. Eisenbach.** 2000. How signals are heard during bacterial chemotaxis: protein-protein interactions in sensory signal propagation. J. Bacteriol. **182:**6865-73.

41. **Bretscher, A. P., and D. Kaiser.** 1978. Nutrition of *Myxococcus xanthus*, a fruiting myxobacterium. J. Bacteriol. **133:**763-8.

42. **Burkart, M., A. Toguchi, and R. M. Harshey.** 1998. The chemotaxis system, but not chemotaxis, is essential for swarming motility in *Escherichia coli*. Proc. Natl. Acad. Sci. USA **95:**2568-73.

43. **Burrows, L. L.** 2005. Weapons of mass retraction. Mol. Microbiol. **57:**878-88.

44. **Caberoy, N. B., R. D. Welch, J. S. Jakobsen, S. C. Slater, and A. G. Garza.** 2003. Global mutational analysis of NtrC-like activators in *Myxococcus xanthus*: identifying activator mutants defective for motility and fruiting body development. J. Bacteriol. **185:**6083-94.

45. **Campos, J. M., and D. R. Zusman.** 1975. Regulation of development in *Myxococcus xanthus*: effect of 3':5'-cyclic AMP, ADP, and nutrition. Proc. Natl. Acad. Sci. USA **72:**518-22.

46. **Chiang, P., M. Habash, and L. L. Burrows.** 2005. Disparate subcellular localization patterns of *Pseudomonas aeruginosa* Type IV pilus ATPases involved in twitching motility. J. Bacteriol. **187:**829-39.

47. **Craig, L., M. E. Pique, and J. A. Tainer.** 2004. Type IV pilus structure and bacterial pathogenicity. Nat. Rev. Microbiol. **2:**363-78.

48. **Dana, J. R., and L. J. Shimkets.** 1993. Regulation of cohesion-dependent cell interactions in *Myxococcus xanthus*. J. Bacteriol. **175:**3636-47.

49. **Darzins, A., and M. A. Russell.** 1997. Molecular genetic analysis of type-4 pilus biogenesis and twitching motility using *Pseudomonas aeruginosa* as a model system - a review. Gene **192:**109-15.

50. **Dawid, W.** 2000. Biology and global distribution of myxobacteria in soils. FEMS Microbiol. Rev. **24:**403-27.

51. **Drews, G.** 2005. Contributions of Theodor Wilhelm Engelmann on phototaxis, chemotaxis, and photosynthesis. Photosynth. Res. **83:**25-34.

52. **Dworkin, M.** 1973. Cell-cell interactions in the myxobacteria. Symp. Soc. Gen. Microbiol. **23:**125-142.

53. **Dworkin, M.** 2000. Introduction to myxobacteria, p. 221-242. *In* Y. V. B. a. L. J. Shimkets (ed.), Prokaryotic development. ASM Press, Washington, D.C.

54. **Dworkin, M.** 1962. Nutritional requirements for vegetative growth of *Myxococcus xanthus*. J. Bacteriol. **84:**250-7.

55. **Dworkin, M.** 1996. Recent advances in the social and developmental biology of the myxobacteria. Microbiol. Rev. **60:**70-102.

56. **Dworkin, M., and D. Kaiser.** 1993. Myxobacteria II. American Society for Microbiology, Washington, D.C.

57. **Fahrner, K. A., W. S. Ryu, and H. C. Berg.** 2003. Biomechanics: bacterial flagellar switching under load. Nature **423:**938.

58. **Falke, J. J., R. B. Bass, S. L. Butler, S. A. Chervitz, and M. A. Danielson.** 1997. The two-component signaling pathway of bacterial chemotaxis: a molecular view of signal transduction by receptors, kinases, and adaptation enzymes. Annu. Rev. Cell. Dev. Biol. **13:**457-512.

59. **Forest, K. T., and J. A. Tainer.** 1997. Type-4 pilus-structure: outside to inside and top to bottom--a minireview. Gene **192:**165-9.

60. **Fudou, R., Y. Jojima, T. Iizuka, and S. Yamanaka.** 2002. *Haliangium ochraceum* gen. nov., sp. nov. and *Haliangium tepidum* sp. nov.: novel moderately halophilic myxobacteria isolated from coastal saline environments. J. Gen. Appl. Microbiol. **48:**109-16.

61. **Gill, J., E. Stellwag, and M. Dworkin.** 1985. Monoclonal antibodies against cell-surface antigens of developing cells of *Myxococcus xanthus*. Ann. Inst. Pasteur. Microbiol. **136A:**11-8.

62. **Giron, J. A., A. S. Ho, and G. K. Schoolnik.** 1991. An inducible bundle-forming pilus of enteropathogenic *Escherichia coli*. Science **254:**710-3.

63. **Hagen, D. C., A. P. Bretscher, and D. Kaiser.** 1978. Synergism between morphogenetic mutants of *Myxococcus xanthus*. Dev. Biol. **64:**284-96.

64. **Harris, B. Z., D. Kaiser, and M. Singer.** 1998. The guanosine nucleotide (p)ppGpp initiates development and A-factor production in *Myxococcus xanthus*. Genes Dev. **12:**1022-35.

65. **Harshey, R. M.** 1994. Bees aren't the only ones: swarming in gram-negative bacteria. Mol. Microbiol. **13:**389-94.

66. **Harshey, R. M., and T. Matsuyama.** 1994. Dimorphic transition in *Escherichia coli* and *Salmonella typhimurium*: surface-induced differentiation into hyperflagellate swarmer cells. Proc. Natl. Acad. Sci. USA **91:**8631-5.

67. **Hartzell, P. L., and P. Youderian.** 1995. Genetics of gliding motility and development in *Myxococcus xanthus*. Arch. Microbiol. **164:**309-23.

68. **He, S. Y., K. Nomura, and T. S. Whittam.** 2004. Type III protein secretion mechanism in mammalian and plant pathogens. Biochim. Biophys. Acta. **1694:**181-206.

69. **Henrichsen, J.** 1972. Bacterial surface translocation: a survey and a classification. Bacteriol. Rev. **36:**478-503.

70. **Hodgkin, J. a. D. K.** 1979. Genetics of gliding motility in *Myxococcus xanthus* (Myxobacterales): genes controlling movement of single cells. Mol. Gen. Genet. **171:**167-176.

71. **Hodgkin, J. a. D. K.** 1979. Genetics of gliding motility in *Myxococcus xanthus*: two gene systems control movement. Mol. Gen. Genet. **171:**177-191.

72. **Hoiczyk, E.** 2000. Gliding motility in cyanobacterial: observations and possible explanations. Arch. Microbiol. **174:**11-7.

73. **Hoiczyk, E., and W. Baumeister.** 1998. The junctional pore complex, a prokaryotic secretion organelle, is the molecular motor underlying gliding motility in cyanobacteria. Curr. Biol. **8:**1161-8.

74. **Hunnicutt, D. W., M. J. Kempf, and M. J. McBride.** 2002. Mutations in *Flavobacterium johnsoniae gldF* and *gldG* disrupt gliding motility and interfere with membrane localization of GldA. J. Bacteriol. **184:**2370-8.

75. **Hunnicutt, D. W., and M. J. McBride.** 2000. Cloning and characterization of the *Flavobacterium johnsoniae* gliding-motility genes *gldB* and *gldC*. J. Bacteriol. **182:**911-8.

76. **Hunnicutt, D. W., and M. J. McBride.** 2001. Cloning and characterization of the *Flavobacterium johnsoniae* gliding motility genes *gldD* and *gldE*. J. Bacteriol. **183:**4167-75.

77. **Iizuka, T., Y. Jojima, R. Fudou, A. Hiraishi, J. W. Ahn, and S. Yamanaka.** 2003. *Plesiocystis pacifica* gen. nov., sp. nov., a marine myxobacterium that contains dihydrogenated menaquinone, isolated from the Pacific coasts of Japan. Int. J. Syst. Evol. Microbiol. **53:**189-95.

78. **Iizuka, T., Y. Jojima, R. Fudou, and S. Yamanaka.** 1998. Isolation of myxobacteria from the marine environment. FEMS Microbiol Lett **169:**317-22.

79. **Julien, B., A. D. Kaiser, and A. Garza.** 2000. Spatial control of cell differentiation in *Myxococcus xanthus*. Proc. Natl. Acad. Sci. USA **97:**9098-103.

80. **Jurica, M. S., and B. L. Stoddard.** 1998. Mind your B's and R's: bacterial chemotaxis, signal transduction and protein recognition. Structure **6:**809-13.

81. **Kaiser, D.** 2000. Bacterial motility: how do pili pull? Curr. Biol. **10:**R777-80.

82. **Kaiser, D.** 2003. Coupling cell movement to multicellular development in myxobacteria. Nat. Rev. Microbiol. **1:**45-54.

83. **Kaiser, D.** 1993. Roland Thaxter's legacy and the origins of multicellular development. Genetics **135:**249-54.

84. **Kaiser, D.** 2004. Signaling in myxobacteria. Annu. Rev. Microbiol. **58:**75-98.

85. **Kaiser, D.** 1979. Social gliding is correlated with the presence of pili in *Myxococcus xanthus*. Proc. Natl. Acad. Sci. USA **76:**5952-6.

86. **Kaiser, D., C. Manoil, and M. Dworkin.** 1979. Myxobacteria: cell interactions, genetics, and development. Annu. Rev. Microbiol. **33:**595-639.

87. **Kaplan, H. B.** 2003. Multicellular development and gliding motility in Myxococcus xanthus. Curr Opin Microbiol **6:**572-7.

88. **Karatan, E., M. M. Saulmon, M. W. Bunn, and G. W. Ordal.** 2001. Phosphorylation of the response regulator CheV is required for adaptation to attractants during *Bacillus subtilis* chemotaxis. J. Biol. Chem. **276:**43618-26.

89. **Kashefi, K., and P. L. Hartzell.** 1995. Genetic suppression and phenotypic masking of a *Myxococcus xanthus frzF-* defect. Mol. Microbiol. **15:**483-94.

90. **Kearns, D. B., P. J. Bonner, D. R. Smith, and L. J. Shimkets.** 2002. An extracellular matrix-associated zinc metalloprotease is required for dilauroyl phosphatidylethanolamine chemotactic excitation in *Myxococcus xanthus*. J. Bacteriol. **184:**1678-84.

91. **Kearns, D. B., B. D. Campbell, and L. J. Shimkets.** 2000. *Myxococcus xanthus* fibril appendages are essential for excitation by a phospholipid attractant. Proc. Natl. Acad. Sci. USA **97:**11505-10.

92. **Kearns, D. B., and L. J. Shimkets.** 1998. Chemotaxis in a gliding bacterium. Proc. Natl. Acad. Sci. USA **95:**11957-62.

93. **Kearns, D. B., and L. J. Shimkets.** 2001. Lipid chemotaxis and signal transduction in *Myxococcus xanthus*. Trends Microbiol. **9:**126-9.

94. **Kim, S. H., S. Ramaswamy, and J. Downard.** 1999. Regulated exopolysaccharide production in *Myxococcus xanthus*. J. Bacteriol. **181:**1496-507.

95. **Kim, S. K., and D. Kaiser.** 1990. Cell alignment required in differentiation of *Myxococcus xanthus*. Science **249:**926-8.

96. **Kirby, J. R., C. J. Kristich, M. M. Saulmon, M. A. Zimmer, L. F. Garrity, I. B. Zhulin, and G. W. Ordal.** 2001. CheC is related to the family of flagellar switch proteins and acts independently from CheD to control chemotaxis in *Bacillus subtilis*. Mol. Microbiol. **42:**573-85.

97. **Kirby, J. R., and D. R. Zusman.** 2003. Chemosensory regulation of developmental gene expression in *Myxococcus xanthus*. Proc. Natl. Acad. Sci. USA **100:**2008-13.

98. **Koomey, M.** 2001. Implications of molecular contacts and signaling initiated by *Neisseria gonorrhoeae*. Curr. Opin. Microbiol. **4:**53-7.

99. **Kroos, L., A. Kuspa, and D. Kaiser.** 1986. A global analysis of developmentally regulated genes in *Myxococcus xanthus*. Dev. Biol. **117:**252-66.

100. **Lancero, H., J. E. Brofft, J. Downard, B. W. Birren, C. Nusbaum, J. Naylor, W. Shi, and L. J. Shimkets.** 2002. Mapping of *Myxococcus xanthus* social motility *dsp* mutations to the *dif* genes. J. Bacteriol. **184:**1462-5.

101. **Lapidus, I. R., and H. C. Berg.** 1982. Gliding motility of *Cytophaga* sp. strain U67. J. Bacteriol. **151:**384-98.

102. **Larsen, S. H., R. W. Reader, E. N. Kort, W. W. Tso, and J. Adler.** 1974. Change in direction of flagellar rotation is the basis of the chemotactic response in *Escherichia coli*. Nature **249:**74-7.

103. **Lee, K., and L. J. Shimkets.** 1994. Cloning and characterization of the *socA* locus which restores development to *Myxococcus xanthus* C-signaling mutants. J. Bacteriol. **176:**2200-9.

104. **Lee, K., and L. J. Shimkets.** 1996. Suppression of a signaling defect during *Myxococcus xanthus* development. J. Bacteriol. **178:**977-84.

105. **Li, Y., H. Sun, X. Ma, A. Lu, R. Lux, D. Zusman, and W. Shi.** 2003. Extracellular polysaccharides mediate pilus retraction during social motility of *Myxococcus xanthus*. Proc. Natl. Acad. Sci. USA **100:**5443-8.

106. **Li, Y. Z., W. Hu, Y. Q. Zhang, Z. Qiu, Y. Zhang, and B. H. Wu.** 2002. A simple method to isolate salt-tolerant myxobacteria from marine samples. J. Microbiol. Methods **50:**205-9.

107. **Lloubes, R., E. Cascales, A. Walburger, E. Bouveret, C. Lazdunski, A. Bernadac, and L. Journet.** 2001. The Tol-Pal proteins of the *Escherichia coli* cell envelope: an energized system required for outer membrane integrity? Res. Microbiol. **152:**523-9.

108. **Lobedanz, S., and L. Sogaard-Andersen.** 2003. Identification of the C-signal, a contact-dependent morphogen coordinating multiple developmental responses in *Myxococcus xanthus*. Genes Dev. **17:**2151-61.

109. **Lu, A., K. Cho, W. P. Black, X. Y. Duan, R. Lux, Z. Yang, H. B. Kaplan, D. R. Zusman, and W. Shi.** 2005. Exopolysaccharide biosynthesis genes required for social motility in *Myxococcus xanthus*. Mol. Microbiol. **55:**206-20.

110. **Lukat, G. S., W. R. McCleary, A. M. Stock, and J. B. Stock.** 1992. Phosphorylation of bacterial response regulator proteins by low molecular weight phospho-donors. Proc. Natl. Acad. Sci. USA **89:**718-22.

111. **Macnab, R. M.** 2004. Type III flagellar protein export and flagellar assembly. Biochim. Biophys. Acta. **1694:**207-17.

112. **MacNeil, S. D., A. Mouzeyan, and P. L. Hartzell.** 1994. Genes required for both gliding motility and development in *Myxococcus xanthus*. Mol. Microbiol. **14:**785-95.

113. **Manson, M. D., P. Tedesco, H. C. Berg, F. M. Harold, and C. Van der Drift.** 1977. A protonmotive force drives bacterial flagella. Proc. Natl. Acad. Sci. USA **74:**3060-4.

114. **Mattick, J. S.** 2002. Type IV pili and twitching motility. Annu. Rev. Microbiol. **56:**289-314.

115. **McBride, M. J.** 2001. Bacterial gliding motility: multiple mechanisms for cell movement over surfaces. Annu. Rev. Microbiol. **55:**49-75.

116. **McBride, M. J.** 2004. Cytophaga-flavobacterium gliding motility. J. Mol. Microbiol. Biotechnol. **7:**63-71.

117. **McBride, M. J., and M. J. Kempf.** 1996. Development of techniques for the genetic manipulation of the gliding bacterium *Cytophaga johnsonae*. J. Bacteriol. **178:**583-90.

118. **McBride, M. J., R. A. Weinberg, and D. R. Zusman.** 1989. "Frizzy" aggregation genes of the gliding bacterium *Myxococcus xanthus* show sequence similarities to the chemotaxis genes of enteric bacteria. Proc. Natl. Acad. Sci. USA **86:**424-8.

119. **McCarter, L. L.** 2001. Polar flagellar motility of the Vibrionaceae. Microbiol. Mol. Biol. Rev. **65:**445-62.

120. **Merroun, M. L., K. Ben Chekroun, J. M. Arias, and M. T. Gonzalez-Munoz.** 2003. Lanthanum fixation by *Myxococcus xanthus*: cellular location and extracellular polysaccharide observation. Chemosphere **52:**113-20.

121. **Merz, A. J., C. A. Enns, and M. So.** 1999. Type IV pili of pathogenic Neisseriae elicit cortical plaque formation in epithelial cells. Mol. Microbiol. **32:**1316-32.

122. **Merz, A. J., M. So, and M. P. Sheetz.** 2000. Pilus retraction powers bacterial twitching motility. Nature **407:**98-102.

123. **Mignot, T., J. P. Merlie, Jr., and D. R. Zusman.** 2005. Regulated pole-to-pole oscillations of a bacterial gliding motility protein. Science **310:**855-7.

124. **Miller, J. H.** 1972. Experiments in molecular genetics. Cold Spring Harbor Laboratory, Cold Spring Harbor, N.Y.

125. **Morand, P. C., E. Bille, S. Morelle, E. Eugene, J. L. Beretti, M. Wolfgang, T. F. Meyer, M. Koomey, and X. Nassif.** 2004. Type IV pilus retraction in pathogenic *Neisseria* is regulated by the PilC proteins. Embo J. **23:**2009-17.

126. **Nassif, X., C. Pujol, P. Morand, and E. Eugene.** 1999. Interactions of pathogenic *Neisseria* with host cells. Is it possible to assemble the puzzle? Mol. Microbiol. **32:**1124-32.

127. **Neidhardt, F. C., and R. Curtiss.** 1996. *Escherichia coli* and *Salmonella*: cellular and molecular biology, 2nd ed. ASM Press, Washington, D.C.

128. **Nudleman, E., and D. Kaiser.** 2004. Pulling together with type IV pili. J. Mol. Microbiol. Biotechnol. **7:**52-62.

129. **Nudleman, E., D. Wall, and D. Kaiser.** 2005. Cell-to-cell transfer of bacterial outer membrane lipoproteins. Science **309:**125-127.

130. **O'Connor, K. A., and D. R. Zusman.** 1986. Genetic analysis of *Myxococcus xanthus* and isolation of gene replacements after transduction under conditions of limited homology. J. Bacteriol. **167:**744-8.

131. **Park, S. Y., X. Chao, G. Gonzalez-Bonet, B. D. Beel, A. M. Bilwes, and B. R. Crane.** 2004. Structure and function of an unusual family of protein phosphatases: the bacterial chemotaxis proteins CheC and CheX. Mol. Cell **16:**563-74.

132. **Parkinson, J. S.** 2003. Bacterial chemotaxis: a new player in response regulator dephosphorylation. J. Bacteriol. **185:**1492-4.

133. **Pate, J. L.** 1988. Gliding motility in procaryotic cells. Can. J. Microbiol. **34:**459-465.

134. **Pate, J. L., and Chang, L. E.** 1979. Evidence that gliding motility in prokaryotic cells is driven by rotary assemblies in the cell envelopes. Curr. Microbiol. **2:**59-64.

135. **Pugsley, A. P.** 1993. The complete general secretory pathway in gram-negative bacteria. Microbiol. Rev. **57:**50-108.

136. **Pujol, C., E. Eugene, M. Marceau, and X. Nassif.** 1999. The meningococcal PilT protein is required for induction of intimate attachment to epithelial cells following pilus-mediated adhesion. Proc. Natl. Acad. Sci. USA **96:**4017-22.

137. **Ramaswamy, S., M. Dworkin, and J. Downard.** 1997. Identification and characterization of *Myxococcus xanthus* mutants deficient in calcofluor white binding. J. Bacteriol. **179:**2863-71.

138. **Reichenbach, H.** 1999. The ecology of the myxobacteria. Environ. Microbiol. **1:**15-21.

139. **Rodriguez-Soto, J. P., and D. Kaiser.** 1997. The *tgl* gene: social motility and stimulation in *Myxococcus xanthus*. J. Bacteriol. **179:**4361-71.

140. **Rodriguez, A. M., and A. M. Spormann.** 1999. Genetic and molecular analysis of *cglB*, a gene essential for single-cell gliding in *Myxococcus xanthus*. J. Bacteriol. **181:**4381-90.

141. **Rosario, M. M., K. L. Fredrick, G. W. Ordal, and J. D. Helmann.** 1994. Chemotaxis in *Bacillus subtilis* requires either of two functionally redundant CheW homologs. J. Bacteriol. **176:**2736-9.

142. **Rosario, M. M., J. R. Kirby, D. A. Bochar, and G. W. Ordal.** 1995. Chemotactic methylation and behavior in *Bacillus subtilis*: role of two unique proteins, CheC and CheD. Biochemistry **34:**3823-31.

143. **Rosenberg, E., K. H. Keller, and M. Dworkin.** 1977. Cell density-dependent growth of *Myxococcus xanthus* on casein. J. Bacteriol. **129:**770-7.

144. **Rubin, E. J., B. J. Akerley, V. N. Novik, D. J. Lampe, R. N. Husson, and J. J. Mekalanos.** 1999. I*n vivo* transposition of *mariner*-based elements in enteric bacteria and mycobacteria. Proc. Natl. Acad. Sci. USA **96:**1645-50.

145. **Russel, M.** 1998. Macromolecular assembly and secretion across the bacterial cell envelope: type II protein secretion systems. J. Mol. Biol. **279:**485-99.

146. **Sambrook, J., and D. W. Russell.** 2001. Molecular cloning : a laboratory manual, 3rd ed. Cold Spring Harbor Laboratory Press, Cold Spring Harbor, N.Y.

147. **Sanford, R. A., J. R. Cole, and J. M. Tiedje.** 2002. Characterization and description of *Anaeromyxobacter dehalogenans* gen. nov., sp. nov., an aryl-halorespiring facultative anaerobic myxobacterium. Appl. Environ. Microbiol. **68:**893-900.

148. **Schmitt, R.** 2002. Sinorhizobial chemotaxis: a departure from the enterobacterial paradigm. Microbiology **148:**627-31.

149. **Semmler, A. B., C. B. Whitchurch, and J. S. Mattick.** 1999. A re-examination of twitching motility in *Pseudomonas aeruginosa*. Microbiology **145:**2863-73.

150. **Shah, D. S., S. L. Porter, A. C. Martin, P. A. Hamblin, and J. P. Armitage.** 2000. Fine tuning bacterial chemotaxis: analysis of *Rhodobacter sphaeroides* behaviour under aerobic and anaerobic conditions by mutation of the major chemotaxis operons and *cheY* genes. Embo J. **19:**4601-13.

151. **Shi, W., T. Kohler, and D. R. Zusman.** 1993. Chemotaxis plays a role in the social behaviour of *Myxococcus xanthus*. Mol. Microbiol. **9:**601-11.

152. **Shi, W., and D. R. Zusman.** 1993. The two motility systems of *Myxococcus xanthus* show different selective advantages on various surfaces. Proc. Natl. Acad. Sci. USA **90:**3378-82.

153. **Shimkets, L., and C. R. Woese.** 1992. A phylogenetic analysis of the myxobacteria: basis for their classification. Proc. Natl. Acad. Sci. USA **89:**9459-63.

154. **Shimkets, L. J.** 1986. Correlation of energy-dependent cell cohesion with social motility in *Myxococcus xanthus*. J. Bacteriol. **166:**837-41.

155. **Shimkets, L. J.** 1999. Intercellular signaling during fruiting-body development of *Myxococcus xanthus*. Annu. Rev. Microbiol. **53:**525-49.

156. **Shimkets, L. J.** 1986. Role of cell cohesion in *Myxococcus xanthus* fruiting body formation. J. Bacteriol. **166:**842-8.

157. **Shimkets, L. J.** 1989. The role of the cell surface in social and adventurous behaviour of myxobacteria. Mol. Microbiol. **3:**1295-9.

158. **Shimkets, L. J.** 1990. Social and developmental biology of the myxobacteria. Microbiol. Rev. **54:**473-501.

159. **Silversmith, R. E., G. P. Guanga, L. Betts, C. Chu, R. Zhao, and R. B. Bourret.** 2003. CheZ-mediated dephosphorylation of the *Escherichia coli* chemotaxis response regulator CheY: role for CheY glutamate 89. J. Bacteriol. **185:**1495-502.

160. **Singer, M., and D. Kaiser.** 1995. Ectopic production of guanosine penta- and tetraphosphate can initiate early developmental gene expression in *Myxococcus xanthus*. Genes Dev. **9:**1633-44.

161. **Skerker, J. M., and H. C. Berg.** 2001. Direct observation of extension and retraction of type IV pili. Proc. Natl. Acad. Sci. USA **98:**6901-4.

162. **Sourjik, V., and R. Schmitt.** 1996. Different roles of CheY1 and CheY2 in the chemotaxis of Rhizobium meliloti. Mol. Microbiol. **22:**427-36.

163. **Sourjik, V., and R. Schmitt.** 1998. Phosphotransfer between CheA, CheY1, and CheY2 in the chemotaxis signal transduction chain of *Rhizobium meliloti*. Biochemistry **37:**2327-35.

164. **Spormann, A. M.** 1999. Gliding motility in bacteria: insights from studies of *Myxococcus xanthus*. Microbiol. Mol. Biol. Rev. **63:**621-41.

165. **Spormann, A. M., and D. Kaiser.** 1999. Gliding mutants of *Myxococcus xanthus* with high reversal frequencies and small displacements. J. Bacteriol. **181:**2593-601.

166. **Sudo, S., and M. Dworkin.** 1972. Bacteriolytic enzymes produced by *Myxococcus xanthus*. J. Bacteriol. **110:**236-45.

167. **Sun, H., D. R. Zusman, and W. Shi.** 2000. Type IV pilus of *Myxococcus xanthus* is a motility apparatus controlled by the *frz* chemosensory system. Curr. Biol. **10:**1143-6.

168. **Szurmant, H., M. W. Bunn, V. J. Cannistraro, and G. W. Ordal.** 2003. *Bacillus subtilis* hydrolyzes CheY-P at the location of its action, the flagellar switch. J. Biol. Chem. **278:**48611-6.

169. **Szurmant, H., T. J. Muff, G. W. Ordal, M. W. Bunn, and V. J. Cannistraro.** 2004. *Bacillus subtilis* CheC and FliY are members of a novel class of CheY-P-

hydrolyzing proteins in the chemotactic signal transduction cascade. J. Biol. Chem. **279:**21787-92.

170. **Szurmant, H., and G. W. Ordal.** 2004. Diversity in chemotaxis mechanisms among the bacteria and archaea. Microbiol. Mol. Biol. Rev. **68:**301-19.

171. **Taylor, B. L., I. B. Zhulin, and M. S. Johnson.** 1999. Aerotaxis and other energy-sensing behavior in bacteria. Annu. Rev. Microbiol. **53:**103-28.

172. **Thaxter, R.** 1897. Further observations on the Myxobacteriaceae. Botanical Gazette **23:**395-411.

173. **Thaxter, R.** 1904. Notes on the Myxobacteriaceae. Botanical Gazette **37:**405-416.

174. **Thaxter, R.** 1892. On the Myxobacteriaceae, a new order of Schizomycetes. Botanical Gazette **17:**389-406.

175. **Tobe, T., and C. Sasakawa.** 2001. Role of bundle-forming pilus of enteropathogenic *Escherichia coli* in host cell adherence and in microcolony development. Cell. Microbiol. **3:**579-85.

176. **Ueki, T., S. Inouye, and M. Inouye.** 1996. Positive-negative KG cassettes for construction of multi-gene deletions using a single drug marker. Gene **183:**153-7.

177. **Vlamakis, H. C., J. R. Kirby, and D. R. Zusman.** 2004. The Che4 pathway of *Myxococcus xanthus* regulates type IV pilus-mediated motility. Mol. Microbiol. **52:**1799-811.

178. **Wadhams, G. H., and J. P. Armitage.** 2004. Making sense of it all: bacterial chemotaxis. Nat. Rev. Mol. Cell Biol. **5:**1024-37.

179. **Wall, D., and D. Kaiser.** 1998. Alignment enhances the cell-to-cell transfer of pilus phenotype. Proc. Natl. Acad. Sci. USA **95:**3054-8.

180. **Wall, D., and D. Kaiser.** 1999. Type IV pili and cell motility. Mol. Microbiol. **32:**1-10.

181. **Wall, D., P. E. Kolenbrander, and D. Kaiser.** 1999. The *Myxococcus xanthus pilQ* (*sglA*) gene encodes a secretin homolog required for type IV pilus biogenesis, social motility, and development. J. Bacteriol. **181:**24-33.

182. **Wall, D., S. S. Wu, and D. Kaiser.** 1998. Contact stimulation of Tgl and type IV pili in *Myxococcus xanthus*. J. Bacteriol. **180:**759-61.

183. **Wang, Q., A. Suzuki, S. Mariconda, S. Porwollik, and R. M. Harshey.** 2005. Sensing wetness: a new role for the bacterial flagellum. Embo J. **24:**2034-42.

184. **Ward, M. J., H. Lew, and D. R. Zusman.** 2000. Social motility in *Myxococcus xanthus* requires FrzS, a protein with an extensive coiled-coil domain. Mol. Microbiol. **37:**1357-71.

185. **Ward, M. J., and D. R. Zusman.** 1999. Motility in *Myxococcus xanthus* and its role in developmental aggregation. Curr. Opin. Microbiol. **2:**624-9.

186. **Ward, M. J., and D. R. Zusman.** 1997. Regulation of directed motility in *Myxococcus xanthus*. Mol. Microbiol. **24:**885-93.

187. **Webre, D. J., P. M. Wolanin, and J. B. Stock.** 2003. Bacterial chemotaxis. Curr. Biol. **13:**R47-9.

188. **Weimer, R. M., C. Creighton, A. Stassinopoulos, P. Youderian, and P. L. Hartzell.** 1998. A chaperone in the HSP70 family controls production of extracellular fibrils in *Myxococcus xanthus*. J. Bacteriol. **180:**5357-68.

189. **Winther-Larsen, H. C., and M. Koomey.** 2002. Transcriptional, chemosensory and cell-contact-dependent regulation of type IV pilus expression. Curr. Opin. Microbiol. **5:**173-8.

190. **Wolgemuth, C., E. Hoiczyk, D. Kaiser, and G. Oster.** 2002. How myxobacteria glide. Curr. Biol. **12:**369-77.

191. **Wolgemuth, C. W., and G. Oster.** 2004. The junctional pore complex and the propulsion of bacterial cells. J. Mol. Microbiol. Biotechnol. **7:**72-7.

192. **Wu, S. S., and D. Kaiser.** 1995. Genetic and functional evidence that Type IV pili are required for social gliding motility in *Myxococcus xanthus*. Mol. Microbiol. **18:**547-58.

193. **Wu, S. S., and D. Kaiser.** 1997. Regulation of expression of the *pilA* gene in *Myxococcus xanthus*. J. Bacteriol. **179:**7748-58.

194. **Wu, S. S., J. Wu, and D. Kaiser.** 1997. The *Myxococcus xanthus pilT* locus is required for social gliding motility although pili are still produced. Mol. Microbiol. **23:**109-21.

195. **Xu, H., and T. R. Hoover.** 2001. Transcriptional regulation at a distance in bacteria. Curr. Opin. Microbiol. **4:**138-44.

196. **Xu, Q., W. P. Black, S. M. Ward, and Z. Yang.** 2005. Nitrate-dependent activation of the Dif signaling pathway of *Myxococcus xanthus* mediated by a NarX-DifA interspecies chimera. J. Bacteriol. **187:**6410-8.

197. **Yang, R., S. Bartle, R. Otto, A. Stassinopoulos, M. Rogers, L. Plamann, and P. Hartzell.** 2004. AglZ is a filament-forming coiled-coil protein required for adventurous gliding motility of *Myxococcus xanthus*. J. Bacteriol. **186:**6168-78.

198. **Yang, Z., Y. Geng, and W. Shi.** 1998. A DnaK homolog in *Myxococcus xanthus* is involved in social motility and fruiting body formation. J. Bacteriol. **180:**218-24.

199. **Yang, Z., Y. Geng, D. Xu, H. B. Kaplan, and W. Shi.** 1998. A new set of chemotaxis homologues is essential for *Myxococcus xanthus* social motility. Mol. Microbiol. **30:**1123-30.

200. **Yang, Z., D. Guo, M. G. Bowden, H. Sun, L. Tong, Z. Li, A. E. Brown, H. B. Kaplan, and W. Shi.** 2000. The *Myxococcus xanthus wbgB* gene encodes a glycosyltransferase homologue required for lipopolysaccharide O-antigen biosynthesis. Arch. Microbiol. **174:**399-405.

201. **Yang, Z., and Z. Li.** 2005. Demonstration of interactions among *Myxococcus xanthus* Dif chemotaxis-like proteins by the yeast two-hybrid system. Arch. Microbiol. **183:**243-52.

202. **Yang, Z., X. Ma, L. Tong, H. B. Kaplan, L. J. Shimkets, and W. Shi.** 2000. *Myxococcus xanthus dif* genes are required for biogenesis of cell surface fibrils essential for social gliding motility. J. Bacteriol. **182:**5793-8.

203. **Youderian, P., N. Burke, D. J. White, and P. L. Hartzell.** 2003. Identification of genes required for adventurous gliding motility in *Myxococcus xanthus* with the transposable element *mariner*. Mol. Microbiol. **49:**555-70.

204. **Zhao, R., E. J. Collins, R. B. Bourret, and R. E. Silversmith.** 2002. Structure and catalytic mechanism of the *E. coli* chemotaxis phosphatase CheZ. Nat. Struct. Biol. **9:**570-5.

205. **Zusman, D. R.** 1982. "Frizzy" mutants: a new class of aggregation-defective developmental mutants of *Myxococcus xanthus*. J. Bacteriol. **150:**1430-7.

# CURRICULUM VITAE

**Wesley P. Black**
Virginia Polytechnic and State University
Department of Biological Sciences
2119 Derring Hall
Blacksburg, VA 24061
(540) 231-9381 (w)   (540) 998-9215 (h)
weblack@vt.edu

## EDUCATION

**Doctorate of Philosophy, Biological Sciences –** December 2005
Virginia Polytechnic and State University – Blacksburg, VA

Research topic: Regulation of exopolysaccharide production in *Myxococcus xanthus*

**Bachelor of Science, Microbiology –** August 2000
Auburn University – Auburn, AL

## RESEARCH EXPERIENCE

Undergraduate Research

**Special Problems in Molecular Biology under Dr. Brent Nielsen.** Identification and characterization of proteins associated with the replication fork of plant chloroplast DNA in *Nicotiana tabacum*.

**Special Problems in Plant Pathology under Dr. Gareth Morgan-Jones.** Characterization of the taxonomy of traditionally identified fungi using a modern molecular based classification system.

Graduate Research

**Research and Thesis under Dr. Thomas Pitta.** Adapted and developed a molecular genetic approach for the identification, isolation, and characterization of various proteases produced by a major catfish pathogen, *Flavobacterium columnare*.

**Research and Dissertation and Special Problems under Dr. Zhaomin Yang.**
**Project 1**: Construction of full in-frame deletion mutants at the *dif* locus, which forms a signal transduction pathway in *Myxococcus xanthus* and analysis of their phenotypic effects on social gliding motility and development.
**Project 2**: Epistatic analysis of the Dif pathway and correlation of the Dif pathway with type IV pili.

**Project 3**: Structure-function examination of DifA, a transmembrane receptor, by specific and random mutational analysis to determine essential amino acid residues involved in signal perception of the Dif pathway.

**Project 4**: Genetic and physical mapping of a *difA* suppressor mutation in order to characterize and identify additional members of the Dif pathway including auxiliary modulatory factors.

**Project 5**: Global mutational analysis of *Myxococcus xanthus* to identify genes specifically involved in the regulation and biogenesis of extracellular fibrils.

## TEACHING EXPERIENCE

GTA Position: Sixteen sections of General Microbiology Lab and one section of Food Microbiology Lab during 2000-2002.

## HONORS

Competitively selected student speaker at Research Day, 2005. Department of Biological Sciences, Virginia Tech.

Outstanding Teaching Award for Lab GTA, 2002. Department of Biological Sciences, Auburn University.

## MEETING ABSTRACTS

Black, W. P., X. Qian and Z. Yang. **2005**. Remote Senses of a Social Gliding Bacterium. 2nd ASM Conference on Prokaryotic Development: Vancouver, British Colombia, Canada.

Black, W. P. and Z. Yang. **2004**. New Developments on the Dif Pathway in *Myxococcus xanthus*. 31th International Conference on the Biology of the Myxobacteria: Helsingør, Denmark.

Black, W. P., K. M. Bellenger, Z. Li and Z. Yang. **2004**. Fibril biogenesis, Dif chemotaxis-like pathway and type IV pili in *Myxococcus xanthus*. Gordon Research Conference: Ventura, CA.

Black, W. P. and Z. Yang. **2003**. Regulation of fibril production by an unusual set of chemotaxis homologues in *Myxococcus xanthus*. Virginia Branch ASM Meeting: Charlottesville, VA.

Black, W. P. and Z. Yang. **2003**. DifD and DifG negatively regulate fibril biogenesis in *Myxococcus xanthus*. 30th International Conference on the biology of the Myxobacteria: Long Beach, CA.

Black, W. and Z. Yang. **2003**. Phenotypic analysis of the *dif* locus in *Myxococcus xanthus*. Graduate Research Symposium: Blacksburg, VA.

Black, W. and Z. Yang. **2003**. Phenotypic analysis of the *dif* locus in *Myxococcus xanthus*. ASM General Meeting: Washington D.C.

Black, W., K. Bellenger and Z. Yang. **2002**. Mutational Analysis of DifA, a MCP Homologue Essential for *Myxococcus xanthus* Fruiting Body Development and S-motility. 1st ASM Conference on Prokaryotic Development: Quebec City, Quebec, Canada.

Bellenger, K., W. Black, W. Shi and Z. Yang. **2002**. Not all *dif* genes are required for *Myxococcus xanthus* S-motility and development. Gordon Research Conference: Ventura, CA.

Burnside, K., W. Black, J. Ramsey, J. Newton and T. Pitta. **2001**. Transposon Insertion Mutations of a Protease Implicated in Virulence of the Catfish Pathogen *Flavobacterium columnare*. ASM General Meeting: Orlando, FL.

## PUBLICATIONS

Xu, Q., Black, W. P., Ward, S. M. and Z. Yang. **2005**. Nitrate-dependent activation of the Dif signaling pathway of *Myxococcus xanthus* mediated by a NarX-DifA interspecies chimera. J. Bacteriol. 187: 6410-6418.

Bonner, P. J., Xu, Q., Black, W. P., Li, Z., Yang, Z. and L. J. Shimkets. **2005**. The Dif chemosensory pathway is directly involved in phosphatidylethanolamine sensory transduction in *Myxococcus xanthus*. Mol. Micro. 57: 1499-1508.

Lu, A., Cho, K., Black, W. P., Duan, X., Lux, R., Yang, Z., Kaplan, H. B., Zusman, D. R. and W. Shi. **2005**. Exopolysaccharide biosynthesis genes required for social motility in *Myxococcus xanthus*. Mol. Micro. 55: 206-220.

Black, W. P. and Z. Yang. **2004**. *Myxococcus xanthus* Chemotaxis Homologs DifD and DifG Negatively Regulate Fibril Polysaccharide Production. J. Bacteriol. 186: 1001-1008.